AD-A171 364 THE PSEUDO-IMAGE METHOD FOR COMPUTING ELECTROMAGNETIC FIELD PENETRATION I (U) SYRACUSE UNIV NY DEPT OF ELECTRICAL AND COMPUTER ENGINEERING X YUAN ET AL. 1/2

UNCLASSIFIED MAY 86 SYRU/DECE/TR-86/1 ARO-21378.6-EL F/G 20/3 NL

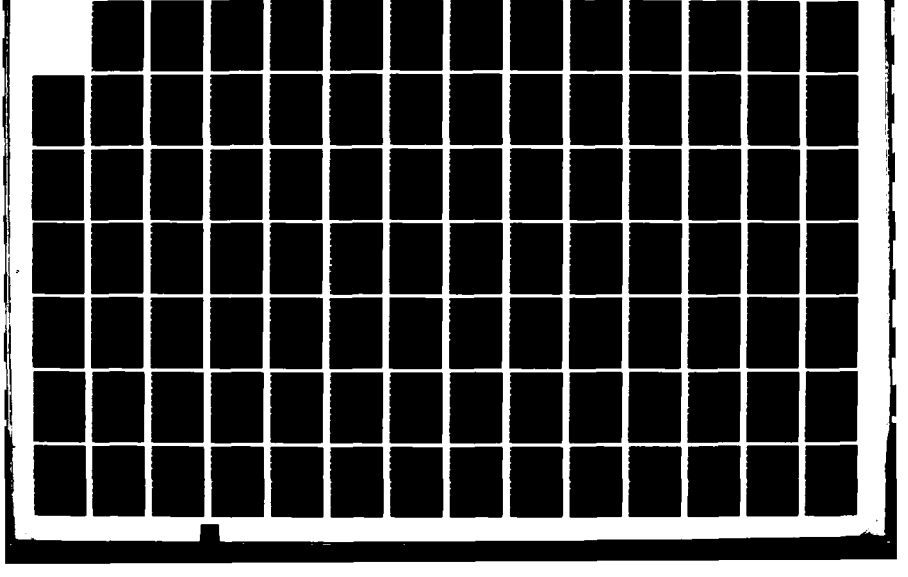

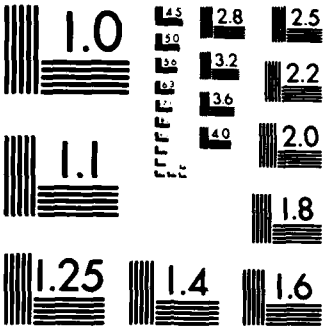

MICROCOPY RESOLUTION TEST CHART
NATIONAL BUREAU OF STANDARDS-1963-A

SYRU/DECE/TR-86/1

THE PSEUDO-IMAGE METHOD FOR COMPUTING ELECTROMAGNETIC FIELD PENETRATION INTO A CYLINDRICAL CAVITY, TM CASE

Interim Technical Report No. 5

by

Xingchao Yuan
Roger F. Harrington
Joseph R. Mautz

May 1986

Department of
Electrical and Computer Engineering
Syracuse University
Syracuse, New York 13210

Contract No. DAAG29-84-K-0078

Approved for Public release; distribution unlimited

Prepared for

ARMY RESEARCH OFFICE
RESEARCH TRIANGLE PARK
NORTH CAROLINA 27709

SYRU/DECE/TR-86/1

THE PSEUDO-IMAGE METHOD FOR COMPUTING ELECTROMAGNETIC FIELD PENETRATION INTO A CYLINDRICAL CAVITY, TM CASE

Interim Technical Report No. 5

by

Xingchao Yuan
Roger F. Harrington
Joseph R. Mautz

May 1986

Department of
Electrical and Computer Engineering
Syracuse University
Syracuse, New York 13210

Contract No. DAAG29-84-K-0078

Approved for Public release; distribution unlimited

Prepared for

ARMY RESEARCH OFFICE
RESEARCH TRIANGLE PARK
NORTH CAROLINA 27709

UNCLASSIFIED
SECURITY CLASSIFICATION OF THIS PAGE (When Data Entered)

REPORT DOCUMENTATION PAGE	READ INSTRUCTIONS BEFORE COMPLETING FORM
1. REPORT NUMBER: ARO 21378.6-EL	2. GOVT ACCESSION NO.: AD-A171 364	3. RECIPIENT'S CATALOG NUMBER
4. TITLE (and Subtitle): THE PSEUDO-IMAGE METHOD FOR COMPUTING ELECTROMAGNETIC FIELD PENETRATION INTO A CYLINDRICAL CAVITY, TM CASE	5. TYPE OF REPORT & PERIOD COVERED: Interim Technical Report #5
	6. PERFORMING ORG. REPORT NUMBER
7. AUTHOR(s): Xingchao Yuan, Roger F. Harrington, Joseph R. Mautz	8. CONTRACT OR GRANT NUMBER(s): DAAG29-84-K-0078
9. PERFORMING ORGANIZATION NAME AND ADDRESS: Department of Electrical & Computer Engineering, Syracuse University, Syracuse, New York 13210	10. PROGRAM ELEMENT, PROJECT, TASK AREA & WORK UNIT NUMBERS
11. CONTROLLING OFFICE NAME AND ADDRESS: U.S. Army Research Office, Post Office Box 12211, Research Triangle Park, NC 27709	12. REPORT DATE: May 1986
	13. NUMBER OF PAGES: 110
14. MONITORING AGENCY NAME & ADDRESS(if different from Controlling Office)	15. SECURITY CLASS. (of this report): UNCLASSIFIED
	15a. DECLASSIFICATION/DOWNGRADING SCHEDULE

16. DISTRIBUTION STATEMENT (of this Report)

Approved for public release; distribution unlimited

17. DISTRIBUTION STATEMENT (of the abstract entered in Block 20, if different from Report)

NA

18. SUPPLEMENTARY NOTES

The view, opinions, and/or findings contained in this report are those of the author(s) and should not be construed as an official Department of the Army position, policy, or decision, unless so designated by other documentation.

19. KEY WORDS (Continue on reverse side if necessary and identify by block number)

Aperture problems
Conducting cylinders
Electromagnetic coupling
Generalized network formulation
Magnetic current
Numerical solutions
Pseudo-image method
Two-dimensional fields

20. ABSTRACT (Continue on reverse side if necessary and identify by block number)

A solution for the electromagnetic coupling through an aperture in an arbitrarily shaped perfect conductor is obtained by the generalized network formulation for aperture problems in conjunction with a new method called the pseudo-image method. The theory developed is applied to a TM curved cylindrical surface with a narrow or a wide slot. The field in an aperture in a circular cylindrical surface is calculated by the pseudo-image method, by a method without a pseudo-image, and by a method in which only an electric current is used. The aperture field calculated by the pseudo-image →

DD FORM 1 JAN 73 1473 EDITION OF 1 NOV 65 IS OBSOLETE
S/N 0102-014-6601

UNCLASSIFIED
SECURITY CLASSIFICATION OF THIS PAGE (When Data Entered)

20. ABSTRACT (continued)

method is the most accurate because it agrees best with a Fourier series solution.

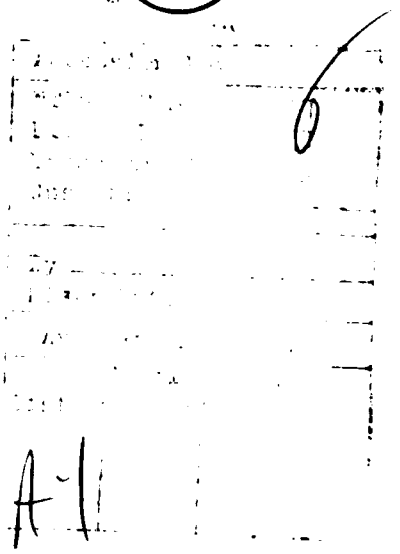

CONTENTS

1. INTRODUCTION

The problem of electromagnetic coupling to a cavity through an aperture is an old problem. For an extensive list of references see [1]. A number of problems are solved by the so-called generalized network formulation for aperture problems [2]-[4]. In this method, the aperture is closed by a perfect conductor, a sheet of unknown magnetic current $\underline{M}$ is placed on one side of the shorted aperture and $-\underline{M}$ is placed on the other side. This insures continuity of the tangential electric field across the aperture. Next, the tangential magnetic field is forced to be continuous across the aperture, resulting in an integral equation for $\underline{M}$. $\underline{M}$ is found numerically by following the method of moments [5]. Unfortunately, this method can be easily implemented only when the aperture is in a perfectly conducting infinite plane so that image theory [6,Sec.3-4] may be applied to find the fields due to $\underline{M}$ [3],[4].

When the aperture is in a finite curved surface, the fields due to $\underline{M}$ (or $-\underline{M}$) radiating in the presence of the complete conducting surface are difficult to find. The complete conducting surface is the conducting surface with its aperture shorted. The present report gives an accurate solution to such problems. We recognize that the problem of obtaining the electromagnetic field due to $\underline{M}$ is a scattering problem in which the impressed source is on the scatterer. A

similar static problem was solved in [7] by a method in which a pseudo-image was used in order to improve the numerical accuracy. For reference, we call this method the pseudo-image method. With this in mind, we approach the problem by following the generalized network formulation method until the point of finding the fields due to $\underline{M}$ radiating in the presence of a complete conducting surface. We then solve this scattering problem by placing an electric current $\underline{J}$ on the complete conducting surface, introducing the pseudo-image as in [7], writing the electric field integral equation for $\underline{J}$ and finally solving this equation for $\underline{J}$ by the method of moments [5]. As shown in the following sections, the theory developed in this way works very well for a non-resonant cavity formed by the complete conducting surface. However, it fails when the cavity is resonant. Further study is needed to treat this special case.

Section 2 states and formulates the general problem shown in Fig.1. The theory developed applies to both two and three dimensional problems. In a two dimensional problem, all quantities are invariant in one direction, for instance, the z-direction. Section 3, which is essentially the application of the theory developed in Section 2, solves the problem of electromagnetic scattering from an infinitely long, infinitesimally thin, perfectly conducting cylindrical surface with an infinitely long slot illuminated by a uniform TM plane wave. Section 4 states the numerical

results obtained for the problem of Section 3. Various methods are compared to show how well the pseudo-image method works. Appendix A evaluates some of the complicated integrals appearing in Section 3. Appendix B summarizes a method for the aperture problem in which the aperture is not closed by a perfect conductor and only an unknown electric current $\underline{J}$ is placed on the conducting surface. This method fails to give accurate fields inside the cavity when the aperture becomes very small.

2. FORMULATION OF THE PROBLEM

2.1 Statement of the Problem

The problem to be considered is shown in Fig.1 where electromagnetic coupling occurs through an aperture of arbitrary shape in a perfectly conducting body which may have finite thickness. If the aperture were closed, there would be a cavity. Some additional complete perfectly conducting bodies may exist either inside or outside the cavity, or both. To keep the formulation of the problem simple, we consider the case where only one additional complete conducting body is located outside the cavity. Other cases are just straightforward extensions of the case under consideration. A homogeneous medium with permeability μ and permittivity ϵ fills all space outside the perfectly conducting bodies. The perfectly conducting body with an aperture is specified by its internal surface, denoted by S_a, and its external surface, denoted by S_b. (Of course, if the body has zero thickness, then the internal and external surface will be indistinguishable.) The additional perfectly conducting body is specified by the surface S_c. It does not matter whether this body is hollow or solid because, due to the fact that S_c is closed, no field can penetrate it. The cross sections of the conducting bodies are shown in Fig.1. The problem is two dimensional if

everything is invariant in the z-direction. In this case the conducting bodies are infinitely long cylinders and the aperture is an infinitely long slot. We formulate the problem without mentioning whether it is a three- or two-dimensional problem.

Next, we define the symbols appearing in Fig.1. $(\underline{J}^{imp},\underline{M}^{imp})$ denotes the known impressed electric current source and impressed magnetic current source. $(\underline{E}^{inc},\underline{H}^{inc})$ denotes the fields that would exist if $(\underline{J}^{imp},\underline{M}^{imp})$ were to radiate into unbounded, homogeneous space with (μ,ϵ) everywhere. Region b denotes the space inside the cavity, and region a denotes the space external to the closed surface that consists of S_∞ and the aperture. $(\underline{E}^{inc}+\underline{E}^{a},\underline{H}^{inc}+\underline{H}^{a})$ denotes the total field in region a, and $(\underline{E}^{b},\underline{H}^{b})$ denotes the total field in region b. The objective is to determine these total fields. In turn, related quantities such as power gain and polarizability can be easily determined. Also, we want to investigate how Bethe hole theory[8],[9] should be modified when a small aperture (compared to wavelength) is in a finite perfectly conducting cavity instead of in an infinite ground plane. Finally, we state the boundary conditions required for solving this problem. First, both the tangential electric field and the tangential magnetic field must be continuous across the aperture. Second, the tangential electric field on the perfectly conducting surfaces, i.e., on S_∞, S_1 and S_∞ must be zero. With this in mind, we proceed to the next section.

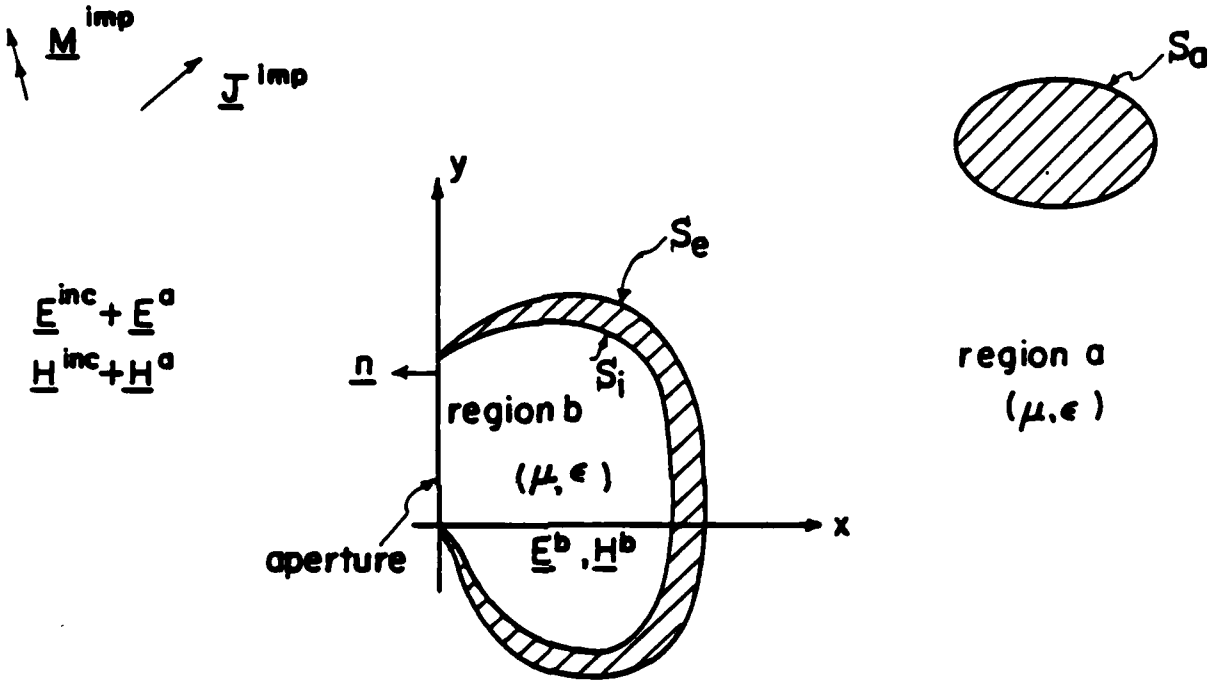

Fig. 1. Original problem: Electromagnetic coupling through an arbitrary shaped aperture in a conducting body. (Only a typical cross section is shown; the shaded area denotes a perfect conductor.) Impressed sources $\underline{J}^{imp}$ and $\underline{M}^{imp}$ radiate in the presence of surfaces S_i, S_e, and S_a.

2.2 Derivation of the Operator Equation

The situation considered in Fig.1 is rather complicated. The approach that we take is to decompose the problem into two parts. The point of departure is the equivalence principle [6,Sec.3-5]. The aperture in Fig.1 is first closed by a perfectly conducting flat plate. (If, in a three dimensional case, it is not possible to close the aperture by a flat plate, then special treatment is needed.) Then the magnetic current sheet $\underline{M}$ is placed on the left-hand side of the flat plate and $-\underline{M}$ is placed on the right-hand side of the flat plate. The $\underline{M}$ is defined as

$$\underline{M} = \underline{E} \times \underline{n} \qquad (2\text{-}1)$$

where n is the unit normal vector on the aperture, pointing toward region a, and E is the electric field in the aperture in Fig.1. In this way, the boundary condition that the tangential electric field is continuous across the aperture is satisfied. The combination of S_a and the flat plate is called S_a^{sc}; and the combination of S_1 and the flat plate is called S_1^{sc}. (Superscript sc stands for short circuit since the closing of the aperture can be viewed as the short circuiting of the aperture). The equivalent problem is shown in Fig.2. Before the problem in Fig.2 is actually equivalent to the problem in Fig.1, we have to impose continuity of the tangential magnetic field across the aperture, as required in the original problem. Namely,

$$\underline{H}_t^a(\underline{J}^{imp},\underline{M}^{imp})+\underline{H}_t^a(\emptyset,\underline{M})=\underline{H}_t^b(\emptyset,-\underline{M}) \qquad \text{on A} \qquad (2\text{-}2)$$

where A denotes the flat plate shorting the aperture. The subscript t in (2-2) denotes the component tangent to A. In (2-2), $\underline{H}^a(\cdot,\cdot)$ is the magnetic field operator in region a with the sources indicated in the parentheses $(\cdot,\cdot)$ radiating in the presence of S_w^{ec} and S_a. $\underline{H}^b(\cdot,\cdot)$ is the magnetic field operator in region b with the sources indicated in the parentheses $(\cdot,\cdot)$ radiating in the presence of S_1^{ec}. Actually, the "a" fields on the left-hand side of (2-2) are evaluated not exactly on A but immediately to the left of any electric current that could flow on the flat plate. Moreover, the "b" field on the right-hand side of (2-2) is evaluated not exactly on A but immediately to the right of any electric current that could flow on the flat plate. Each magnetic field in (2-2) has two arguments. The first argument is an electric current source and the second argument is a magnetic current source. Equation (2-2) states that the tangential magnetic field must be continuous across the aperture.

The impressed sources $\underline{J}^{imp}$ and $\underline{M}^{imp}$ and the boundary conditions on the fields on A, S_1, S_w, and S_a in Fig.2 are the same as in Fig.1. It is evident from [10,Theorem I] that the electric field in an infinite region outside a closed surface is uniquely specified by its impressed sources in the region and its tangential components on the surface. Consequently, the fields in Fig.2 are identical to those in

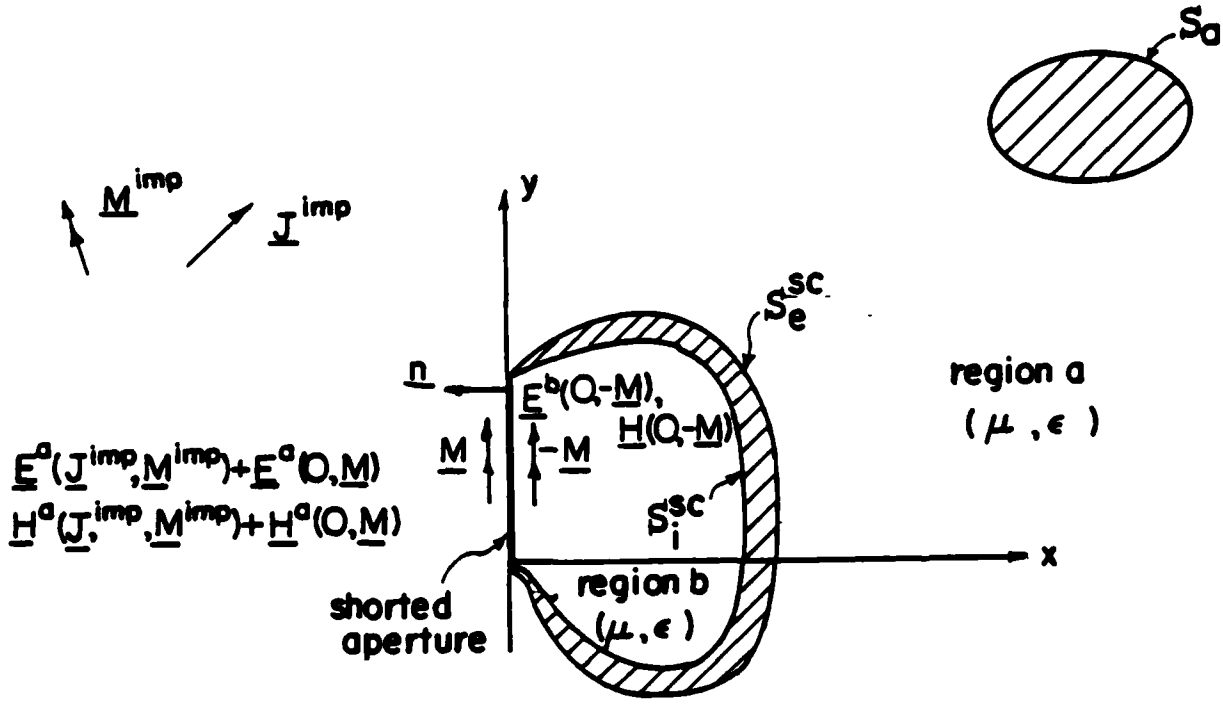

Fig. 2. The equivalent problem as viewed in the xy plane. The space inside the cavity formed by S_i^{sc} is called region b and the space outside S_e^{sc} is called region a.

Fig.1 so that the problem in Fig.2 is equivalent to that in Fig.1. Comparing Fig.1 with Fig.2, we find that

$$(\underline{E}^{inc}+\underline{E}^{a},\underline{H}^{inc}+\underline{H}^{a})= \tag{2-3}$$

$$\{\underline{E}^{a}(\underline{J}^{imp},\underline{M}^{imp})+\underline{E}^{a}(\underline{0},\underline{M}),\underline{H}^{a}(\underline{J}^{imp},\underline{M}^{imp})+\underline{H}^{a}(\underline{0},\underline{M})\}$$

in region a

$$(\underline{E}^{b},\underline{H}^{b})=(\underline{E}^{b}(\underline{0},-\underline{M}),\underline{H}^{b}(\underline{0},-\underline{M})) \quad \text{in region b} \tag{2-4}$$

The electric fields on the right-hand sides of (2-3) and (2-4) correspond to the magnetic fields in (2-2). $\underline{E}^{a}(\cdot,\cdot)$ is the electric field operator in region a with the sources indicated in the parentheses radiating in the presence of $S_{a}^{a c}$ and S_{a}. $\underline{E}^{b}(\cdot,\cdot)$ is the electric field operator in region b with the sources indicated in the parentheses radiating in the presence of $S_{A}^{a c}$. For example, $\underline{E}^{b}(\underline{0},-\underline{M})$ is the electric field in region b due to $-\underline{M}$ placed on the right-hand side of the flat plate that shorts A.

To find the unknown magnetic current $\underline{M}$, we appeal to (2-2). Rearranging the terms in (2-2) and using the linearity of the operators, we obtain

$$-\underline{H}_{t}^{a}(\underline{0},\underline{M})-\underline{H}_{t}^{b}(\underline{0},\underline{M})=\underline{H}_{t}^{a}(\underline{J}^{imp},\underline{M}^{imp}) \quad \text{on A} \tag{2-5}$$

2.3 Numerical Solution of the Operator Equation

To find $\underline{M}$ using (2-5), we first approximate $\underline{M}$ by

$$\underline{M} = \sum_{n} V_{n}\,\underline{M}_{n} \tag{2-6}$$

where $\underline{M}_n$ are known (to be chosen) vector expansion functions, and V_n are scalar coefficients. Substituting (2-6) into (2-5), we have, by the linearity of the operators in (2-5),

$$\sum_n V_n(-\underline{\overset{a}{H}}_e(\emptyset,\underline{M}_n)-\underline{\overset{b}{H}}_e(\emptyset,\underline{M}_n))=\underline{\overset{a}{H}}_e(\underline{J}^{imp},\underline{M}^{imp}) \qquad (2\text{-}7)$$

Next, we define a symmetric product as

$$< \underline{A},\underline{B} >= \int_S \underline{A} \cdot \underline{B}\, ds \qquad (2\text{-}8)$$

where $\underline{A}$ and $\underline{B}$ are vector functions, S is the surface on which they are defined, and ds is the differential element of surface area on S. Taking the symmetric product of (2-7) with $\underline{M}_m$, m=1,2,···, we obtain

$$\left[[Y^a]+[Y^b] \right] \vec{V} = \vec{I}^{inc} \qquad (2\text{-}9)$$

where $\vec{V}$ and $\vec{I}^{inc}$ are column vectors. The n^{th} element of $\vec{V}$ is V_n. The m^{th} element of $\vec{I}^{inc}$ is I_m^{inc} given by

$$I_m^{inc} = <\underline{M}_m, \underline{\overset{a}{H}}_e(\underline{J}^{imp},\underline{M}^{imp})> \qquad (2\text{-}10)$$

Moreover, $[Y^a]$ and $[Y^b]$ are square matrices whose mn^{th} elements are given by

$$Y_{mn}^a = -\int_A \underline{M}_m \cdot \underline{\overset{a}{H}}_e(\emptyset,\underline{M}_n)\, ds \qquad (2\text{-}11)$$

$$Y_{mn}^b = -\int_A \underline{M}_m \cdot \underline{\overset{b}{H}}_e(\emptyset,\underline{M}_n)\, ds \qquad (2\text{-}12)$$

In (2-11) $\underline{H}^a(\underline{\emptyset},\underline{M}_n)$ is evaluated on the region a side of A. Similarly, in (2-12), $\underline{H}^b(\underline{\emptyset},\underline{M}_n)$ is evaluated on the region b side of A. If $[Y^a]$, $[Y^b]$, and $\vec{I}^{inc}$ are found, $\vec{V}$ can be found by solving the set of linear equations given in (2-9). A standard computer routine for this purpose is available.

Substituting (2-6) into (2-3) and (2-4), we relate each field component in those two equations to the fields due to the known expansion functions (sources). Now the problem of finding the fields due to the unknown source $\underline{M}$ is reduced to the problem of finding the fields due to known sources radiating in the presence of complete perfect conductors. The fields in each region can be written as follows: In region a,

$$\underline{E}^{inc}+\underline{E}^a = \underline{E}^a(\underline{J}^{imp},\underline{M}^{imp})+\sum_n V_n \underline{E}^a(\underline{\emptyset},\underline{M}_n) \qquad (2\text{-}13)$$

$$\underline{H}^{inc}+\underline{H}^a = \underline{H}^a(\underline{J}^{imp},\underline{M}^{imp})+\sum_n V_n \underline{H}^a(\underline{\emptyset},\underline{M}_n) \qquad (2\text{-}14)$$

In region b,

$$\underline{E}^b = -\sum_n V_n \underline{E}^b(\underline{\emptyset},\underline{M}_n) \qquad (2\text{-}15)$$

$$\underline{H}^b = -\sum_n V_n \underline{H}^b(\underline{\emptyset},\underline{M}_n) \qquad (2\text{-}16)$$

The fields on the right-hand sides of equations (2-13)-(2-16) have the same meaning as in (2-3) and (2-4). The fields on the left-hand sides of (2-13)-(2-16) are those in the original problem Fig.1.

In the following sections, we evaluate the fields on the right-hand sides of (2-13)-(2-16) one by one. The

results obtained are not only substituted into (2-13)-(2-16) but also into (2-10)-(2-12) to find the coefficients of the magnetic current expansion functions, i.e., V_n, n=1,2,....

2.4 Short-Circuit Field due to the Impressed Sources

$(\underline{E}^a(\underline{J}^{imp},\underline{M}^{imp}),\underline{H}^a(\underline{J}^{imp},\underline{M}^{imp}))$ in (2-13) and (2-14) are the fields in region a due to the impressed sources $(\underline{J}^{imp},\underline{M}^{imp})$ radiating in the presence of S_b^{sc} and S_a (See Fig.2). These fields can be viewed as the sum of the fields due to the impressed sources radiating in an unbounded homogeneous space with (μ,ϵ) and the fields due to the electric current induced on S_b^{sc} and S_a radiating also in the unbounded homogeneous space with (μ,ϵ). Namely, in region a,

$$\underline{E}^a(\underline{J}^{imp},\underline{M}^{imp}) = \underline{E}^{inc}+\underline{E}(\underline{J}^{ex},\underline{0}) \qquad (2\text{-}17)$$

$$\underline{H}^a(\underline{J}^{imp},\underline{M}^{imp}) = \underline{H}^{inc}+\underline{H}(\underline{J}^{ex},\underline{0}) \qquad (2\text{-}18)$$

where $(\underline{E}^{inc},\underline{H}^{inc})$ is defined in the last paragraph of section (2.1); $(\underline{E}(\underline{J}^{ex},\underline{0}),\underline{H}(\underline{J}^{ex},\underline{0}))$ are the fields due to induced current $\underline{J}^{ex}$ on S_b^{sc} and S_a, radiating in an unbounded homogeneous space with (μ,ϵ).

On the surfaces of the perfectly conducting bodies S_b^{sc} and S_a

$$\underline{E}_t^a(\underline{J}^{imp},\underline{M}^{imp}) = \underline{E}_t^{inc} + \underline{E}_t(\underline{J}^{ex},\underline{0}) = \underline{0} \qquad (2\text{-}19)$$

where the subscript t denotes the component tangent to either S_b^{sc} or S_a. Rearranging (2-19), we obtain

$$-\underline{E}_s(\underline{J}^{ex},\underline{0}) = \underline{E}_s^{inc} \qquad (2\text{-}20)$$

on S_m^{ec} and S_a

The electric current $\underline{J}^{ex}$ is approximated by

$$\underline{J}^{ex} = \sum_j I_j^{ex}\ \underline{J}_j^a \qquad (2\text{-}21)$$

where $\{\underline{J}_j^a\}$ are expansion functions that are chosen later when particular impressed fields are given. The function $\underline{J}_j^a$ is on either S_m^{ec} or S_a and is tangent to whichever surface it is on. Seeking to determine the unknown coefficients I_j^{ex}, we substitute (2-21) into (2-20) and take the symmetric product of (2-20) with $\underline{J}_i^a$, i=1,2,···, to obtain

$$[Z^a]\ \vec{I}^{ex} = \vec{V}^{ex} \qquad (2\text{-}22)$$

where $\vec{I}^{ex}$ and $\vec{V}^{ex}$ are column vectors. The j^{th} element of $\vec{I}^{ex}$ is I_j^{ex}. The i^{th} element of $\vec{V}^{ex}$ is V_i^{ex} given by

$$V_i^{ex} = \langle \underline{J}_i^a\ ,\underline{E}^{inc}\rangle \qquad (2\text{-}23)$$

Furthermore, $[Z^a]$ is a square matrix whose ij^{th} element is given by

$$Z_{ij}^a = \langle \underline{J}_i^a\ ,-\underline{E}(\underline{J}_j^a,\underline{0})\rangle = -\int_{S_m^{ec}+S_a} \underline{J}_i^a \cdot \underline{E}(\underline{J}_j^a\ ,\underline{0})\ ds \qquad (2\text{-}24)$$

where $\int_{S_m^{ec}+S_a}$ denotes that the surface integral is performed on both S_m^{ec} and S_a. Note that $\underline{E}^{inc}$ and $\underline{E}(\underline{J}_j^a,\underline{0})$ are due to their corresponding sources radiating in empty space. They can be found by the well known formulas in empty space. In turn (2-

23) and (2-24) can be computed. With $[Z^a]$ and $\vec{V}^{ex}$ available, $\{I_j^{ex}\}$ can be found by solving the matrix equation (2-22). Substituting (2-21) into (2-17) and (2-18), we obtain, in region a,

$$\underline{E}^a(\underline{J}^{imp},\underline{M}^{imp})=\underline{E}^{inc} + \sum_j I_j^{ex}\ \underline{E}(\underline{J}_j^a,\underline{\emptyset}) \qquad (2\text{-}25)$$

$$\underline{H}^a(\underline{J}^{imp},\underline{M}^{imp})=\underline{H}^{inc} + \sum_j I_j^{ex}\ \underline{H}(\underline{J}_j^a,\underline{\emptyset}) \qquad (2\text{-}26)$$

As introduced in Fig.2, the fields on the left-hand sides of (2-25) and (2-26) exist only in region a so that (2-25) and (2-26) are only valid in region a even though $(\underline{E}^{inc},\underline{H}^{inc})$ and $(\underline{E}(\underline{J}_j^a,\underline{\emptyset}),\underline{H}(\underline{J}_j^a,\underline{\emptyset}))$ are valid everywhere in space.

2.5 Short-Circuit Fields due to the Magnetic Current Expansion Functions

a) Finding $(\underline{E}^a(\underline{\emptyset},\underline{M}_n),\underline{H}^a(\underline{\emptyset},\underline{M}_n))$

The field $(\underline{E}^a(\underline{\emptyset},\underline{M}_n),\underline{H}^a(\underline{\emptyset},\underline{M}_n))$ appearing in (2-13) and (2-14) is the field in region a due to the magnetic current sheet $\underline{M}_n$ placed on the region a side of the shorted aperture and radiating in the presence of S_a^{sc} and S_a. Since S_a^{sc} is perfectly conducting, the region inside it is completely isolated from region a. Therefore, any medium and any source can be placed inside S_a^{sc} without affecting the field in region a. We fill the region inside S_a^{sc} with the medium characterized by (μ,ϵ) and place the magnetic current sheet $\underline{M}_n$ on the right-hand side of the shorted aperture as shown in Fig.3. The magnetic current sheet on the right-hand side

of the shorted aperture in Fig.3 is called the pseudo-image of the one on the left-hand side of the shorted aperture. Now, the electromagnetic field $(\underline{E}^a(\underline{\emptyset},\underline{M}_n),\underline{H}^a(\underline{\emptyset},\underline{M}_n))$ in region a is written as

$$\underline{E}^a(\underline{\emptyset},\underline{M}_n)=\underline{E}(\underline{\emptyset},2\underline{M}_n)+\underline{E}(\underline{\mathcal{J}}_n^a,\underline{\emptyset}) \tag{2-27}$$

$$\underline{H}^a(\underline{\emptyset},\underline{M}_n)=\underline{H}(\underline{\emptyset},2\underline{M}_n)+\underline{H}(\underline{\mathcal{J}}_n^a,\underline{\emptyset}) \tag{2-28}$$

The fields on the right-hand sides of (2-27) and (2-28) are due to their corresponding sources given in the associated parentheses radiating in the unbounded homogeneous medium as on the right-hand sides of (2-17) and (2-18). Here, $\underline{\mathcal{J}}_n^a$ is the electric current induced on S_e^c and S_a by $2\underline{M}_n$ where $2\underline{M}_n$ represents the combination of the two magnetic current sheets in Fig.3. Now, $\underline{\mathcal{J}}_n^a$ adjusts itself so that

$$\underline{E}_t^a(\underline{\emptyset},\underline{M}_n) = \underline{\emptyset} \qquad \text{on } S_e^c \text{ and } S_a \tag{2-29}$$

where subscript t denotes tangential component. Combining (2-27) and (2-29), we obtain

$$-\underline{E}_t(\underline{\mathcal{J}}_n^a,\underline{\emptyset}) = \underline{E}_t(\underline{\emptyset},2\underline{M}_n) \tag{2-30}$$

$\underline{\mathcal{J}}_n^a$ is now approximated by

$$\underline{\mathcal{J}}_n^a = \sum_j I_{jn}^a \underline{J}_j^a \tag{2-31}$$

where I_{jn}^a, $j=1,2,\cdots$ are coefficients to be determined, and $\underline{J}_j^a$ are the same as in (2-21). Substituting (2-31) into (2-30) and taking the symmetric product of (2-30) with each $\underline{J}_i^a$, we obtain

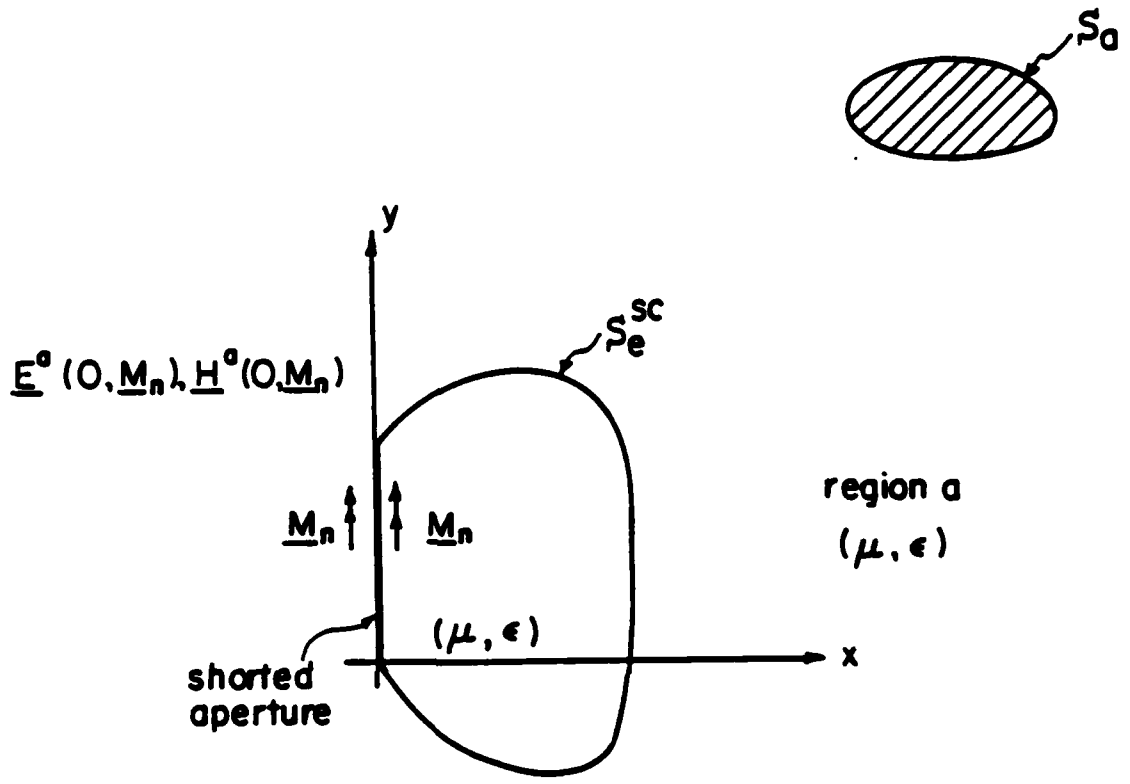

Fig. 3. The xy cross section of a situation in which $(\underline{E}^a(0, \underline{M}_n), \underline{H}^a(0, \underline{M}_n))$ can exist. The magnetic current sheet immediately to the right of the shorted aperture is called the pseudo-image of the one immediately to the left.

$$[Z^a]\ \vec{I}_n^a = \vec{V}_n^a \tag{2-32}$$

Here, $[Z^a]$ is given in (2-24), and $\vec{I}_n^a$ and $\vec{V}_n^a$ are column vectors. The j^{th} element of $\vec{I}_n^a$ is $I_{j,n}^a$, and the i^{th} element of $\vec{V}_n^a$ is $V_{i,n}^a$ given by

$$V_{i,n}^a = \langle \underline{J}_i^a , \underline{E}_t(\underline{\emptyset}, 2\underline{M}_n) \rangle \tag{2-33}$$

Because $\underline{E}(\underline{\emptyset}, 2\underline{M}_n)$ is the field due to $2\underline{M}_n$ radiating in unbounded homogeneous space, it can be evaluated easily. Thus, (2-33) can be computed. Therefore $\vec{I}_n^a$ can be found by solving the linear equations in (2-32), i.e., $\underline{J}_n^a$ is completely determined. Substituting (2-31) into (2-27) and (2-28), we obtain, in region a,

$$\underline{E}^a(\underline{\emptyset}, \underline{M}_n) = \underline{E}(\underline{\emptyset}, 2\underline{M}_n) + \sum_j I_{j,n}^a \, \underline{E}(\underline{J}_j^a, \underline{\emptyset}) \tag{2-34}$$

$$\underline{H}^a(\underline{\emptyset}, \underline{M}_n) = \underline{H}(\underline{\emptyset}, 2\underline{M}_n) + \sum_j I_{j,n}^a \, \underline{H}(\underline{J}_j^a, \underline{\emptyset}) \tag{2-35}$$

In (2-33)-(2-35), $2\underline{M}_n$ represents the combination of the magnetic current sheets placed on both sides of the flat plate that shorts the aperture in Fig.3. At any point not on the shorting plate $\underline{E}(\underline{\emptyset}, 2\underline{M}_n)$ and $H(\underline{\emptyset}, 2\underline{M}_n)$ are simply twice the fields due to $\underline{M}_n$ because the two $\underline{M}_n$'s are infinitesimally close to each other. On the shorting plate the normal electric field $\underline{E}_n(\underline{\emptyset}, 2\underline{M}_n)$ and the tangential magnetic field $\underline{H}_t(\underline{\emptyset}, 2\underline{M}_n)$ are simply twice those due to $\underline{M}_n$, but $\underline{E}_t(\underline{\emptyset}, 2\underline{M}_n)$ and $\underline{H}_n(\underline{\emptyset}, 2\underline{M}_n)$ vanish. Because $\underline{E}_t(\underline{\emptyset}, 2\underline{M}_n)$ vanishes on the shorting plate, the magnitude of the electric current on it is considerably reduced. Hopefully,

this reduction will improve the behavior of the electric current on the shorting plate and consequently a more accurate numerical solution to the problem can be obtained.

b) Finding $(\underline{E}^b(\underline{\emptyset},\underline{M}_n),\underline{H}^b(\underline{\emptyset},\underline{M}_n))$

$(\underline{E}^b(\underline{\emptyset},\underline{M}_n),\underline{H}^b(\underline{\emptyset},\underline{M}_n))$ in (2-15) and (2-16) are the fields due to $\underline{M}_n$ placed on the right-hand side of the shorted aperture radiating in the presence of $\overset{\bullet c}{S_1}$. Since $\overset{\bullet c}{S_1}$ forms a cavity, $\underline{M}_n$ will produce zero fields in region a. With the same idea as in Section 2.5a, we write for region b

$$\underline{E}^b(\underline{\emptyset},\underline{M}_n)=\underline{E}(\underline{\emptyset},2\underline{M}_n)+\underline{E}(\overset{b}{\underline{J}}_n,\underline{\emptyset}) \qquad (2\text{-}36)$$

$$\underline{H}^b(\underline{\emptyset},\underline{M}_n)=\underline{H}(\underline{\emptyset},2\underline{M}_n)+\underline{H}(\overset{b}{\underline{J}}_n,\underline{\emptyset}) \qquad (2\text{-}37)$$

where $(\underline{E}(\underline{\emptyset},2\underline{M}_n),\underline{H}(\underline{\emptyset},2\underline{M}_n))$ is the electromagnetic field due to $2\underline{M}_n$ radiating in unbounded homogeneous space where $2\underline{M}_n$ represents the combination of the two magnetic current sheets shown in Fig.4. There, the $\underline{M}_n$ placed on the right-hand side of the shorted aperture is the original $\underline{M}_n$,and the $\underline{M}_n$ placed on the left-hand side of the shorted aperture is called the pseudo-image of $\underline{M}_n$. $\overset{b}{\underline{J}}_n$ is the electric current induced by $2\underline{M}_n$ on $\overset{\bullet c}{S_1}$. $(\underline{E}(\overset{b}{\underline{J}}_n,\underline{\emptyset}),\underline{H}(\overset{b}{\underline{J}}_n,\underline{\emptyset}))$ is the electromagnetic field due to $\overset{b}{\underline{J}}_n$ radiating in homogeneous space. Now, $\overset{b}{\underline{J}}_n$ adjusts itself such that

$$\overset{b}{\underline{E}}_t(\underline{\emptyset},\underline{M}_n) = \underline{\emptyset} \qquad \text{on } \overset{\bullet c}{S_1} \qquad (2\text{-}38)$$

where subscript t denotes tangential component. Combining (2-36) and (2-38), we obtain

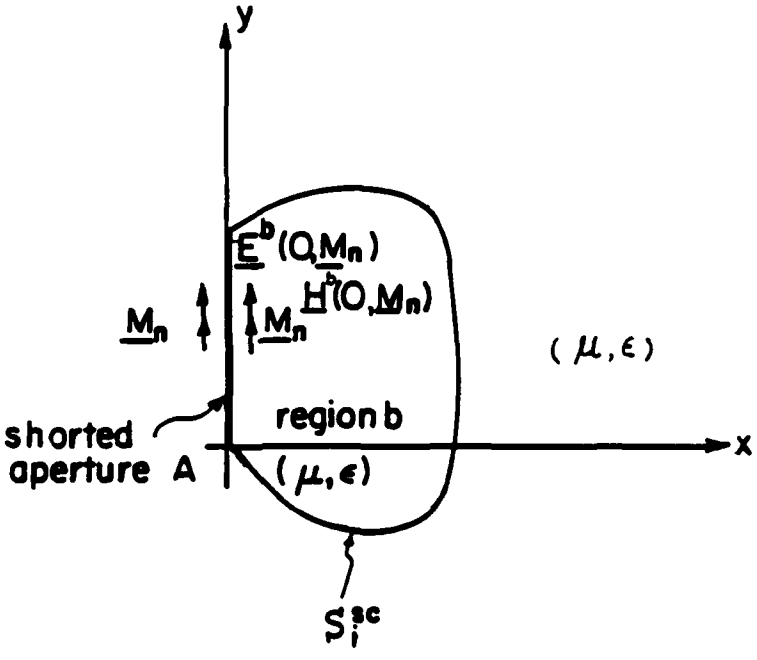

Fig. 4. The xy cross section of a situation in which ($\underline{E}^b(0, \underline{M}_n)$, $\underline{H}^b(0, \underline{M}_n)$) can exist. The magnetic current sheet immediately to the left of the shorted aperture is called the pseudo-image of the one immediately to the right.

$$-\underline{E}_c(\underline{\mathcal{J}}_n^b,\underline{\emptyset})=\underline{E}_c(\underline{\emptyset},2\underline{M}_n) \qquad \text{on } S_i^{mc} \tag{2-39}$$

$\underline{\mathcal{J}}_n^b$ is next approximated by

$$\underline{\mathcal{J}}_n^b = \sum_j I_{jn}^b \ \underline{J}_j^b \tag{2-40}$$

where $\underline{J}_j^b$ is an expansion function on S_i^{mc}. Substituting (2-40) into (2-39) and taking the symmetric product of (2-39) with $\underline{J}_i^b$, we obtain

$$[Z^b]\ \vec{I}_n^b = \vec{V}_n^b \tag{2-41}$$

where $\vec{I}_n^b$ and $\vec{V}_n^b$ are column vectors. The j^{th} element of $\vec{I}_n^b$ is I_{jn}^b. The i^{th} element of $\vec{V}_n^b$ is V_{in}^b given by

$$V_{in}^b = \langle \underline{J}_i^b, \underline{E}(\underline{\emptyset},2\underline{M}_n)\rangle \tag{2-42}$$

Furthermore, $[Z^b]$ is a square matrix whose ij^{th} element is given by

$$Z_{ij}^b = -\int_{S_i^{mc}} \underline{J}_i^b \cdot \underline{E}(\underline{J}_j^b,\underline{\emptyset})\ ds \tag{2-43}$$

Once $(\underline{J}_j^b,\underline{M}_n)$ are chosen, (2-42) and (2-43) can be evaluated. Thus, $\vec{I}_n^b$ can be found by solving (2-41). Substituting (2-40) into (2-36) and (2-37), we obtain, in region b,

$$\underline{E}^b(\underline{\emptyset},\underline{M}_n)=\underline{E}(\underline{\emptyset},2\underline{M}_n) + \sum_j I_{jn}^b \ \underline{E}(\underline{J}_j^b,\underline{\emptyset}) \tag{2-44}$$

$$\underline{H}^b(\underline{\emptyset},\underline{M}_n)=\underline{H}(\underline{\emptyset},2\underline{M}_n) + \sum_j I_{jn}^b \ \underline{H}(\underline{J}_j^b,\underline{\emptyset}) \tag{2-45}$$

2.6 Summary

In section 2.4 through 2.5, we have evaluated all the field quantities in (2-13)-(2-16). Substituting (2-25) and (2-34) into (2-13), (2-26) and (2-35) into (2-14), (2-44) into (2-15), and (2-45) into (2-16), we obtain, in region a,

$$\underline{E}^{inc} + \underline{E}^{a} = \underline{E}^{inc} + \sum_{j} \overset{ex}{I}_{j} \; \underline{E}(\underline{J}_{j}^{a}, \underline{\emptyset}) + \sum_{n} V_n [\underline{E}(\underline{\emptyset}, 2\underline{M}_n) + \sum_{j} \overset{a}{I}_{jn} \; \underline{E}(\underline{J}_{j}^{a}, \underline{\emptyset})] \tag{2-46}$$

$$\underline{H}^{inc} + \underline{H}^{a} = \underline{H}^{inc} + \sum_{j} \overset{ex}{I}_{j} \; \underline{H}(\underline{J}_{j}^{a}, \underline{\emptyset}) + \sum_{n} V_n [\underline{H}(\underline{\emptyset}, 2\underline{M}_n) + \sum_{j} \overset{a}{I}_{jn} \; \underline{H}(\underline{J}_{j}^{a}, \underline{\emptyset})] \tag{2-47}$$

and, in region b,

$$\underline{E}^{b} = - \sum_{n} V_n \; [\underline{E}(\underline{\emptyset}, 2\underline{M}_n) + \sum_{j} \overset{b}{I}_{jn} \; \underline{E}(\underline{J}_{j}^{b}, \underline{\emptyset}) \;] \tag{2-48}$$

$$\underline{H}^{b} = - \sum_{n} V_n \; [\underline{H}(\underline{\emptyset}, 2\underline{M}_n) + \sum_{j} \overset{b}{I}_{jn} \; \underline{H}(\underline{J}_{j}^{b}, \underline{\emptyset}) \;] \tag{2-49}$$

To evaluate V_n, we must solve (2-9) . Before (2-9) can be solved, $[Y^a]$, $[Y^b]$ and $\vec{I}^{inc}$ have to be evaluated. Substituting (2-35) into (2-11) and (2-45) into (2-12), we obtain

$$\overset{a}{Y}_{mn} = \overset{ns}{Y}_{mn} + \Delta \overset{a}{Y}_{mn} \tag{2-50}$$

$$\overset{b}{Y}_{mn} = \overset{ns}{Y}_{mn} + \Delta \overset{b}{Y}_{mn} \tag{2-51}$$

where

$$\overset{ns}{Y}_{mn} = -\int_{A} \underline{M}_m \cdot \underline{H}_e(\underline{\emptyset}, 2\underline{M}_n) \; ds \tag{2-52}$$

$$\Delta \overset{a}{Y}_{mn} = -\sum_{j} \overset{a}{I}_{jn} \int_{A} \underline{M}_m \cdot \underline{\bar{H}}_e(\underline{J}_{j}^{a}, \underline{\emptyset}) \; ds \tag{2-53}$$

$$\Delta Y^{b}_{mn} = -\sum_{j} I^{b}_{j,n} \int_{A} \underline{M}_{m} \cdot \underline{H}^{+}_{e}(\underline{J}^{b}_{j},\underline{0})\, ds \qquad (2\text{-}54)$$

In (2-53), $\underline{H}^{-}_{e}(\underline{J}^{a}_{j},\underline{0})$ is $\underline{H}_{e}(\underline{J}^{a}_{j},\underline{0})$ evaluated immediately to the left of the shorted aperture on which $\underline{J}^{a}_{j}$ may flow. In (2-54), $\underline{H}^{+}_{e}(\underline{J}^{b}_{j},\underline{0})$ is $\underline{H}_{e}(\underline{J}^{b}_{j},\underline{0})$ evaluated immediately to the right of the shorted aperture on which $\underline{J}^{b}_{j}$ may flow. $[Y^{hs}_{mn}]$ is called the half-space admittance matrix. The terminology comes from the fact that it is the admittance matrix for the case of electromagnetic coupling through an aperture in an infinitely large ground plane, which has been investigated extensively in the literature, e.g., Bethe hole theory [8] is developed for the small circular hole in the ground plane. Imagining the infinitely large ground plane being shrunk down to a finite size and bent over to form a cavity, we can view $[\Delta Y^{a}]$ and $[\Delta Y^{b}]$ in (2-50) and (2-51) as modifying terms. We want to state how Bethe hole theory should be modified for an aperture in a finite body. Substituting (2-26) into (2-10), we find that the m^{th} element of $\vec{I}^{inc}$ is given by

$$I^{inc}_{m} = \int_{A} \underline{M}_{m} \cdot \underline{H}^{inc}\, ds + \sum_{j} I^{ex}_{j} \int_{A} \underline{M}_{m} \cdot \underline{H}^{-}(\underline{J}^{a}_{j},\underline{0})\, ds \qquad (2\text{-}55)$$

In summary, we first shorted the aperture in the conducting body with a perfectly conducting flat plate and then put magnetic current sheets on both sides of the plate,

$\underline{M}$ on one side and $-\underline{M}$ on the other to render the tangential electric field continuous across the aperture. By requiring the tangential magnetic field to be continuous across the aperture, we found an integral equation for $\underline{M}$. Solving this integral equation by the method of moments [5], we obtained $\underline{M}$ as the linear combination (2-6) of the magnetic current expansion functions $\underline{M}_n$. In (2-13)-(2-16), we expressed the electromagnetic field of the original problem of Fig.1 as the sum of the field due to the impressed sources and linear combinations of the fields due to the magnetic currents $\underline{M}_n$, all sources radiating in the presence of the conducting body with its aperture shorted. In turn, each of these fields was expressed as the sum of the field due to its source radiating in homogeneous space and the field due to the electric current induced on the body with its aperture shorted. This electric current was obtained by solving its integral equation by the method of moments. Collecting results, we were able to express the electromagnetic field of the original problem of Fig.1 as the summations (2-46)-(2-49).

3. ELECTROMAGNETIC COUPLING TO AN INFINITELY LONG CYLINDER, TM CASE

3.1 Remarks and Simplifications

Although the formulas derived in Section 2 are valid for both two and three dimensional problems, it is difficult to evaluate all the integrals in the three dimensional case. Because of complication, we may lose insight to the problem. Therefore, we shall make the following simplifications.

A). Everything is invariant in the z-direction. Namely, the conducting bodies (three dimensional) become infinitely long cylinders and they are completely specified by their xy cross sections. The aperture becomes an infinitely long slot. The impressed sources ($\underline{J}^{imp}$,$\underline{M}^{imp}$) produce two dimensional fields. All field quantities in Section 2 are now only functions of the coordinates (x,y). (The time dependence exp(jwt) is suppressed).

B). Conductor S_∞ given in Fig. 1 is removed since its presence entails only minor modifications.

C). The conductor with an aperture which is now a slotted cylinder has zero thickness, i.e., S_1 and S_∞ in Fig.1 become indistinguishable so that the slotted cylinder is completely specified by one contour denoted by C in the xy plane.

D). In Section 3, we consider the case where a TM plane wave is incident on the cylinder. The plane wave is specified by

$$\underline{E}^{inc} = \underline{u}_z \exp[jk(x\cos\phi^i + y\sin\phi^i)] \qquad (3\text{-}1)$$

where $\underline{u}_z$ is the unit vector in the z direction, $k=w\sqrt{\mu\epsilon}$, and ϕ^i is the polar angle of the direction from which the plane wave comes.

E). As shown in Fig.5, the contour C of the cylinder is a chain of L-1 straight line segments. The end points of the j^{th} segment are labeled t_j and t_{j+1} where t_j is the value of t at the beginning of the segment and t_{j+1} is the value of t at the end of the segment. Measured from the " beginning " of C at $t_1=0$, t is the arc length along C.

F). As shown in Fig.5, the contour ($x=0$, $|y| \leq W$) of the slot is partitioned into M straight line segments. The end points of these segments are specified by their values of t. Here, t is the arc length along C extended onto the contour of the slot. At ($x=0$, $y=-W$), we have $t=t_L$, and at ($x=0$, $y=W$), we have $t=t_{L+M} = t_L+2W$.

G). The combination of C and the contour of the slot is called C^{inc}. Now, $\underline{J}_j^a$ and $\underline{J}_j^b$ are both on C^{inc}. We choose

$$\underline{J}_j^a = \underline{J}_j^b = \underline{J}_j(t) \qquad (3\text{-}2)$$

where

$$\underline{J}_j(t) = \begin{cases} \underline{u}_z & t_j \leq t \leq t_{j+1} \\ 0 & \text{elsewhere} \end{cases}, \quad j=1,2,\ldots,N \qquad (3\text{-}3)$$

.

where

$$N = L+M-1 \qquad (3\text{-}4)$$

The magnetic current expansion function $\underline{M}_n(t)$ will be

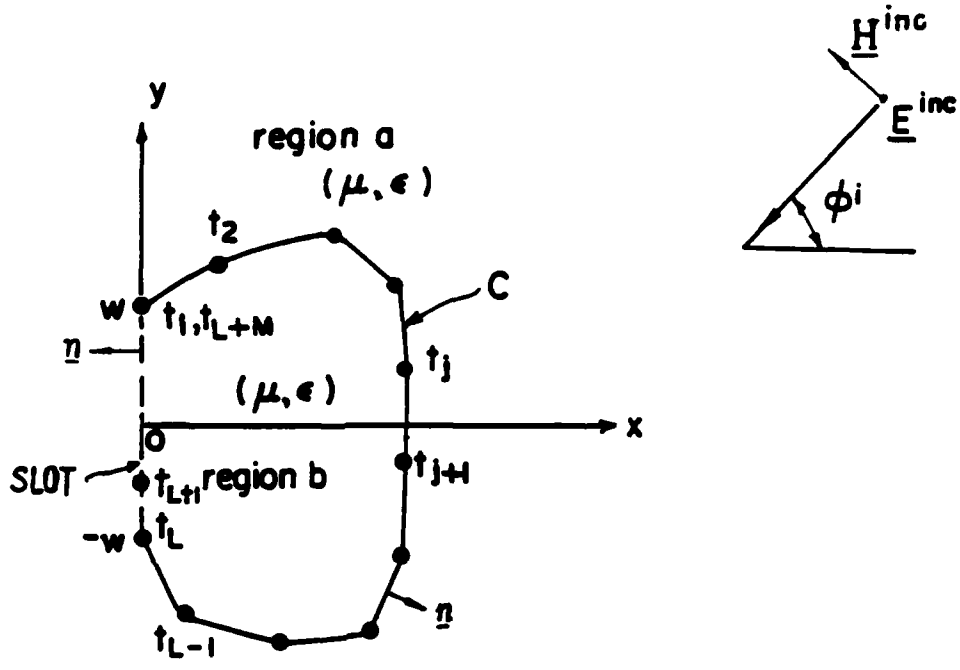

Fig. 5. xy plane view of the slotted cylinder. The dotted line on the y axis represents the slot. C^{sc} is the combination of the contour C of the cylinder and the contour ($x=0$, $|y| \leq W$) of the slot.

specified in Section 3.3.

Assuming that both $\underline{J}_s(t)$ and $\underline{M}_m(t)$ are tangent to C^{sc} and independent of z, the two-dimensional fields due to the electric current $\underline{J}_s(t)$ on C^{sc} and the magnetic current $\underline{M}_m(t)$ on the contour of the slot, both radiating in the unbounded homogeneous space with constitutive parameters (μ,ϵ), are given by [5,Eq.3-27],[11,Eqs.(5) and (6)]

$$\underline{E}(\underline{J}_s,\underline{\emptyset}) = -\frac{\eta}{4}\left[k\int_{\emptyset}^{t_{L+m}} \underline{J}_s(t')\, H_0^{(2)}(k|\underline{\rho}-\underline{\rho}'|)\, dt' + \frac{\nabla}{k}\int_{\emptyset}^{t_{L+m}} \frac{d(\hat{\underline{t}}\cdot\underline{J}_s(t'))}{dt'} H_0^{(2)}(k|\underline{\rho}-\underline{\rho}'|)\, dt' \right] \tag{3-5}$$

$$\underline{H}(\underline{J}_s,\underline{\emptyset}) = \epsilon_m\, \underline{J}_s(t)\times\underline{n} - \frac{1}{4j}\int_{\emptyset}^{t_{L+m}} \underline{J}_s(t')\times\nabla H_0^{(2)}(k|\underline{\rho}-\underline{\rho}'|)\, dt' \tag{3-6}$$

$$\underline{E}(\underline{\emptyset},\underline{M}_m) = -\epsilon_m\, \underline{M}_m(t)\times\underline{n} + \frac{1}{4j}\int_{t_L}^{t_{L+m}} \underline{M}_m(t')\times\nabla H_0^{(2)}(k|\underline{\rho}-\underline{\rho}'|)\, dt' \tag{3-7}$$

$$\underline{H}(\underline{\emptyset},\underline{M}_m) = -\frac{1}{4\eta}\left[k\int_{t_L}^{t_{L+m}} \underline{M}_m(t')\, H_0^{(2)}(k|\underline{\rho}-\underline{\rho}'|)\, dt' + \frac{\nabla}{k}\int_{t_L}^{t_{L+m}} \frac{d(\hat{\underline{t}}\cdot\underline{M}_m(t'))}{dt'} H_0^{(2)}(k|\underline{\rho}-\underline{\rho}'|)\, dt' \right] \tag{3-8}$$

where $\hat{\underline{t}}$ is the unit tangential vector on C^{sc}, $\underline{\rho}'$ is the two-dimensional radius vector to the point on C^{sc} whose arc length is t', and $\underline{\rho}$ is the two-dimensional radius vector to

the field point. The field point is the point at which an electromagnetic field in (3-5)-(3-8) is evaluated. In (3-5)-(3-8), k is the wave number $w\sqrt{\mu\epsilon}$ where w is the angular frequency, η is the intrinsic impedance $\sqrt{\mu/\epsilon}$, $\underline{n}$ is the unit normal vector that points outward from C^{sc} as shown in Fig.5 and $H_m^{(2)}$ is the Hankel function of the second kind of order zero. If the field point is remote from C^{sc}, then ϵ_m is zero. If the field point clings to either side of C^{sc}, then ϵ_m is $\pm 1/2$. Specifically, ϵ_m is 1/2 if the field point is on the region a side of C^{sc}, and ϵ_m is -1/2 if the field point is on the region b side of C^{sc}. If $\epsilon_m = \pm 1/2$, then the t that appears in (3-6) and (3-7) is the arc length of the field point on C^{sc}.

3.2 Evaluation of Quantities That Do Not Depend on M_n

In this section we specialize $\overset{a}{Z}_{ij}$ of (2-24), $\overset{b}{Z}_{ij}$ of (2-43), and $\overset{ex}{V}_i$ of (2-23) to the case in which both $\underline{\overset{a}{J}}_j$ and $\underline{\overset{b}{J}}_j$ are the same electric current $\underline{J}_j$ of (3-2).

a) Evaluation of $\overset{a}{Z}_{ij}$ of (2-24) and $\overset{b}{Z}_{ij}$ of (2-43)

Substituting (3-2) into (2-24) and (2-43) and integrating only over the contour C^{sc} rather than a surface, we obtain

$$\overset{a}{Z}_{ij} = \overset{b}{Z}_{ij} = Z_{ij} \tag{3-9}$$

where

$$Z_{ij} = -\int_{\emptyset}^{t_{i+m}} \underline{J}_i(t) \cdot \underline{E}(\underline{J}_j, \emptyset)\, dt \tag{3-10}$$

Substituting (3-3) into (3-5), we obtain

$$\underline{E}(\underline{J}_j,\underline{\emptyset}) = \underline{u}_z \left[-\frac{k\eta}{4} \int_{t_j}^{t_{j+1}} H_0^{(2)}(k|\underline{\rho}-\underline{\rho}'|)dt' \right] \tag{3-11}$$

Substitution of (3-11) and (3-3) into (3-10) yields

$$Z_{ij} = \frac{k\eta}{4} \int_{t_i}^{t_{i+1}} dt \int_{t_j}^{t_{j+1}} dt' \, H_0^{(2)}(k|\underline{\rho}-\underline{\rho}'|) \tag{3-12}$$

New variables of integration u and u' are defined by

$$u = 2(t-t_i-\Delta C_i/2)/\Delta C_i \tag{3-13}$$

$$u' = 2(t'-t_j-\Delta C_j/2)/\Delta C_j \tag{3-14}$$

where

$$\Delta C_j = t_{j+1} - t_j \ , \qquad j=1,2,\ldots,N \tag{3-15}$$

Substitution of (3-13) and (3-14) into (3-12) leads to

$$Z_{ij} = \begin{cases} \dfrac{\eta\Gamma_i\Gamma_j}{16k} \displaystyle\int_{-1}^{1} du \int_{-1}^{1} du' \, H_0^{(2)}(|\underline{\Gamma}_{ij}(u,u')|) & , \ i \neq j \\ \dfrac{\eta\,\Gamma_i^2}{16k} \displaystyle\int_{-1}^{1} du \int_{-1}^{1} du' \, H_0^{(2)}(\Gamma_i/2|u-u'|) & , \ i=j \end{cases} \tag{3-16}$$

where

$$\Gamma_i = k\Delta C_i \ , \qquad i=1,2,\ldots,N \tag{3-17}$$

$$\underline{\Gamma}_{ij}(u,u') = k\underline{R}_{ij} + (\Gamma_i u\hat{\underline{t}}_i - \Gamma_j u'\hat{\underline{t}}_j)/2 \tag{3-18}$$

In (3-18), $\underline{R}_{ij}$ is the vector from the midpoint of C_j to the midpoint of C_i where C_i and C_j are the straight line segments of C^{oc} whose end points are (t_i,t_{i+1}) and (t_j,t_{j+1}), respectively. Moreover, $\hat{\underline{t}}_i$ and $\hat{\underline{t}}_j$ are the unit

vectors tangent to C_i and C_j, respectively. Here, $\hat{\underline{t}}_i$ points from t_i toward t_{i+1}, and $\hat{\underline{t}}_j$ points from t_j toward t_{j+1}. The vectors $\underline{R}_{ij}$, $\hat{\underline{t}}_i$, and $\hat{\underline{t}}_j$ can be expressed in terms of the (x,y) coordinates of the end points of C_i and C_j.

If $i \neq j$, Z_{ij} is found by the two-dimensional Gaussian quadrature method [12]. If i=j, we recast (3-16) as

$$Z_{ij} = \frac{\eta \Gamma_i^2}{16k} \int_{-1}^{1} du \int_{-1}^{1} du' [H_0^{(2)}(|u-u'|\Gamma_i/2) - g(|u-u'|\Gamma_i/2)]$$

$$+ \frac{\eta \Gamma_i^2}{16k} \int_{-1}^{1} du \int_{-1}^{1} du' \; g(|u-u'|\Gamma_i/2) \qquad (3\text{-}19)$$

where g(x) is the small argument approximation of $H_0^{(2)}(x)$ [6,p.462], i.e.,

$$g(x) = 1 - j\frac{2}{\pi}\log(\tau x/2) \qquad (3\text{-}20)$$

where log denotes the natural logarithm, $\log\tau$ is Euler's constant, and τ=1.781. The first integral in (3-19) now has no singularity at u=u' and can be evaluated by the two-dimensional Gaussian quadrature method. The second integral in (3-19) is found analytically as [13, Eqs.(62) and (63)]

$$\int_{-1}^{1} du \int_{-1}^{1} du' \; g(|u-u'|\Gamma_i/2)$$

$$= 4 + j4(3-2\log(\Gamma_i\tau/2))/\pi \qquad (3\text{-}21)$$

Substituting (3-20) and (3-21) into (3-19), we obtain

$$Z_{ii} = \eta \Gamma_i^2 [1+j(3-2\log(\Gamma_i\tau/2))/\pi]/4k \; +$$

$$\frac{\eta\Gamma_i^m}{16k}\int_{-1}^{1} du \int_{-1}^{1} du' [H_0^{(2)}(|u-u'|\Gamma_i/2) - 1 + \frac{2}{\pi} j\log(|u-u'|\Gamma_i\tau/4)] \qquad (3\text{-}22)$$

b) Evaluation of V_i^{mx} of (2-23)

Substituting (3-1)-(3-3) into (2-23), and integrating only over the contour C^{mc} rather than a surface, we find that the i^{th} element of $\vec{V}^{mx}$ is given by

$$V_i^{mx} = \int_{t_i}^{t_{i+1}} e^{jk(x\cos\phi^i + y\sin\phi^i)}\, dt \qquad (3\text{-}23)$$

where (x,y) are the rectangular coordinates of the point t on C^{mc}. Performing the integration of (3-23), we obtain

$$V_i^{mx} = \frac{\Delta C_i \sin k\beta_i}{k\beta_i} e^{jk\alpha_i} \qquad (3\text{-}24)$$

where $\alpha_i = [(x_{i+1}+x_i)\cos\phi^i + (y_{i+1}+y_i)\sin\phi^i]/2 \qquad (3\text{-}25)$

$\beta_i = [(x_{i+1}-x_i)\cos\phi^i + (y_{i+1}-y_i)\sin\phi^i]/2 \qquad (3\text{-}26)$

Here, (x_i, y_i) are the (x,y) coordinates of the point t_i on C^{mc}.

Now that the elements of Z^m and $\vec{V}^{mx}$ have been evaluated, we can solve (2-22) for $\vec{I}^{mx}$.

3.3 One Magnetic Current Expansion Function for the Narrow Slot

In this section, we assume that kw « 1. Considering that the slot is narrow, we take only one expansion function for the magnetic current $\underline{M}$. We choose

$$\underline{M}_1 = \begin{cases} \underline{u}_y \sqrt{1-(y/W)^2} & x=0,\ |y| \le W \\ 0 & \text{elsewhere} \end{cases} \qquad (3\text{-}27)$$

because it is a simple vector function that, for the TM case, has the correct direction and the correct behavior as y approaches $\pm W$. In the rest of this section, formulas involving the magnetic current expansion functions $\underline{M}_n$ are specialized to the case where $\underline{M}_1$ of (3-27) is the only magnetic current expansion function.

a) Evaluation of V_{1n}^{a} of (2-33) and V_{1n}^{b} of (2-42)

Substituting (3-2) into (2-33) and (2-42) and integrating only over C^{ec} rather than a surface, we find that the i^{th} elements of $\vec{V}_n^{a}$ and $\vec{V}_n^{b}$ are given by

$$V_{1n}^{a} = V_{1n}^{b} = V_{1n} \qquad (3\text{-}28)$$

where

$$V_{1n} = \int_0^{t_{L\leftarrow M}} \underline{J}_1(t) \cdot \underline{E}_s(0, 2\underline{M}_n)\, dt \qquad (3\text{-}29)$$

Referring to the last paragraph in Section 2.5a, and using (3-7) with [6,Eq.(D-15)]

$$\nabla H_0^{(2)}(k|\rho-\rho'|) = \frac{-k(\rho-\rho')}{|\rho-\rho'|} H_1^{(2)}(k|\rho-\rho'|) \qquad (3\text{-}30)$$

substituted into it, we obtain

$$\underline{E}_t(\underline{\rho},\underline{M}_n)=\begin{cases}\dfrac{-k}{2j}\displaystyle\int_{t_L}^{t_{L+M}}(\underline{M}_n(t')\times(\underline{\rho}-\underline{\rho}'))_t\,\frac{H_1^{(2)}(k|\underline{\rho}-\underline{\rho}'|)}{|\underline{\rho}-\underline{\rho}'|}\,dt' & ,\ 0<t<t_L\\ 0 & ,\ t_L<t<t_{L+M}\end{cases} \tag{3-31}$$

The subscript t on both sides of (3-31) denotes the component tangent to C^{ec}. Substitution of (3-31) into (3-29) yields

$$V_{in}=\begin{cases}\dfrac{jk}{2}\displaystyle\int_0^{t_{L+M}}dt\underline{J}_i(t)\cdot\int_{t_L}^{t_{L+M}}dt'(\underline{M}_n(t')\times(\underline{\rho}-\underline{\rho}'))\frac{H_1^{(2)}(k|\underline{\rho}-\underline{\rho}'|}{|\underline{\rho}-\underline{\rho}'|} & i=1,2,\ldots,L-1\\ 0 & i=L,L+1,\ldots,N\end{cases} \tag{3-32}$$

where N is given by (3-4).

Substituting (3-3) and (3-27) into (3-32) and introducing new variables of integration u defined by (3-13) and u' defined by

$$u' = (t-t_L-W)/W \tag{3-33}$$

we obtain

$$V_{ii}=\begin{cases}-\dfrac{jkW\Delta C_i}{4}\displaystyle\int_{-1}^{1}du\int_{-1}^{1}du'\frac{\sqrt{1-(u')^2}\,(\underline{u}_x\cdot\underline{\Gamma}_{ip}(u,u'))H_1^{(2)}(|\underline{\Gamma}_{ip}(u,u')|)}{|\underline{\Gamma}_{ip}(u,u')|} & ,\ i=1,2,\ldots,L-1\\ 0 & ,\ i=L,L+1,\ldots,N\end{cases} \tag{3-34}$$

where

$$\underline{\Gamma}_{ip}(u,u')=k\underline{R}_{ip}+(\Gamma_i u/2)\underline{t}_i-kWu'\underline{u}_y \tag{3-35}$$

and $R_{i\alpha}$ is the vector from the origin at the center of the slot to the midpoint of C_i.

Now that the elements of Z^a, Z^b, $\vec{V}_i^a$, and $\vec{V}_i^b$ have been evaluated, we can solve (2-32) for $\vec{I}_i^a$ and (2-41) for $\vec{I}_i^b$. Because of (3-9) and (3-28), the solution $\vec{I}_i^a$ to (2-32) is the same as the solution $\vec{I}_i^b$ to (2-41). Calling this common solution $\vec{I}_i$, we write

$$I_{ji}^a = I_{ji}^b = I_{ji} \tag{3-36}$$

b) Evaluation of $\overset{nm}{Y}_{mn}$ of (2-52)

Replacing the surface integral by a line integral over the contour ($x=0$, $|y|\leq W$) of the shorting strip, substituting (3-8) into (2-52), and performing an integration by parts, we obtain

$$2kn\overset{nm}{Y}_{mn} = k^2\int_{t_L}^{t_{L+M}} dt\ \underline{M}_m(t)\cdot\int_{t_L}^{t_{L+M}} dt'\underline{M}_n(t')H_0^{(2)}(k|\rho-\rho'|)$$

$$-\int_{t_L}^{t_{L+M}} dt\ \frac{d}{dt}(\underline{t}\cdot\underline{M}_m(t))\int_{t_L}^{t_{L+M}} dt'\frac{d}{dt'}(\underline{t}\cdot\underline{M}_n(t'))\ H_0^{(2)}(k|\rho-\rho'|) \tag{3-37}$$

Substituting (3-27) into (3-37), anticipating that $\hat{\underline{t}}=\underline{u}_y$ when $t_L<t<t_{L+M}$, and introducing new variables of integration u and u' defined by

$$u = (t-t_L-W)/W \tag{3-38}$$

$$u' = (t'-t_L-W)/W \tag{3-39}$$

we obtain

$$2k\eta Y_{11}^{nn} = (kW)^2 U_1 - U_2 \tag{3-40}$$

where

$$U_1 = \int_{-1}^{1} du\sqrt{1-u^2} \int_{-1}^{1} du'\sqrt{1-(u')^2}\, H_0^{(2)}(kW|u-u'|) \tag{3-41}$$

$$U_2 = \int_{-1}^{1} du \frac{u}{\sqrt{1-u^2}} \int_{-1}^{1} du' \frac{u'}{\sqrt{1-(u')^2}} H_0^{(2)}(kW|u-u'|) \tag{3-42}$$

We recast (3-41) and (3-42) as

$$U_1 = I_1 + \int_{-1}^{1} du\sqrt{1-u^2} \int_{-1}^{1} du'\sqrt{1-(u')^2} \left[H_0^{(2)}(kW|u-u'|) - g(kW|u-u'|) \right] \tag{3-43}$$

$$U_2 = I_2 + \int_{-1}^{1} du \frac{u}{\sqrt{1-u^2}} \int_{-1}^{1} du' \frac{u'}{\sqrt{1-(u')^2}} \left[H_0^{(2)}(kW|u-u'|) - g(kW|u-u'|) \right] \tag{3-44}$$

where g is given by (3-20) and

$$I_1 = \int_{-1}^{1} du\sqrt{1-u^2} \int_{-1}^{1} du'\sqrt{1-(u')^2}\, g(kw|u-u'|) \tag{3-45}$$

$$I_2 = \int_{-1}^{1} du \frac{u}{\sqrt{1-u^2}} \int_{-1}^{1} du' \frac{u'}{\sqrt{1-(u')^2}} g(kW|u-u'|) \tag{3-46}$$

By straightforward integration, we have

$$\int_{-1}^{1} \sqrt{1-u^2}\, du = \pi/2 \tag{3-47}$$

$$\int_{-1}^{1} u^2\sqrt{1-u^2}\, du = \pi/8 \tag{3-48}$$

$$\int_{-1}^{1} \frac{u^2}{\sqrt{1-u^2}}\, du = \pi/2 \tag{3-49}$$

It is evident from [14,Eqs.(A6a) and (A6c)] that

$$\int_{-1}^{1} \sqrt{1-u'^2}\,\log|u-u'|\,du' = \frac{\pi}{2}\,(u^2 - 1/2 - \log 2) \qquad (3\text{-}50)$$

It is evident from [14,Eq.(A6b)] that

$$\int_{-1}^{1} \frac{u'}{\sqrt{1-(u')^2}}\log|u-u'|\,du' = -\pi u \qquad (3\text{-}51)$$

Thanks to (3-47), (3-48), and (3-50), I_1 of (3-45) becomes

$$I_1 = \pi^2/4 + j\pi(1/4 - \log(\tau kW/4))/2 \qquad (3\text{-}52)$$

Thanks to (3-49) and (3-51), I_2 of (3-46) becomes

$$I_2 = j\pi \qquad (3\text{-}53)$$

Now, $2k\eta Y^{nn}_{11}$ is given by (3-40) where U_1 and U_2 are obtained from (3-43) and (3-44) in which the explicit integrals are evaluated by the two-dimensional Gaussian quadrature method, and I_1 and I_2 are given by (3-52) and (3-53).

c) Evaluation of ΔY^{a}_{mn} of (2-53) and ΔY^{b}_{mn} of (2-54)

Replacing the surface integrals in (2-53) and (2-54) by line integrals over the contour ($x=0, |y| \le W$) of the shorting strip, we obtain

$$\Delta Y^{a}_{mn} = \sum_{j=1}^{N} I^{a}_{jn}\, C^{a}_{jm} \qquad (3\text{-}54)$$

$$\Delta Y^{b}_{mn} = \sum_{j=1}^{N} I^{b}_{jn}\, C^{b}_{jm} \tag{3-55}$$

where

$$C^{a}_{jm} = -\int_{t_L}^{t_{L+M}} \underline{M}_m(t) \cdot \underline{H}^{-}_{e}(\underline{J}^{a}_{j},\underline{\emptyset})\, dt \tag{3-56}$$

$$C^{b}_{jm} = -\int_{t_L}^{t_{L+M}} \underline{M}_m(t) \cdot \underline{H}^{+}_{e}(\underline{J}^{b}_{j},\underline{\emptyset})\, dt \tag{3-57}$$

Substitution of (3-2) into (3-56) and (3-57) yields

$$C^{a}_{jm} = -\int_{t_L}^{t_{L+M}} \underline{M}_m(t) \cdot \underline{H}^{-}_{e}(\underline{J}_{j},\underline{\emptyset})\, dt \tag{3-58}$$

$$C^{b}_{jm} = -\int_{t_L}^{t_{L+M}} \underline{M}_m(t) \cdot \underline{H}^{+}_{e}(\underline{J}_{j},\underline{\emptyset})\, dt \tag{3-59}$$

First substituting (3-30) into (3-6), then substituting (3-6) into (3-58) and (3-59), and finally noting that $\underline{J}_j(t)$ is on the shorting strip ($t_L < t < t_{L+M}$) only when $j \geq L$, we obtain

$$C^{a}_{jm} = C^{b}_{jm} = \frac{jk}{4}\int_{t_L}^{t_{L+M}} dt\ \underline{M}_m(t)\cdot\int_{\emptyset}^{t_{L+M}} dt'(\underline{J}_j(t')\times(\rho-\rho'))\frac{H_1^{(2)}(k|\rho-\rho'|)}{|\rho-\rho'|}$$

$$j=1,2,\ldots,L-1 \tag{3-60}$$

$$C^{a}_{jm} = -C^{b}_{jm} = -\frac{1}{2}\int_{t_L}^{t_{L+M}} \underline{M}_m(t)\cdot(\underline{J}_j(t)\times\underline{n})\, dt$$

$$,j=L,L+1,\ldots,N \tag{3-61}$$

If, after interchanging t and t' in (3-60), we interchange the order of integration in (3-60), then it is evident from comparison with (3-32) that

$$\overset{a}{C}_{jm} = \overset{b}{C}_{jm} = \frac{1}{2} V_{jm} \quad , j=1,2,\ldots,L-1 \tag{3-62}$$

Since $\underline{J}_j(t)$ is given by (3-3) and $\underline{M}_m$ is $\underline{M}_1$ of (3-27), (3-62) specializes to

$$\overset{a}{C}_{j1} = \overset{b}{C}_{j1} = \frac{1}{2} V_{j1} \quad , j=1,2,\ldots,L-1 \tag{3-63}$$

where V_{j1} is given by (3-34). Substituting (3-3) and (3-27) into (3-61) and introducing the new variable of integration u defined by (3-38), we obtain

$$\overset{a}{C}_{j1} = -\overset{b}{C}_{j1} = \frac{W}{2} \int_{u_j}^{u_{j+1}} \sqrt{1-u^2}\, du \quad , \quad j=L,L+1,\ldots,N \tag{3-64}$$

where

$$u_j = (t_j - t_L - W)/W \quad , \quad j=L,L+1,\ldots,N+1 \tag{3-65}$$

Performing the integration in (3-64), we obtain

$$\overset{a}{C}_{j1} = -\overset{b}{C}_{j1} = \frac{W}{4} \left[\sin^{-1} u + u\sqrt{1-u^2}\right]_{u_j}^{u_{j+1}} \quad , j=L,L+1,\ldots,N \tag{3-66}$$

where the principal value of $\sin^{-1}u$ is taken.

Substitution of (3-36), (3-63), and (3-66) into (3-54) and (3-55) gives

$$\overset{a}{\Delta Y}_{i1} = -\frac{1}{2} \sum_{j=1}^{L-1} I_{j1} V_{j1} + \sum_{j=L}^{N} I_{j1} \overset{a}{C}_{j1} \tag{3-67}$$

$$\Delta Y_{i1}^{b} = \frac{1}{2}\sum_{j=1}^{L-1} I_{j1}\, V_{j1} - \sum_{j=L}^{N} I_{j1}\, C_{j1}^{a} \qquad (3\text{-}68)$$

Setting m=n=1 in (2-50) and (2-51), adding them, and substituting (3-67) and (3-68), we obtain

$$Y_{i1}^{a} + Y_{i1}^{b} = 2\, Y_{i1}^{ns} + \sum_{j=1}^{L-1} I_{j1}\, V_{j1} \qquad (3\text{-}69)$$

where Y_{i1}^{ns} was evaluated in Section 3.3b, I_{j1} is the j^{th} element of the column vector $\vec{I}_1^{a} = \vec{I}_1^{b} = \vec{I}_1$ that satisfies both (2-32) and (2-41), and V_{j1} is given by (3-34) with i replaced by j.

d) Evaluation of I_m^{inc} of (2-55)

Replacing the surface integrals in (2-55) by line integrals over the contour ($x=0$, $|y| \leq W$) of the shorting strip, we obtain

$$I_m^{inc} = C_m^{inc} - \sum_{j=1}^{N} I_j^{ex}\, C_{jm}^{a} \qquad (3\text{-}70)$$

where I_j^{ex} is the j^{th} element of the column vector $\vec{I}^{ex}$ that satisfies (2-22), C_{jm}^{a} is given by (3-56), and

$$C_m^{inc} = \int_{t_L}^{t_{L+M}} \underline{M}_m \cdot \underline{H}^{inc}\, dt \qquad (3\text{-}71)$$

Substitution of (3-1) into the Maxwell equation

$$\underline{H}^{inc} = \frac{j}{k\eta} \nabla \times \underline{E}^{inc} \qquad (3\text{-}72)$$

leads to

$$\underline{H}^{inc} = \frac{1}{\eta}(-\underline{u}_x \sin\phi^i + \underline{u}_y \cos\phi^i)\, e^{jk(x\cos\phi^i + y\sin\phi^i)} \qquad (3\text{-}73)$$

where $\underline{u}_x$ is the unit vector on x axis. Substituting (3-73) into (3-71) and anticipating that $\underline{M}_m$ will lie on the y axis and have no x-component, we obtain

$$C_m^{inc} = \frac{\cos\phi^i}{\eta}\int_{t_L}^{t_{L+M}} (\underline{M}_m \cdot \underline{u}_y)\, e^{jk(t-t_L-W)\sin\phi^i}\, dt \qquad (3\text{-}74)$$

In Section 3.3c, expressions (3-61) and (3-62) were found for $C^{a}_{j,m}$.

When $\underline{M}_1$ of (3-27) is the only magnetic current expansion function, $C^{a}_{j,1}$ is given by (3-63) and (3-66) so that (3-70) becomes

$$I_1^{inc} = C_1^{inc} - \frac{1}{2}\sum_{j=1}^{L-1} I_j V^{ex}_{j,1} - \sum_{j=L}^{N} I_j C^{a}_{j,1} \qquad (3\text{-}75)$$

where $C^{a}_{j,1}$ is given by (3-66) and, as obtained by substituting (3-27) into (3-74) and introducing the new variable of integration u defined by (3-38),

$$C_1^{inc} = \frac{W}{\eta}\cos\phi^i \int_{-1}^{1} \sqrt{1-u^2}\, \cos(kWu\sin\phi^i)\, du \qquad (3\text{-}76)$$

e) Summary

When $\underline{M}_1$ of (3-27) is the only magnetic current expansion function, the matrix equation (2-9) reduces to the single algebraic equation

$$(Y_{11}^{a} + Y_{11}^{b}) V_1 = I_1^{inc} \qquad (3\text{-}77)$$

Substituting (3-69) and (3-75) into (3-77) and solving for V_1, we obtain

$$V_1 = \frac{C_1^{inc} - \sum_{j=1}^{N} I_j^{ex} C_{j1}^{a}}{2 Y_{11}^{hs} + \sum_{j=1}^{L-1} I_{j1} V_{j1}} \qquad (3\text{-}78)$$

where I_j^{ex} is the j^{th} element of the column vector $\vec{I}^{ex}$ that satisfies (2-22), V_{j1} is given by (3-34) with i replaced by j, I_{j1} is the j^{th} element of the column vector $\vec{I}_1^{a} = \vec{I}_1^{b} = \vec{I}_1$ that satisfies both (2-32) and (2-41), Y_{11}^{hs} is given by (3-40), C_{j1}^{a} is given by (3-63) and (3-66), and C_1^{inc} is given by (3-76).

Thus, when $\underline{M}_1(t)$ of (3-27) is the only magnetic current expansion function, the constants I_j^{ex}, I_{j1}^{a}, I_{j1}^{b}, and V_1 in (2-46)-(2-49) can be evaluated. The fields $\underline{E}^{inc}$ and $\underline{H}^{inc}$ are given by (3-1) and (3-73), respectively. The remaining fields in (2-46)-(2-49) are due to the sources $\underline{J}_j^{a}$ and $\underline{J}_j^{b}$ defined by (3-2) and (3-3) and $2\underline{M}_1$ where $\underline{M}_1$ is defined by (3-27). With the meaning of $2\underline{M}_1$ clarified in the last paragraph of Section 2.5a, these fields are given by (3-5)-(3-8). Having evaluated all quantities on the right-hand sides of (2-46)-(2-49) under the assumption that $\underline{M}_1$ of (3-27) is the only magnetic current expansion function, we have achieved our objective , which was to determine the total

fields ($\underline{E}^{inc\,a}+\underline{E}$, $\underline{H}^{inc\,a}+\underline{H}$) and ($\underline{E}^{b}$, $\underline{H}^{b}$) in regions a and b.

3.4 Several Magnetic Current Expansion Functions for the Wider Slot

In this Section, we assume that the width of the slot is comparable to the wavelength so that several magnetic current expansion functions are needed. The slot is partitioned into at least three straight line segments of equal length ΔC. Otherwise stated,

$$t_{n+1} - t_n = \Delta C, \quad n=L,L+1,\ldots,N \tag{3-79}$$

where N is given by (3-4) in which $M \geq 3$. See Fig.5. The magnetic current expansion functions are now defined by

$$\underline{M}_1(t)=\begin{cases} \sqrt{1-((t_{L+1}-t)/\Delta C)^2}\ \underline{u}_y & t_L \leq t \leq t_{L+1} \\ \dfrac{t_{L+2}-t}{\Delta C}\ \underline{u}_y & t_{L+1} \leq t \leq t_{L+2} \\ 0 & \text{elsewhere} \end{cases} \tag{3-80}$$

$$\underline{M}_n(t)=\begin{cases} \dfrac{t-t_{L+n-1}}{\Delta C}\ \underline{u}_y & t_{L+n-1} \leq t \leq t_{L+n} \\ \dfrac{t_{L+n+1}-t}{\Delta C}\ \underline{u}_y & t_{L+n} \leq t \leq t_{L+n+1} \\ 0 & \text{elsewhere} \end{cases} \tag{3-81}$$

with $n=2,3,\ldots,M-2$

$$\underline{M}_{m-1}(t)=\begin{cases}\dfrac{t-t_{L+m-2}}{\Delta C}\,\underline{u}_y & t_{L+m-2}\le t\le t_{L+m-1}\\ \sqrt{1-((t-t_{L+m-1})/\Delta C)^2}\;\underline{u}_y & t_{L+m-1}\le t\le t_{L+m}\\ \emptyset & \text{elsewhere}\end{cases} \tag{3-82}$$

If M=3, then (3-81) is to be discarded. The expansion functions (3-80)-(3-82) are continuous and have the correct behavior as t approaches t_L and as t approaches t_{L+m}.

a) Evaluation of $\overset{a}{V}_{im}$ of (2-33) and $\overset{b}{V}_{im}$ of (2-42)

Equations (3-28)-(3-32) are still valid because they were obtained without knowledge of $\underline{M}_m$. Hence, $\overset{a}{V}_{im}$ and $\overset{b}{V}_{im}$ are given by (3-28) where V_{im} is given by (3-32). Substituting (3-3) and (3-80)-(3-82) into (3-32), introducing the new variable of integration defined by (3-13), replacing the integral with respect to t' by the sum of the integrals over the two straight line segments C_{L+m-1} and C_{L+m} on which $\underline{M}_m(t')$ exists, and introducing a new variable of integration u' that goes from -1 to 1 as t' goes from the beginning to the end of the pertinent straight line segment, we obtain, for i=1,2,...,L-1,

$$V_{i1}=\frac{-jk\Delta C_\Delta C_i}{16}\left[\int_{-1}^{1}du\int_{-1}^{1}du'\sqrt{4-(1-u')^2}\,\frac{(\underline{u}_R\cdot\underline{\Gamma}_{iL}(u,u'))}{|\underline{\Gamma}_{iL}(u,u')|}H_1^{(2)}(|\underline{\Gamma}_{iL}(u,u')|)\right.$$

$$\left.+\int_{-1}^{1}du\int_{-1}^{1}du'(1-u')\frac{(\underline{u}_R\cdot\underline{\Gamma}_{i,L+1}(u,u'))}{|\underline{\Gamma}_{i,L+1}(u,u')|}H_1^{(2)}(|\underline{\Gamma}_{i,L+1}(u,u')|)\right] \tag{3-83}$$

$$V_{i,n}=\frac{k\Delta C_i\Delta C_i}{j16}\left\{\int_{-1}^{1}du\int_{-1}^{1}du'(1+u')\frac{(\underline{u}_w\cdot\underline{\Gamma}_{i,L+n-1}(u,u'))}{|\underline{\Gamma}_{i,L+n-1}(u,u')|}H_1^{(e)}(|\underline{\Gamma}_{i,L+n-1}(u,u')|)\right.$$

$$\left.+\int_{-1}^{1}du\int_{-1}^{1}du'(1-u')\frac{(\underline{u}_w\cdot\underline{\Gamma}_{i,L+n}(u,u'))}{|\underline{\Gamma}_{i,L+n}(u,u')|}H_1^{(e)}(|\underline{\Gamma}_{i,L+n}(u,u')|)\right\}$$

$$, \quad n=2,3,\ldots,M-2 \tag{3-84}$$

$$V_{i,M-1}=-\frac{jk\Delta C\Delta C_i}{16}\left|\int_{-1}^{1}du\int_{-1}^{1}du'(1+u')\frac{(\underline{u}_w\cdot\underline{\Gamma}_{i,L+M-2}(u,u'))}{|\underline{\Gamma}_{i,L+M-2}(u,u')|}H_1^{(e)}(|\underline{\Gamma}_{i,L+M-2}(u,u')|)\right.$$

$$\left.+\int_{-1}^{1}du\int_{-1}^{1}du'\sqrt{4-(1+u')^2}\frac{(\underline{u}_w\cdot\underline{\Gamma}_{i,L+M-1}(u,u'))}{|\underline{\Gamma}_{i,L+M-1}(u,u')|}H_1^{(e)}(|\underline{\Gamma}_{i,L+M-1}(u,u')|)\right| \tag{3-85}$$

where $\underline{\Gamma}_{i,j}(u,u')$ is given by (3-18). From (3-32), we have

$$V_{i,n}=\emptyset \quad \begin{cases} i=L,L+1,\ldots,N \\ n=1,2,\ldots,M-1 \end{cases} \tag{3-86}$$

Knowing the elements of Z^a, Z^b, $\vec{V}^a_n$, and $\vec{V}^b_n$, we can solve (2-32) for $\vec{I}^a_n$ and (2-41) for $\vec{I}^b_n$. Because of (3-9) and (3-28), the solution $\vec{I}^a_n$ to (2-32) is the same as the solution $\vec{I}^b_n$ to (2-41). Calling this common solution $\vec{I}_n$, we write

$$I^a_{j,n}=I^b_{j,n}=I_{j,n} \tag{3-87}$$

b) Evaluation of Y^{ba}_{mn} of (2-52)

Equation (3-37) is still valid because it was obtained without knowledge of $\underline{M}_m$ and $\underline{M}_n$. Substituting (3-80)-(3-82) into (3-37), replacing the integral with respect to t' by the sum of the integrals over the two straight line segments C_{L+n-1} and C_{L+n} on which $\underline{M}_n(t')$ exists, introducing a new variable of integration v' that goes from 0 to 1 as t' goes from one end to the other end of the straight line segment, and dealing similarly with the integral with respect to t to introduce a corresponding variable of integration v, we find that the first row of Y^{ne} is given by

$$
\begin{aligned}
2k\eta Y_{11}^{ne} = (k\Delta C)^2 \Bigg[& \int_0^1 dv \sqrt{1-v^2} \int_0^1 dv' \sqrt{1-v'^2}\, H_0^{(2)}(k\Delta C|v-v'|) \\
& + 2\int_0^1 dv\, v \int_0^1 dv' \sqrt{1-v'^2}\, H_0^{(2)}(k\Delta C|v-v'-1|) \\
& + \int_0^1 dv\, v \int_0^1 dv' v'\, H_0^{(2)}(k\Delta C|v-v'|) \Bigg] \\
& - \int_0^1 dv \frac{v}{\sqrt{1-v^2}} \int_0^1 dv' \frac{v'}{\sqrt{1-v'^2}} H_0^{(2)}(k\Delta C|v-v'|) \\
& + 2\int_0^1 dv \int_0^1 dv' \frac{v'}{\sqrt{1-v'^2}} H_0^{(2)}(k\Delta C|v-v'-1|) - \int_0^1 dv \int_0^1 dv'\, H_0^{(2)}(k\Delta C|v-v'|)
\end{aligned}
\tag{3-88}
$$

$$
\begin{aligned}
2k\eta Y_{1n}^{ne} = (k\Delta C)^2 \Bigg[& \int_0^1 dv \sqrt{1-v^2} \int_0^1 dv'\, v' \left[H_0^{(2)}(k\Delta C|v+v'+n-2|) + H_0^{(2)}(k\Delta C|v-v'+n|) \right] \\
& + \int_0^1 dv\, v \int_0^1 dv'\, v' \left[H_0^{(2)}(k\Delta C|v+v'+n-3|) + H_0^{(2)}(k\Delta C|v-v'+n-1|) \right] \Bigg] \\
& - \int_0^1 dv \frac{v}{\sqrt{1-v^2}} \int_0^1 dv' \left[H_0^{(2)}(k\Delta C|v+v'+n-2|) - H_0^{(2)}(k\Delta C|v-v'+n|) \right]
\end{aligned}
$$

$$+\int_0^1 dv \int_0^1 dv' \; [H_o^{(e)}(k\Delta C|v+v'+n-3|) - H_o^{(e)}(k\Delta C|v-v'+n-1|)\;]$$

$$n=2,3,\ldots,M-2 \qquad (3\text{-}89)$$

$$2k\eta Y_{1,M-1}^{ne} = (k\Delta C)^e \Bigg[\int_0^1 dv\sqrt{1-v^2} \int_0^1 dv'\sqrt{1-v'^2}\, H_o^{(e)}(k\Delta C|v+v'+M-2|)$$

$$+\int_0^1 dv\; v \int_0^1 dv'\; v' H_o^{(e)}(k\Delta C|v+v'+M-4|)$$

$$+2\int_0^1 dv\; v \int_0^1 dv'\sqrt{1-v'^2}\; H_o^{(e)}(k\Delta C|v+v'+M-3|)\;\Bigg]$$

$$+\int_0^1 dv \frac{v}{\sqrt{1-v^2}} \int_0^1 dv' \frac{v'}{\sqrt{1-v'^2}} H_o^{(e)}(k\Delta C|v+v'+M-2|)$$

$$+\int_0^1 dv \int_0^1 dv'\; H_o^{(e)}(k\Delta C|v+v'+M-4|) \qquad (3\text{-}90)$$

$$-2\int_0^1 dv \int_0^1 dv' \frac{v'}{\sqrt{1-v'^2}} H_o^{(e)}(k\Delta C|v+v'+M-3|)$$

and that the "internal" elements of Y^{ne} are given by

$$2k\eta Y_{mn}^{ne} = (k\Delta C)^e \Bigg[\int_0^1 dv\; v \int_0^1 dv'\; v' [\, H_o^{(e)}(k\Delta C|v-v'+m-n|)$$

$$+ H_o^{(e)}(k\Delta C|v-v'+n-m|)\;]$$

$$+\int_0^1 dv\; v \int_0^1 dv'\; v' [H_o^{(e)}(k\Delta C|v+v'+m-n-2|) + H_o^{(e)}(k\Delta C|v+v'+n-m-2|)\;]$$

$$-\int_0^1 dv \int_0^1 dv' \; [\, H_o^{(e)}(k\Delta C|v-v'+m-n|) + H_o^{(e)}(k\Delta C|v-v'+n-m|)\;] \qquad (3\text{-}91)$$

$$+\int_0^1 dv \int_0^1 dv' \; [\, H_o^{(e)}(k\Delta C|v+v'+m-n-2|) + H_o^{(e)}(k\Delta C|v+v'+n-m-2|)\;]$$

with $m=2,3,\ldots,M-2$, and $n=2,3,\ldots,M-2$.

Since t and t' can be interchanged without affecting $|\rho-\rho'|$ in (3-37), Y^{hs} is symmetric.

$$Y^{hs}_{mn} = Y^{hs}_{nm} \tag{3-92}$$

If both $\underline{M}_m$ and $\underline{M}_n$ are reflected about the xz plane, then Y^{hs}_{mn} does not change. Since the reflection of $\underline{M}_m$ is $\underline{M}_{M-m}$ and that of $\underline{M}_n$ is $\underline{M}_{M-n}$, it is evident that

$$Y^{hs}_{M-m,M-n} = Y^{hs}_{mn} \tag{3-93}$$

From (3-92) and (3-93), we obtain

$$\left.\begin{aligned} Y^{hs}_{n1} &= Y^{hs}_{1n} \\ Y^{hs}_{M-1,n} &= Y^{hs}_{1,M-n} \\ Y^{hs}_{n,M-1} &= Y^{hs}_{1,M-n} \end{aligned}\right\} \quad n=1,2,\ldots,M-1 \tag{3-94}$$

Therefore, the first column, the last row, and the last column of Y^{hs} can all be generated from the first row of Y^{hs} given by (3-88)-(3-90). It is not necessary to compute all the internal elements of Y^{hs} because, as given by (3-91), they depend only on $|m-n|$ rather than on m and n individually.

Each integral in (3-88)-(3-91) whose integrand does not have any singularity interior to the region of integration is evaluated by the method of two-dimensional Gaussian quadrature. Each integral that has a singularity interior to the region of integration is treated in Appendix A by

"subtracting out" the singularity before applying the method of two-dimensional Gaussian quadrature.

c) Evaluation of $\overset{a}{\Delta Y_{mn}}$ of (2-53) and $\overset{b}{\Delta Y_{mn}}$ of (2-54)

What was done in the first two paragraphs of Section 3.3c is still valid because it was accomplished without knowledge of the magnetic current expansion functions. In those two paragraphs, we found that $\overset{a}{\Delta Y_{mn}}$ and $\overset{b}{\Delta Y_{mn}}$ are given by (3-54) and (3-55) where $\overset{a}{C_{jm}}$ and $\overset{b}{C_{jm}}$ are given by (3-62) and (3-61).

Since $\underline{J}_j(t)$ is given by (3-3) and $\underline{M}_m$ is given by (3-80)-(3-82), (3-62) specializes to

$$\overset{a}{C_{jm}} = \overset{b}{C_{jm}} = \frac{1}{2} V_{jm} \quad , \begin{cases} j=1,2,\ldots,L-1 \\ m=1,2,\ldots,M-1 \end{cases} \tag{3-95}$$

where V_{jm} is given by (3-83)-(3-85). Substituting (3-3) and (3-80)-(3-82) into (3-61) and evaluating the resulting integrals, we obtain

$$\left.\begin{aligned} \overset{a}{C_{L,1}} &= -\overset{b}{C_{L,1}} = \frac{\pi\Delta C}{8} \\ \overset{a}{C_{L+1,1}} &= -\overset{b}{C_{L+1,1}} = \frac{\Delta C}{4} \end{aligned}\right\} \tag{3-96}$$

$$\left.\begin{aligned} \overset{a}{C_{L+m-1,m}} &= -\overset{b}{C_{L+m-1,m}} = \frac{\Delta C}{4} \\ \overset{a}{C_{L+m,m}} &= -\overset{b}{C_{L+m,m}} = \frac{\Delta C}{4} \end{aligned}\right\} \quad m=2,3,\ldots,M-2 \tag{3-97}$$

$$\left.\begin{aligned} C^{a}_{L+M-2,M-1} &= -C^{b}_{L+M-2,M-1} = \frac{\Delta C}{4} \\ C^{a}_{L+M-1,M-1} &= -C^{b}_{L+M-1,M-1} = \frac{\pi \Delta C}{8} \end{aligned}\right\} \qquad (3\text{-}98)$$

The rest of the C^{a}'s and C^{b}'s, those that do not appear in (3-95)-(3-98), are zero.

Substitution of (3-87), and (3-95)-(3-98) into (3-54) and (3-55) gives

$$\Delta Y^{a}_{mn} = \frac{1}{2} \sum_{j=1}^{L-1} I_{jn} V_{jm} + \Delta Y_{mn} \qquad (3\text{-}99)$$

$$\Delta Y^{b}_{mn} = \frac{1}{2} \sum_{j=1}^{L-1} I_{jn} V_{jm} - \Delta Y_{mn} \qquad (3\text{-}100)$$

where

$$Y_{mn} = \begin{cases} \dfrac{\Delta C}{4}\left(\dfrac{\pi}{2} I_{Ln} + I_{L+1,n}\right) & ,m=1 \\ \dfrac{\Delta C}{4}\left(I_{L+m-1,n} + I_{L+m,n}\right) & ,m=2,3,\ldots,M-2 \\ \dfrac{\Delta C}{4}\left(I_{L+M-2,n} + \dfrac{\pi}{2} I_{L+M-1,n}\right) & ,m=M-1 \end{cases} \qquad (3\text{-}101)$$

Substituting (3-99) and (3-100) into the sum of (2-50) and (2-51), we obtain

$$Y^{a}_{mn} + Y^{b}_{mn} = 2\, Y^{ns}_{mn} + \sum_{j=1}^{L-1} I_{jn} V_{jm} \qquad (3\text{-}102)$$

where Y^{ns}_{mn} was evaluated in Section 3.4b, I_{jn} is the j^{th} element of the column vector $\vec{I}^{a}_{n} = \vec{I}^{b}_{n}$ that satisfies both (2-

32) and (2-41), and V_{jm} is given by (3-83)-(3-85) with i replaced by j.

d) Evaluation of I_m^{inc} of (2-55)

What was done in the first paragraph of Section 3.3d is still valid because it was accomplished without knowledge of the magnetic current expansion functions. In that paragraph, we found that I_m^{inc} is given by (3-70) in which I_j^{ex} is the j^{th} element of the column vector $\vec{I}^{ex}$ that satisfies (2-22), $\bar{C}_{jm}$ is given by (3-56), and C_m^{inc} is given by (3-74)

When the magnetic current expansion functions are given by (3-80)-(3-82), the non-zero $\bar{C}_{jm}$'s are given by (3-95)-(3-98) so that (3-70) becomes

$$I_m^{inc} = C_m^{inc} - \frac{1}{2}\sum_{j=1}^{L-1} I_j^{ex} V_{jm} - \begin{cases} \frac{\Delta C}{4}\left(\frac{\pi}{2} I_L^{ex} + I_{L+1}^{ex}\right), & m=1 \\ \frac{\Delta C}{4}\left(I_{L+m-1}^{ex} + I_{L+m}^{ex}\right), & m=2,3,\ldots,M-2 \\ \frac{\Delta C}{4}\left(I_{L+M-2}^{ex} + \frac{\pi}{2} I_{L+M-1}^{ex}\right), & m=M-1 \end{cases} \quad (3\text{-}103)$$

Substituting (3-80)-(3-82) into (3-74), we obtain

$$C_1^{inc} = \frac{\Delta C \cos\phi_1}{\eta} e^{j(\phi_1+\phi_2)} \left[\int_0^1 \frac{1}{\sqrt{1-v^2}} e^{-j\phi_1 v} dv + e^{j\phi_1} \int_0^1 v\, e^{-j\phi_1 v} dv \right] \quad (3\text{-}104)$$

$$C_m^{inc} = \frac{\Delta C \cos\phi^i}{\eta} e^{j(m\phi_1+\phi_2)} \left[e^{-j\phi_1} \int_{\emptyset}^{1} \frac{1}{v} e^{j\phi_1 v} dv + e^{j\phi_1} \int_{\emptyset}^{1} \frac{1}{v} e^{-j\phi_1 v} dv \right] \quad (3\text{-}105)$$

$$, \; m=2,3,\ldots,M-2$$

$$C_{M-1}^{inc} = \frac{\Delta C \cos\phi^i}{\eta} e^{j((M-1)\phi_1+\phi_2)} \left[\int_{\emptyset}^{1} \frac{1}{\sqrt{1-v^2}} e^{j\phi_1 v} dv + e^{-j\phi_1} \int_{\emptyset}^{1} \frac{1}{v} e^{j\phi_1 v} dv \right] \quad (3\text{-}106)$$

where

$$\phi_1 = k\Delta C \sin\phi^i \quad (3\text{-}107)$$

$$\phi_2 = - KW \sin\phi^i \quad (3\text{-}108)$$

If $\sin\phi^i \neq \emptyset$, then $\phi_1 \neq \emptyset$ and, thanks to [15,Formula 567.1.], (3-104)-(3-106) become

$$C_1^{inc} = \frac{\Delta C \cos\phi^i}{\eta} e^{j(\phi_1+\phi_2)} \left[\int_{\emptyset}^{1} \frac{1}{\sqrt{1-v^2}} e^{-j\phi_1 v} dv + \frac{1-\cos\phi_1 + j(\phi_1-\sin\phi_1)}{\phi_1^2} \right] \quad (3\text{-}109)$$

$$C_m^{inc} = \frac{2\Delta C \cos\phi^i}{\eta \, \phi_1^2} e^{j(m\phi_1+\phi_2)} \left[1-\cos\phi_1 \right] \quad ,m=2,3,\ldots,M-2 \quad (3\text{-}110)$$

$$C_{M-1}^{inc} = \frac{\Delta C \cos\phi^i}{\eta} e^{j((M-1)\phi_1+\phi_2)} \left[\int_{\emptyset}^{1} \frac{1}{\sqrt{1-v^2}} e^{j\phi_1 v} dv + \frac{1-\cos\phi_1 - j(\phi_1-\sin\phi_1)}{\phi_1^2} \right] \quad (3\text{-}111)$$

If $\sin\phi^{i} = 0$, then $\phi_1 = \phi_M = 0$ and (3-104)-(3-106) reduce to

$$C_1^{inc} = \frac{\Delta C \cos\phi^{i}}{2\eta}\left(1 + \frac{\pi}{2}\right) \qquad (3\text{-}112)$$

$$C_m^{inc} = \frac{\Delta C \cos\phi^{i}}{\eta}, \quad m=2,3,\ldots,M-2 \qquad (3\text{-}113)$$

$$C_{M-1}^{inc} = C_1^{inc} \qquad (3\text{-}114)$$

Now, I_m^{inc} of (2-55) is given by (3-103) in which I_j^{ex} is the j^{th} element of the column vector $\vec{I}^{ex}$ that satisfies (2-22), V_{jm} is given by (3-83)-(3-85), and C_m^{inc} is given by either (3-109)-(3-111) or (3-112)-(3-114).

e) Summary

Substituting (3-102) and (3-103) into (2-9), we can solve (2-9) for $\vec{V}$, whose n^{th} element V_n appears in (2-46)-(2-49). Of the remaining constants in (2-46)-(2-49), I_j^{ex} is the j^{th} element of the column vector $\vec{I}^{ex}$ that satisfies (2-22), and I_{jn}^{a} and I_{jn}^{b} are given by (3-87) in which I_{jn} is the j^{th} element of the column vector $\vec{I}^{a} = \vec{I}^{b} = \vec{I}$ that satisfies both (2-32) and (2-41).

Thus, when the magnetic current expansion functions are given by (3-80)-(3-82), the constants V_n, I_j^{ex}, I_{jn}^{a}, and I_{jn}^{b} in (2-46)-(2-49) can be evaluated. The fields $\underline{E}^{inc}$ and $\underline{H}^{inc}$ are given by (3-1) and (3-73), respectively. The remaining fields in (2-46)-(2-49) are due to the sources $\underline{J}_j^{a}$ and $\underline{J}_j^{b}$ defined by (3-2) and (3-3) and $2\underline{M}_n$ where $\underline{M}_n$ is defined by (3-80)-(3-82). With the meaning of $2\underline{M}_n$ clarified in the last

paragraph of Section 2.5a, these fields are given by (3-5)-(3-8). Having evaluated all quantities on the right-hand sides of (2-46)-(2-49) with the magnetic current expansion functions given by (3-80)-(3-82), we have achieved our objective, which was to determine the total fields $(\underline{E}^{inc}+\underline{E}^{a},\underline{H}^{inc}+\underline{H}^{a})$ and $(\underline{E}^{b},\underline{H}^{b})$ in regions a and b.

4. NUMERICAL RESULTS AND DISCUSSION

Programs have been written in FORTRAN for both a narrow slot and a wide slot. More general than the theory presented in Sections 3.3 and 3.4, these programs apply when the wall of the cavity is finitely thick and when an additional conductor is either inside or outside the cavity. A report on the usage of the programs is in preparation. Since the magnetic current (or the aperture field) is our main interest, it has been computed for different widths of the aperture, different sizes of the cavity and different angles of incidence. Some far field patterns are also computed.

4.1 Remarks and Definitions

The numerical results presented in this report are all for the case where the uniform TM plane wave given in (3-1) impinges on the aperture with the incident angle ϕ^i being defined in Fig.5. We decided to plot the magnitude of the magnetic current versus the position in the aperture since our computations show that the phase of the magnetic current changes little in the aperture. All numerical integrations are performed by 10 point Gaussian quadrature.

The name pseudo-image method 1 is attached to the solution developed in Section 3.3, where only one special expansion function is used for the magnetic current. The name pseudo-image method 2 is attached to the solution developed in Section 3.4, where no less than two expansion

functions are chosen for the magnetic current. The Fourier Series method is the method presented in [13,Appendix B] for a circular cylindrical cavity with very narrow slot. The scattering method is the method used in [16] and summarized in Appendix B, where only an electric current is solved for. In the scattering method, a matrix equation is extracted from the electric field integral equation either by Galerkin's method [5,Section 1-3], or by point matching. In Galerkin's method, the symmetric product of the integral equation is taken with each expansion function. In point matching [5,Section 1-4], the integral equation is enforced at discrete points. The non-pseudo-image method is the method where the pseudo-image introduced in Section 2.5 is eliminated. This method is summarized in [13, Appendix A]. Finally, if the plots are for the pseudo-image method, then the magnetic current expansion functions used are triangles only (i.e., $M_1(t)$ of (3-80) and $M_{m-1}(t)$ of (3-82) are replaced by triangles) unless we state otherwise. The reason for this is explained in Section 4.4.

4.2 Validity of Results

We have to check whether we obtain correct and accurate results. This is not only an important task but also a difficult one since no exact solution is available to compare with. That is why we started with the simplest case: a circular cylindrical shell of zero thickness. This shell was treated by the Fourier series method in [13] where the magnetic current distribution (3-27) was on the arc in

Fig.6 instead of on the plane strip. For ease of comparison and simplicity, most of our computations are made for circular cylinders and zero thickness of the cavity wall even though the programs work for thick cylinders of arbitrary cross section. The comparison is made as follows:

It is very interesting to note the following from Figs.7-16:

a) The results obtained by the different methods are of the same order of magnitude (Fig.7). The pseudo-image methods and the Fourier series method give especially close results. For instance, at the center of the aperture the magnetic current is obtained as Ø.15234 /-1Ø3.18° by the pseudo-image method 1; Ø.15384 /-1Ø3.49° by the pseudo-image method 2, and Ø.1535 /-1Ø2.97° by the Fourier series method.

b) The scattering method yields larger results than other methods. Scattering (Galerkin's method) yields the second largest and Scattering (point matching) yields the largest. (see Figs.8-1Ø). The results obtained by the scattering methods monotonically approach the results obtained by the pseudo-image method as N increases. This is true for both a large aperture (e.g., ϕ_o=3Ø°) and a small aperture (e.g., ϕ_o=5°). (see Figs.11-16). Furthermore, Scattering (Galerkin's method) approaches faster than Scattering (point matching). (see Fig.13). The magnetic currents of both scattering methods are usually within 1Ø% of each other. Scattering (Galerkin's method) is more accurate since Galerkin's method tests the equation over an

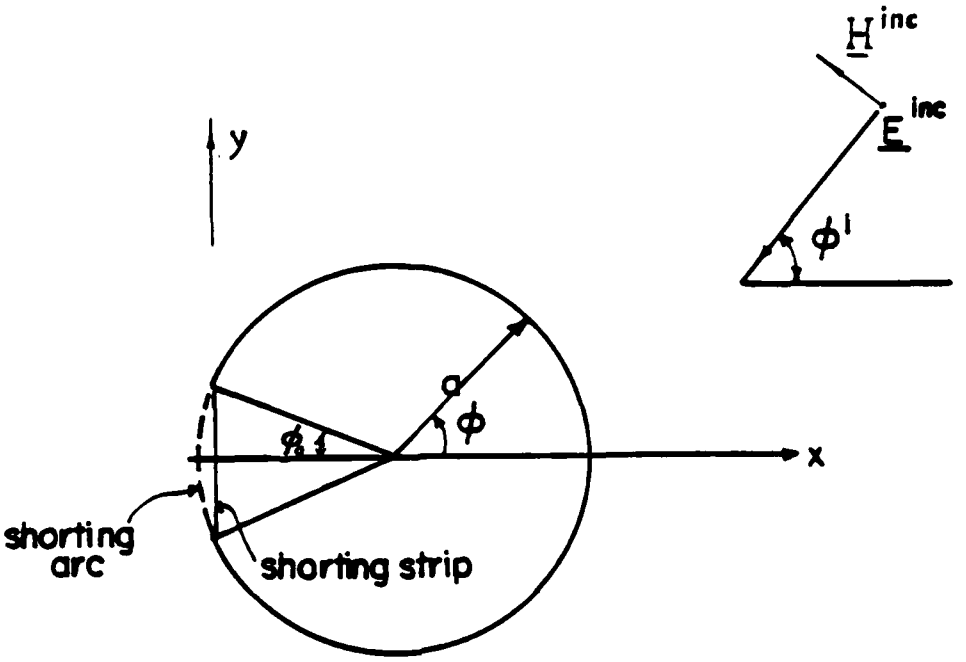

Fig. 6. An infinitely long circular cylinder with a slot. $k = \omega\sqrt{\mu\varepsilon}$ is the wavenumber and a is the radius of the circular cylinder. $-\pi + \phi_o \leq \phi \leq \pi - \phi_o$ defines the conducting part of the cylinder. The edges of the shell are at ($x = 0$, $y = \pm a \sin \phi_o$).

interval instead of at one point as point matching does [5,Sections 1-3 and 1-4].

As a further check, we compare our results with those obtained in [16] and [17] for two special cases. At the center of the aperture, the magnitudes of the electric field are obtained as: case i) Ø.31 by [16] and [17], Ø.235 by Scattering (point matching) with N=31, Ø.22 by Scattering (Galerkin's method) with N=31, and Ø.19 by the pseudo-image method with M=15 and L=18, where ϕ^i=Ø°, ϕ_o=1Ø°,and ka=1. Case ii) Ø.75 by [16] and [17], Ø.54 by Scattering (Galerkin's method) with N=31, and Ø.52 by the pseudo-image method with M=15 and L=18, where ϕ^i=Ø°, ϕ_o=3Ø°,and ka=1. ϕ^i, ϕ_o, and ka are defined in Fig.6.

In the previous paragraph, the numbers obtained in [16] and [17] are the largest. The reasons are twofold. First of all, [16] and [17] evaluate the electric field on the arc part of the cavity (Fig.6), whereas we evaluate the electric field on the plane strip connecting the cavity edges. Ours should be smaller since we are further inside the cavity. However, This should not yield a big difference when the aperture is small. Secondly, in [16] and [17] point matching is used to apply the moment method, and the integrals are approximated by the interval of integration times the integrand sampled at the center of the interval with special treatment of the singularity of the integrand. Gaussian quadrature yields results that are more accurate than those of any other technique for well behaved functions

[12]. Hence, our results should be more accurate than theirs.

On the whole,the comparisons and discussion presented above lead to the conclusion that the results we obtained are correct and that the pseudo-image method yields very accurate results.

4.3 Usefulness of the Pseudo-image

On the surface, the introduction of the pseudo-image in Section 2.5 seems a little artificial. However, as shown in Figs.17-19, the pseudo-image method does give better results than the non-pseudo-image method. First of all,the non-pseudo-image method yields unexpected overshoots near the edges. We say that they are unexpected overshoots since no other method mentioned in Section 4.1 predicts them. Secondly, the non-pseudo-image method gives larger amplitude (within 10%) but essentially the same phase for the magnetic current (within 1%).

From the results discussed in Section 4.2 and those shown in Figs.17-19, we conclude that the pseudo-image method gives a more accurate magnetic current than the non-pseudo-image method.

4.4 Edge Conditions

In Section 3.4, we have chosen the two special expansion functions $M_1(t)$ and $M_{m-1}(t)$ to obtain the proper edge behavior [14] because we initially believed that this would yield more accurate results. Alternatively, we could

use only triangle functions. For comparison we carry out both solutions. Figs. 20-22 show that the results of these two methods are very close to each other, even near the edges. Not much advantage is gained by satisfying the edge conditions in the examples we computed. The addition of the special expansion functions results in much more complicated equations, and more effort and computer time are needed.

4.5 Speed of Convergence

Given a certain size of aperture, how many expansion functions should be used? In other words, how fast do the results converge ? It can be seen from Figs.23-26 that M=10 suffices to obtain convergence for a small aperture and M=16 suffices for a large aperture. The larger M is, the smoother the plots are. Hence, as a rule of thumb, M should be large enough to obtain a smooth curve.

4.6 Other Numerical Examples

Fig.27 shows that the magnitude of the aperture field increases with the width of the aperture. Figures 28 and 29 show that oblique incidence causes noticeable asymmetry of the aperture field only when the aperture is large. Figs.30 and 31 give results for the case where the cavity wall is finitely thick (see Fig.32). It is interesting to note that the aperture field increases with the wall thickness.

The far scattered field is obtained by replacing the Hankel function by its large argument approximation [6, eq.(D-13)]. Although the aperture fields obtained by the

different methods mentioned in Section 4.1 are different, the far fields are nearly the same. Their difference is less than 1%. This is expected since the aperture field only affects the electric current in the vicinity of the aperture. However, the field inside the cavity is proportional to the aperture field. Examples of far field scattering patterns are given in Fig.33 and Fig.34. If the angle of incidence ϕ^i increases by $\delta\phi^i$, then the far field scattering pattern rotates through the angle $\delta\phi^i$ as does the scattering pattern of an infinitely long complete circular cylinder. Again, this shows that the small aperture has little effect on the far field scattering pattern.

4.7 Concluding Remarks

In this report, a new method called the pseudo-image method, incorporated in the generalized network formulation for aperture problems, is developed to accurately determine the field inside and outside a conducting cavity with a small aperture. The theory can be applied to both two and three dimensional cavities of arbitrary shape.

A number of computations have been made for an infinitely long slot in a perfectly conducting cylindrical surface illuminated by a uniform TM plane wave. The programs developed apply to a cavity with finite thickness and an additional conductor may be either inside or outside the cavity. With some modifications, the main program can apply to a multi-conductor system as well. As further work, we could solve the problem of an infinitely long cylinder with

a slot illuminated by a uniform TE plane wave instead of a uniform TM plane wave.

Finally, we should point out that, although the pseudo-image method works well for a non-resonant cavity, it fails when the cavity is resonant. There two reasons. One is that the resonant electric current on the conducting surface S_{sc} produces tangential electric field on this surface so that $\underline{J}_n^a$ can not be uniquely determined by using the electric field integral equation only [18, Section 2]. The other is that the field inside the cavity would go to infinity if the magnetic current $\underline{M}_n$ on the right hand side of the shorted aperture in Fig.4 excited the resonant mode of the cavity. A special technique has to be developed to treat the resonant cavity.

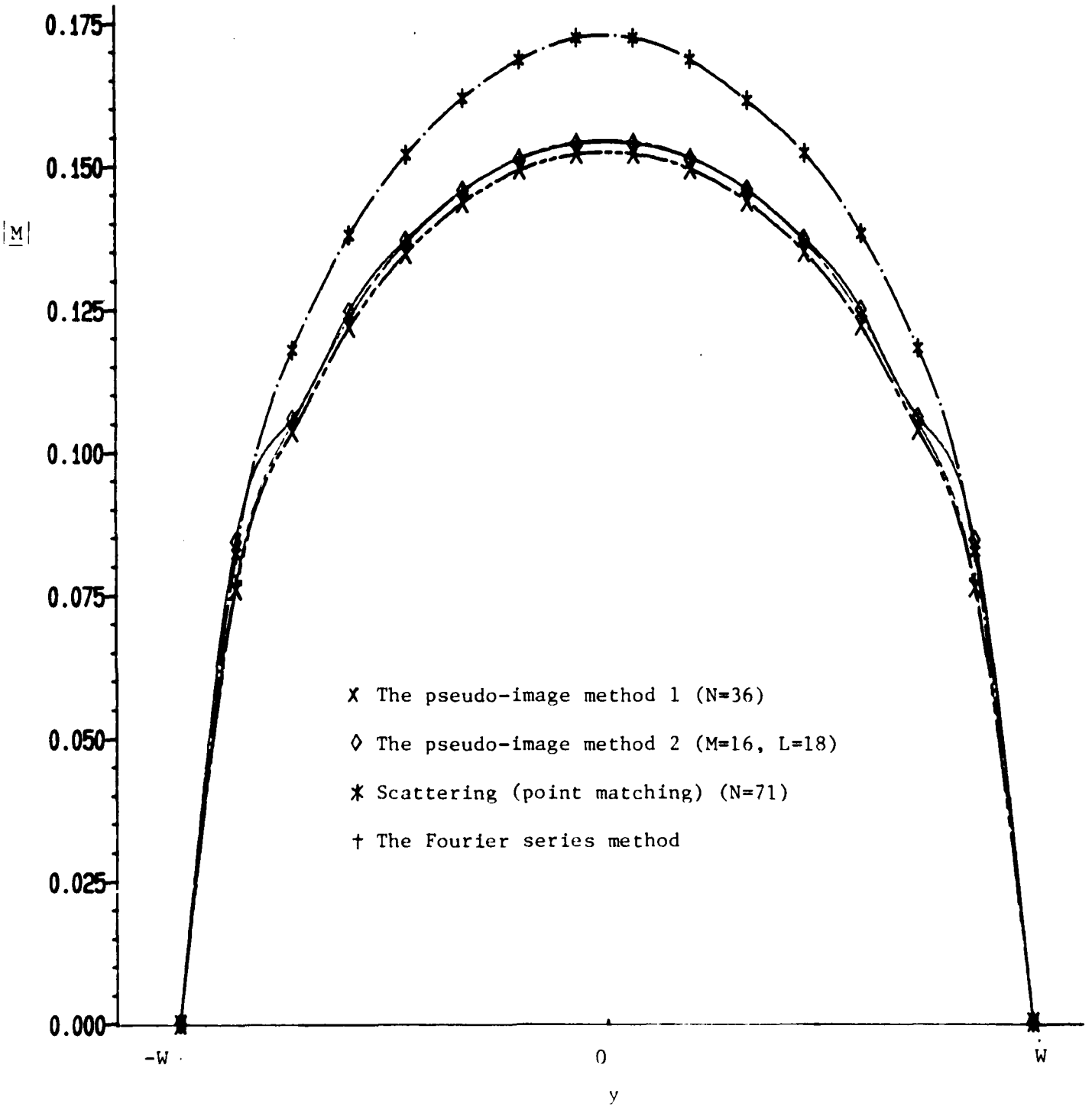

Fig. 7. The magnitude of the magnetic current in the aperture obtained by different methods for $\phi^i = 180°$, $\phi_o = 5°$, $ka = \pi/2$.

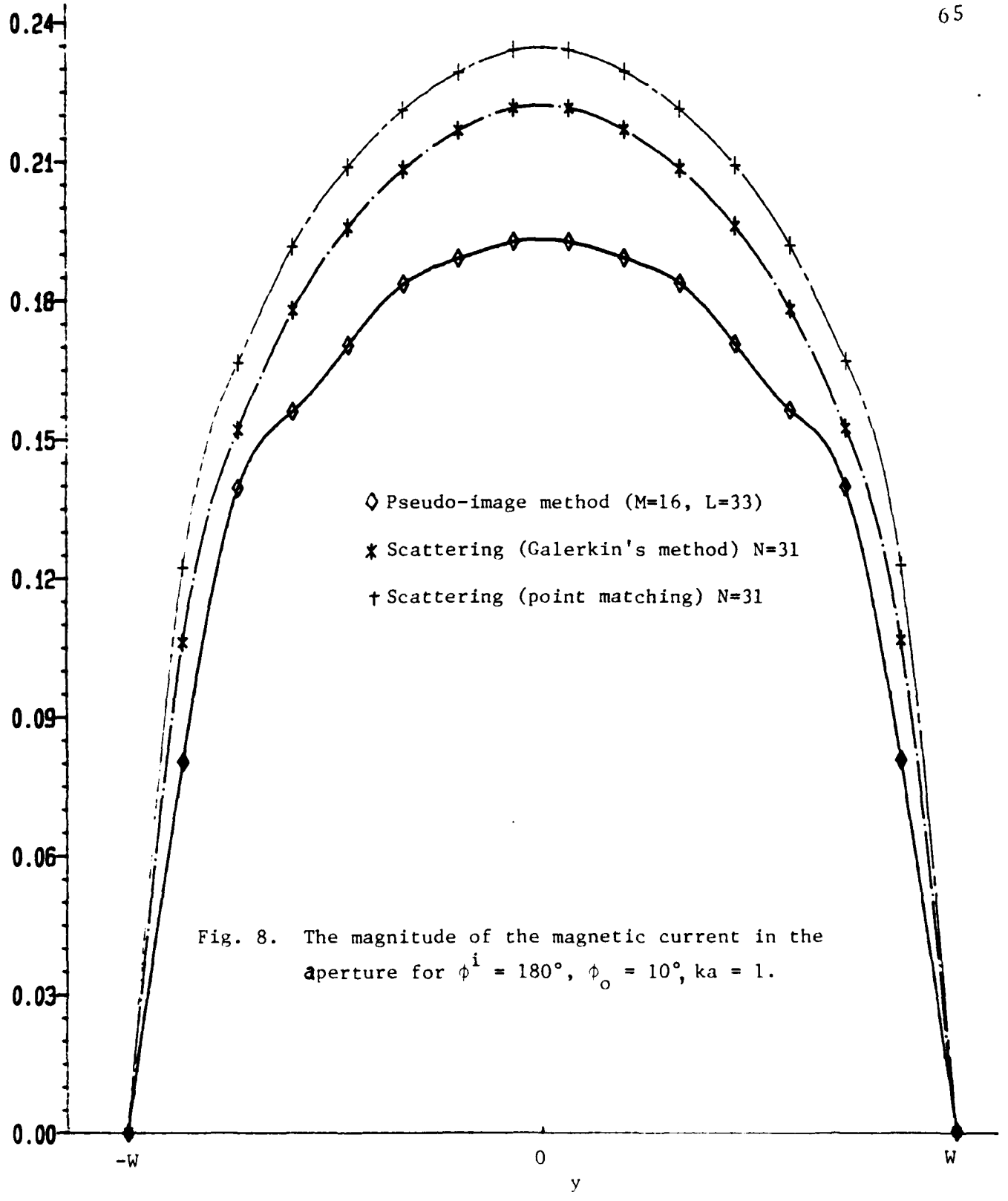

Fig. 8. The magnitude of the magnetic current in the aperture for $\phi^i = 180°$, $\phi_o = 10°$, ka = 1.

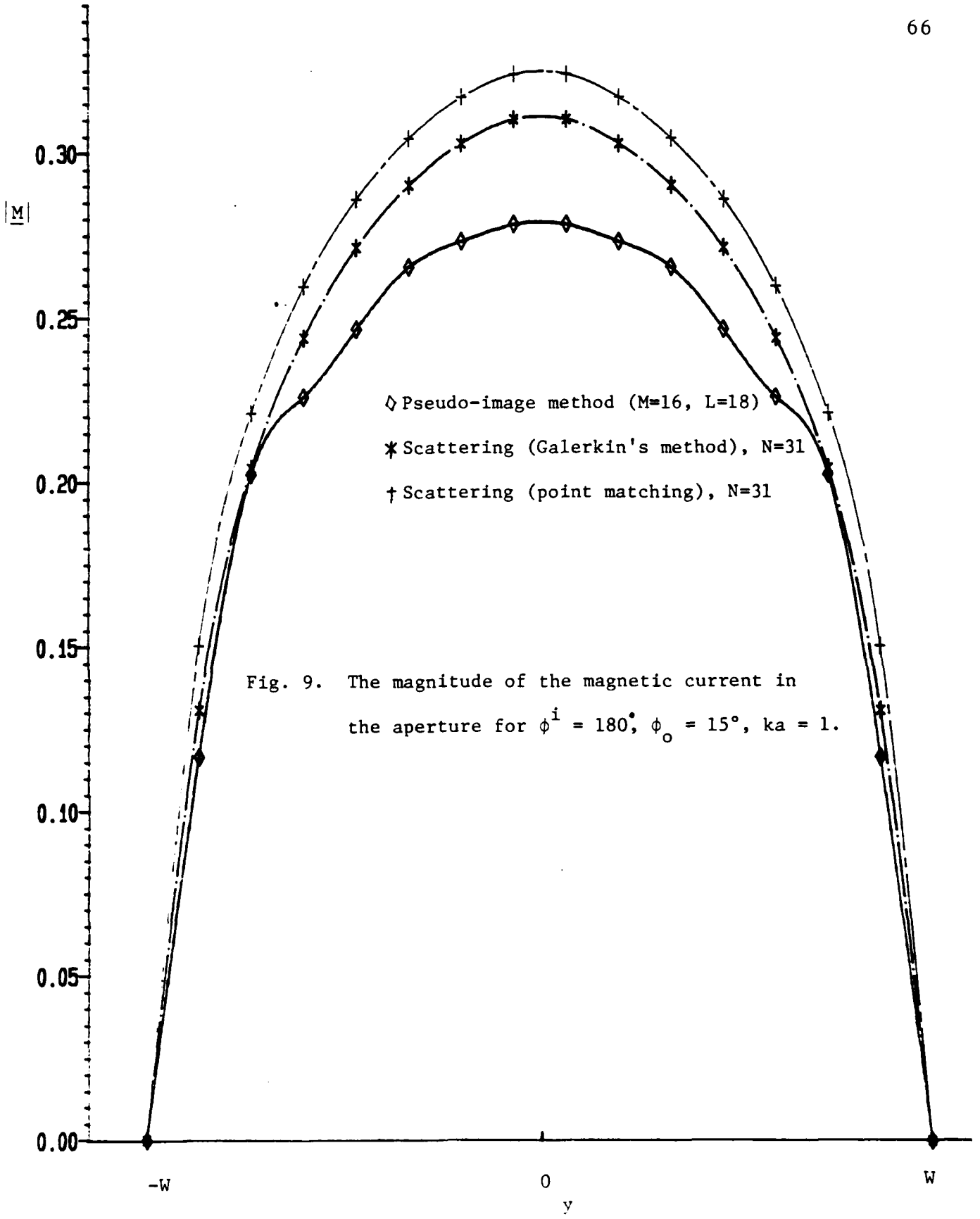

Fig. 9. The magnitude of the magnetic current in the aperture for $\phi^i = 180°$, $\phi_o = 15°$, ka = 1.

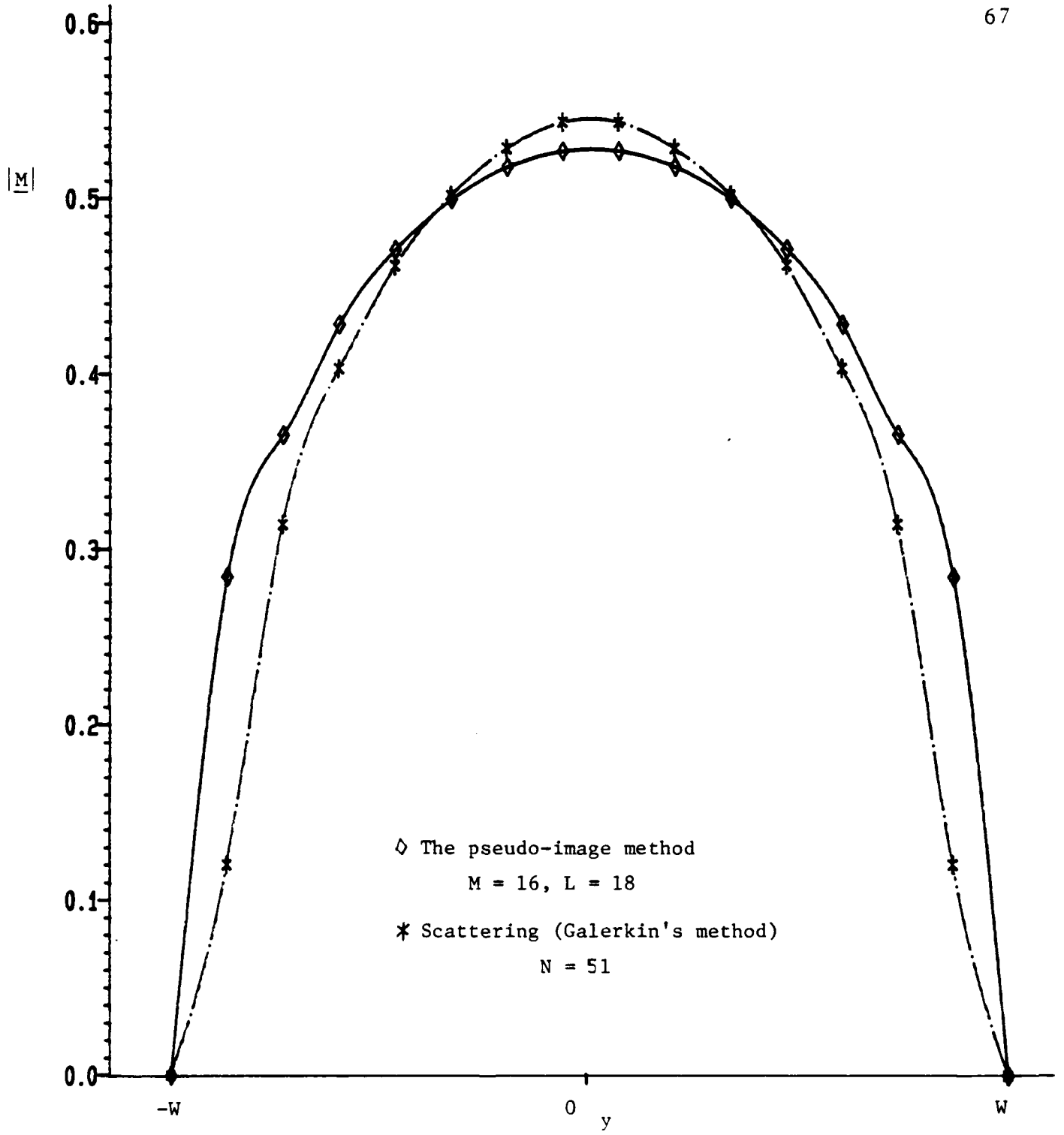

Fig. 10. The magnitude of the magnetic current in the aperture for $\phi^i = 180°$, $\phi_o = 30°$, ka = 1.

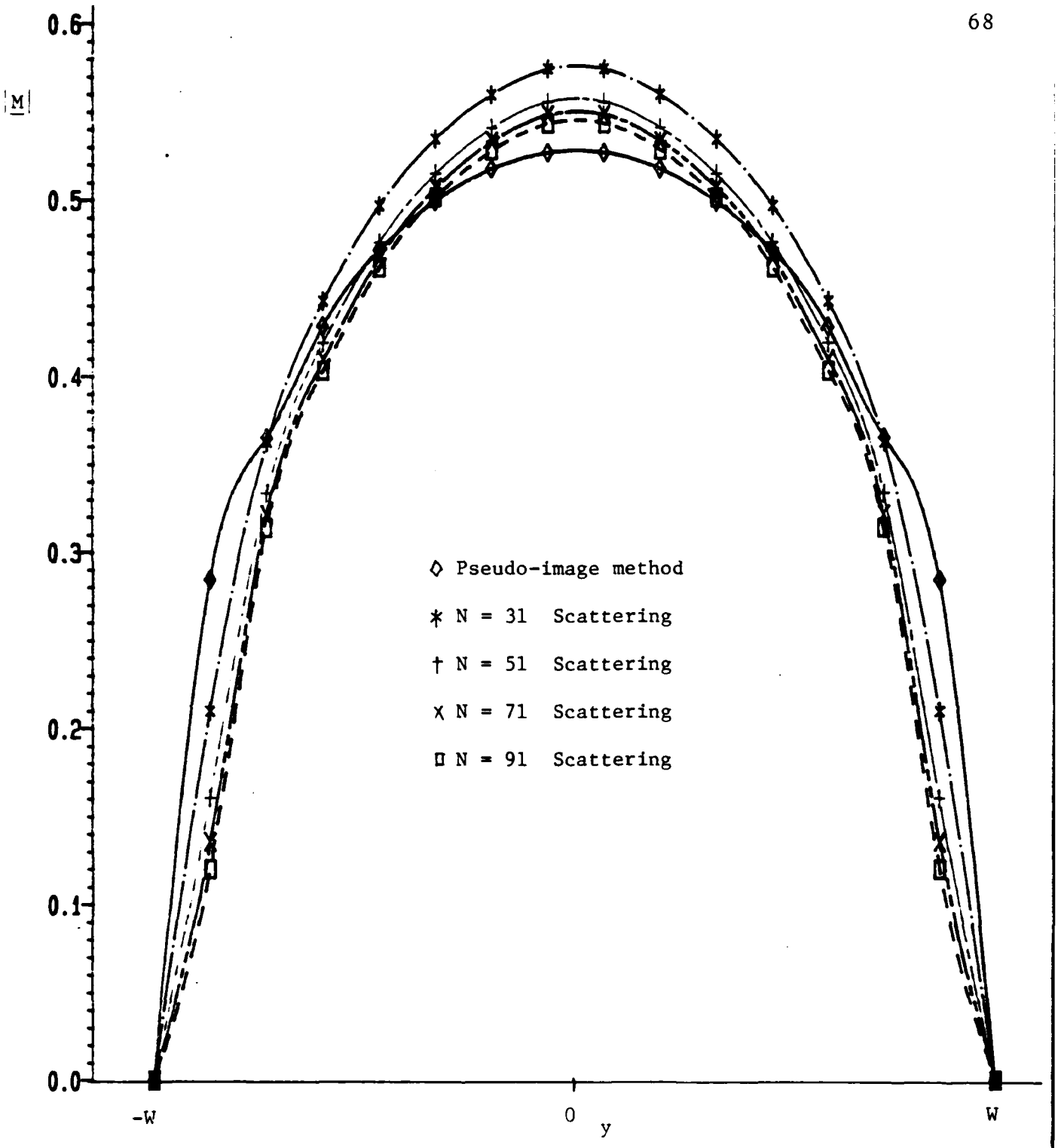

Fig. 11. The magnetic current magnitude in the aperture obtained by the pseudo-image method (M = 20, L = 18) and the scattering (point matching) method for $\phi^i = 180°$, $\phi_o = 30°$, ka = 1.

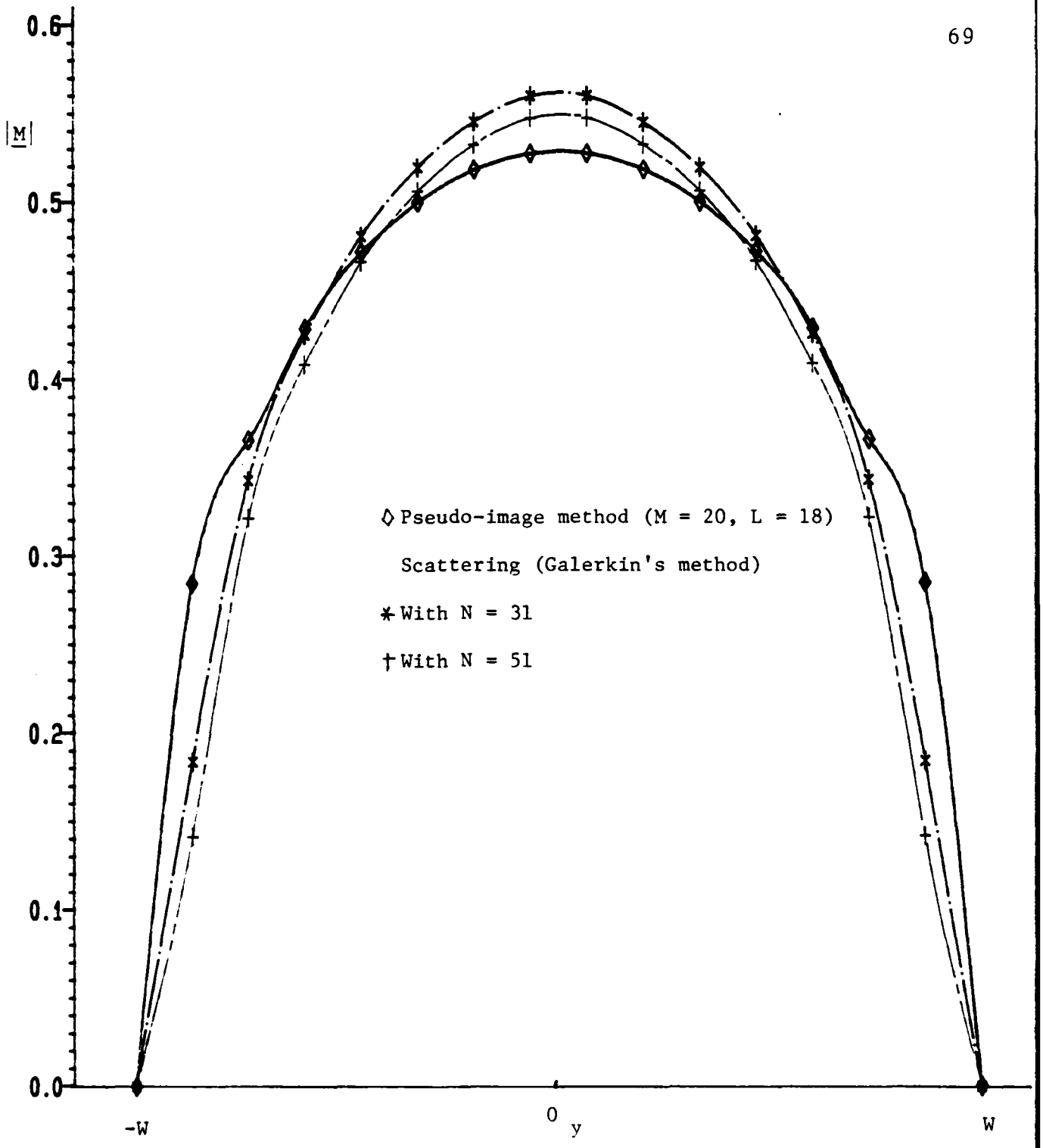

Fig. 12. The magnitude of the magnetic current in the aperture for $\phi^i = 180^\circ$, $\phi_o = 30^\circ$, ka = 1.

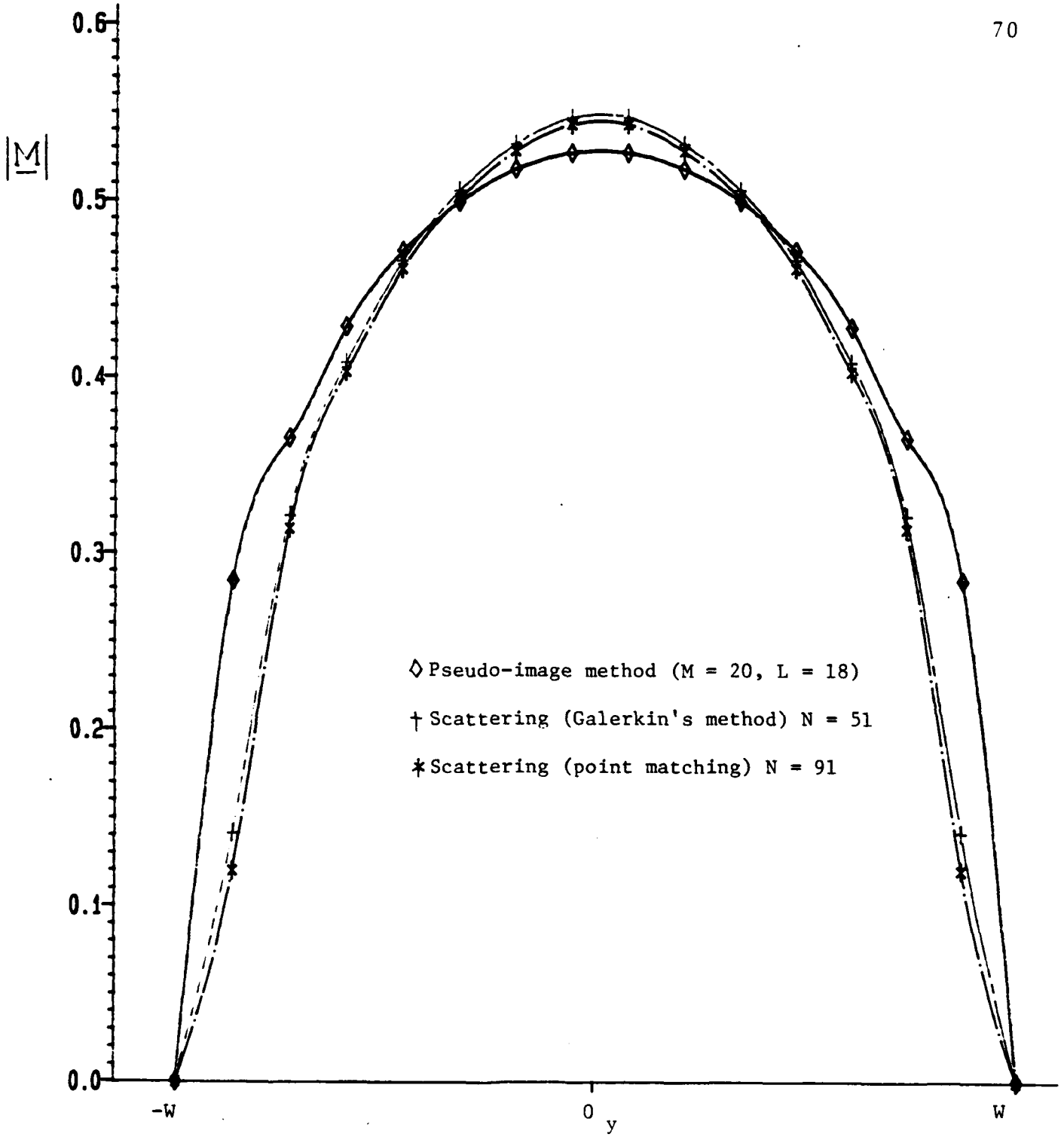

Fig. 13. The magnitude of the magnetic current in the aperture for $\phi^i = 180°$, $\phi_o = 30°$, ka = 1.

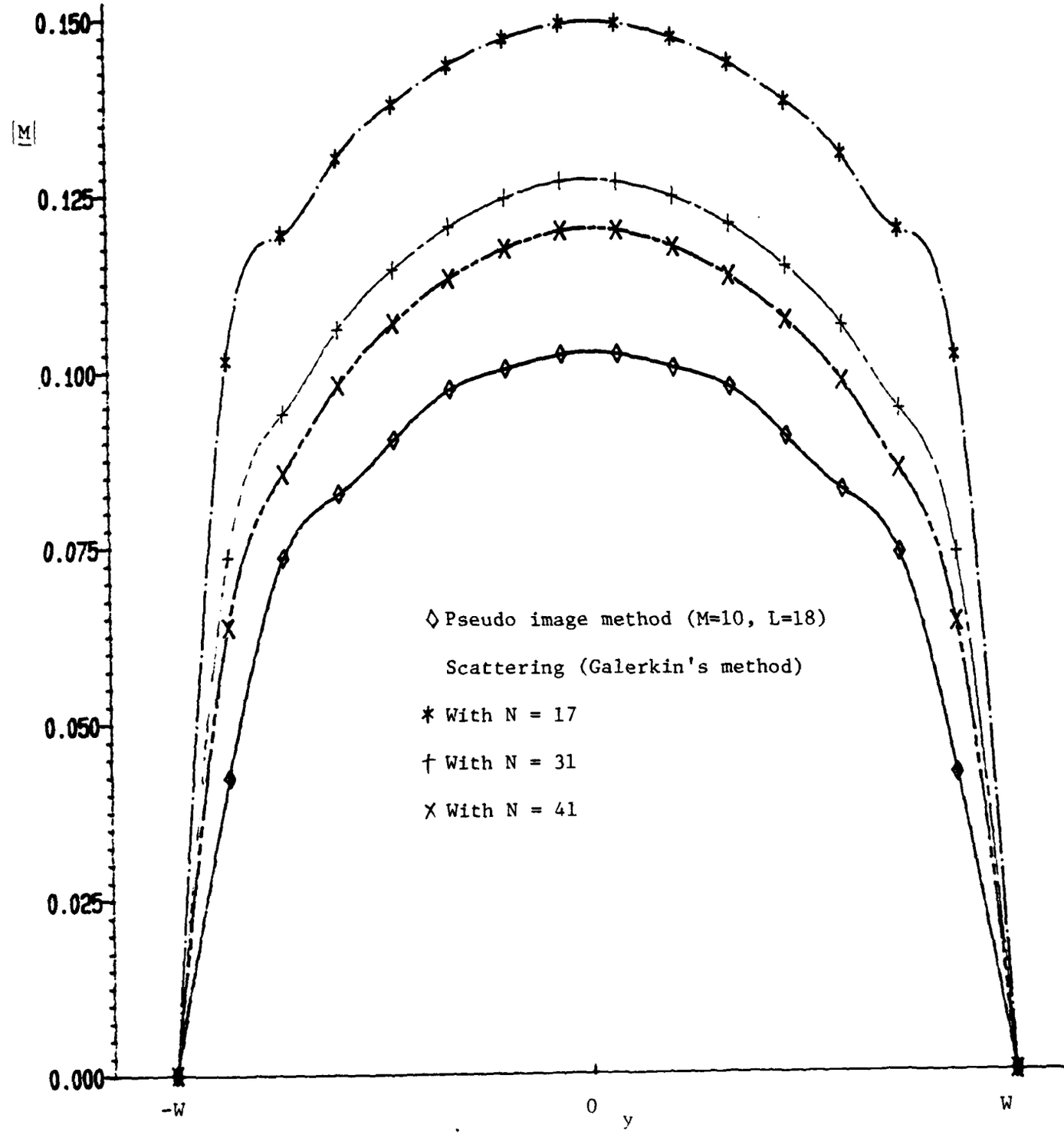

Fig. 14. The magnitude of the magnetic current in the aperture for $\phi^i = 180°$, $\phi_o = 5°$, ka = 1.

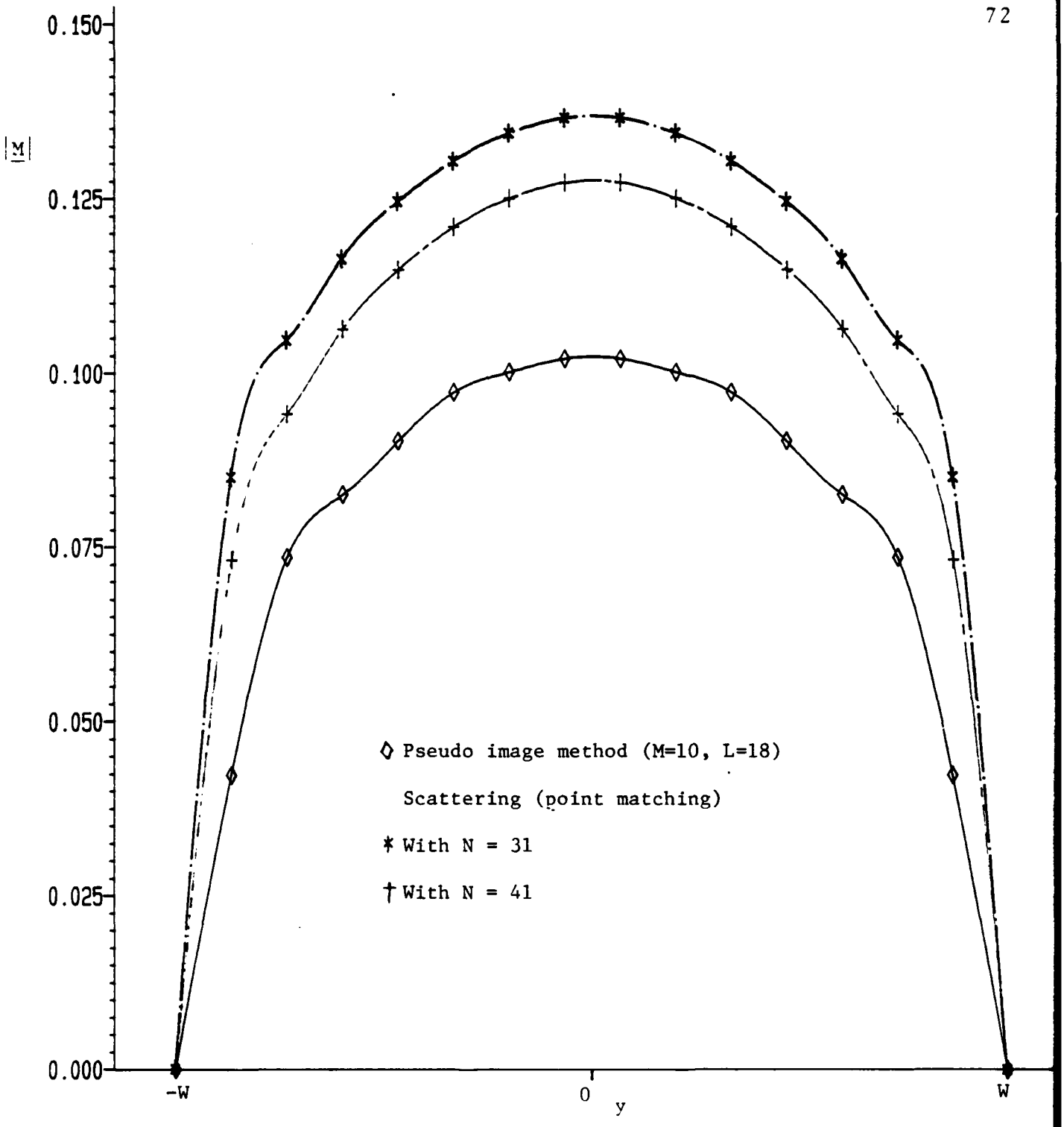

Fig. 15. The magnitude of the magnetic current in the aperture for $\phi^i = 180°$, $\phi_o = 5°$, ka = 1.

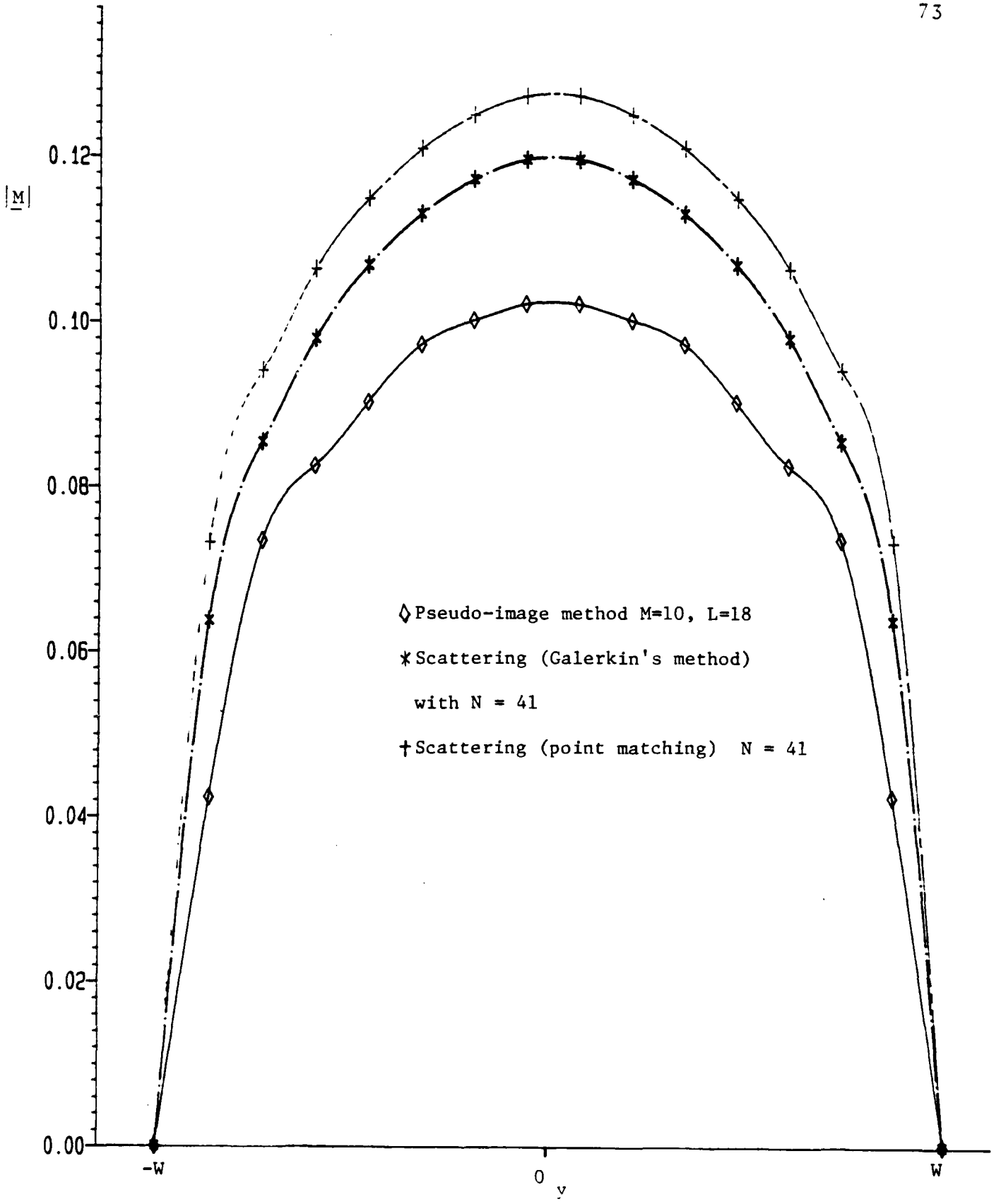

Fig. 16. The magnitude of the magnetic current in the aperture for $\phi^i = 180°$, $\phi_o = 5°$, ka = 1.

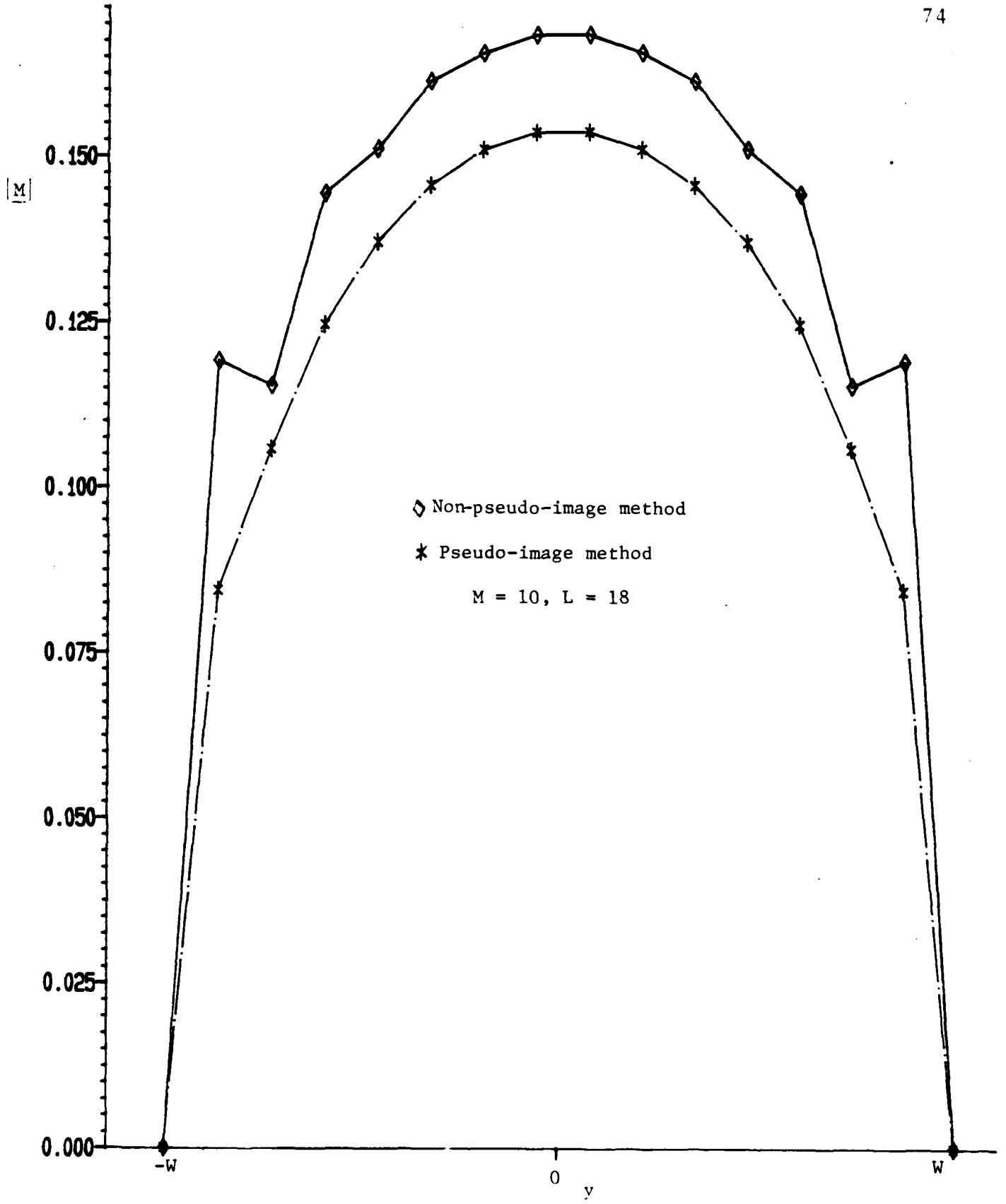

Fig. 17. The magnitude of the magnetic current for $\phi^i = 180°$, $\phi_o = 5°$, ka = $\pi/2$.

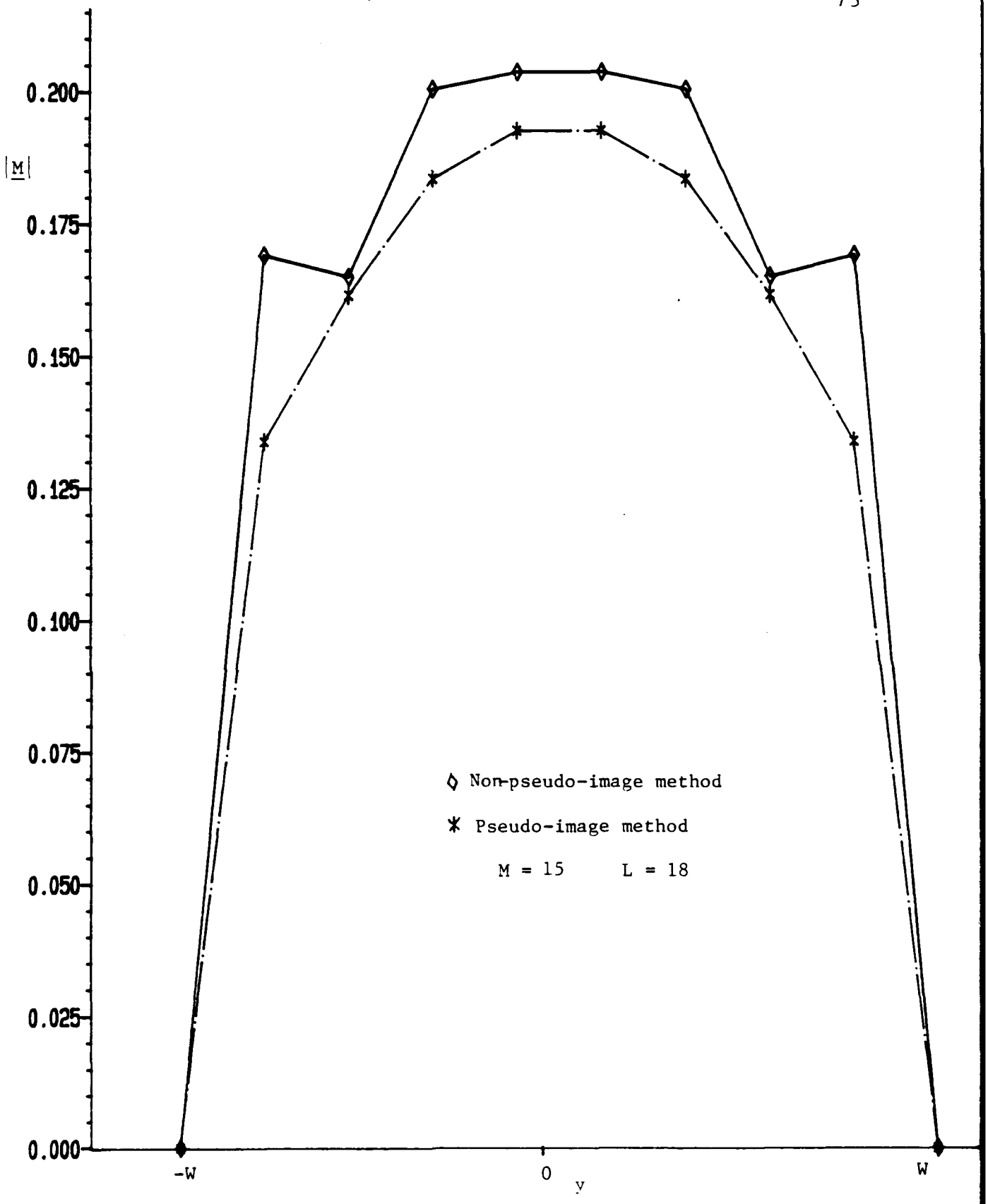

Fig. 18. The magnitude of the magnetic current in the aperture for $\phi^i = 180°$, $\phi_o = 10°$, ka = 1.

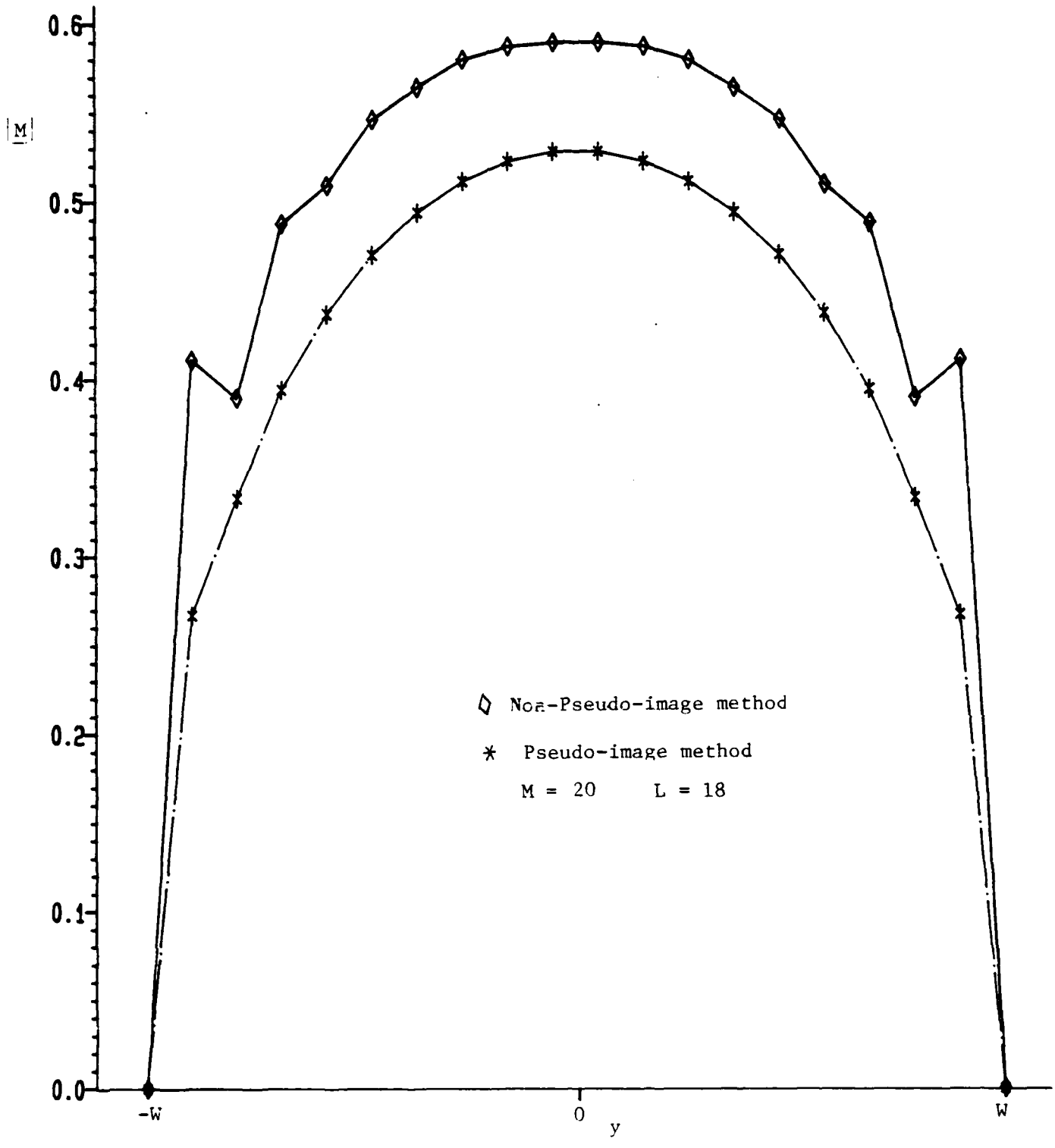

Fig.19. The magnitude of the magnetic current in the aperture for $\phi^i = 180°$, $\phi_o = 30°$, ka = 1.

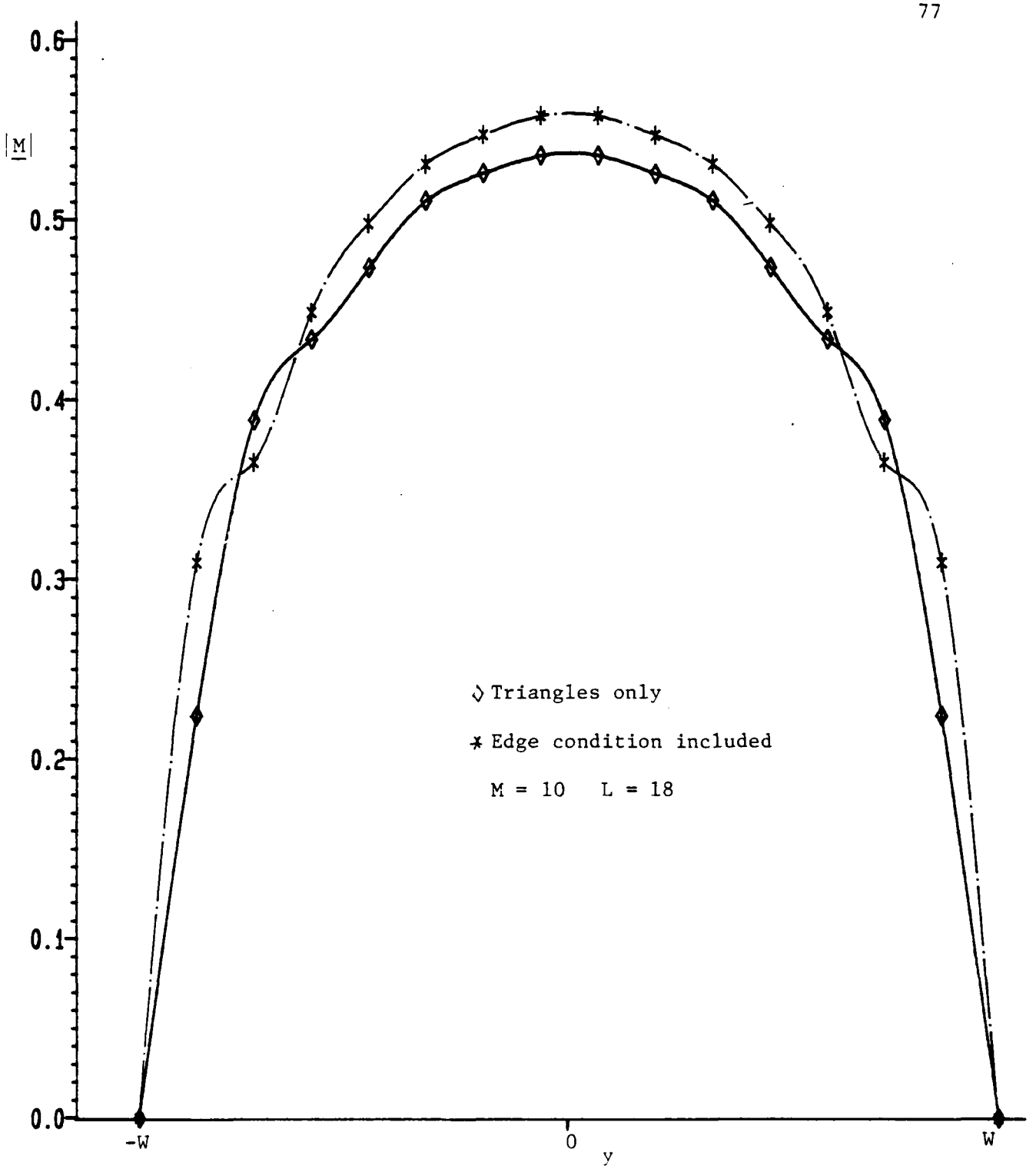

Fig. 20. The magnitude of the magnetic current in the aperture obtained by the pseudo image method with and without the satisfaction of the edge condition $\phi^i = 180°$, $\phi_o = 1.25°$, ka = 2.

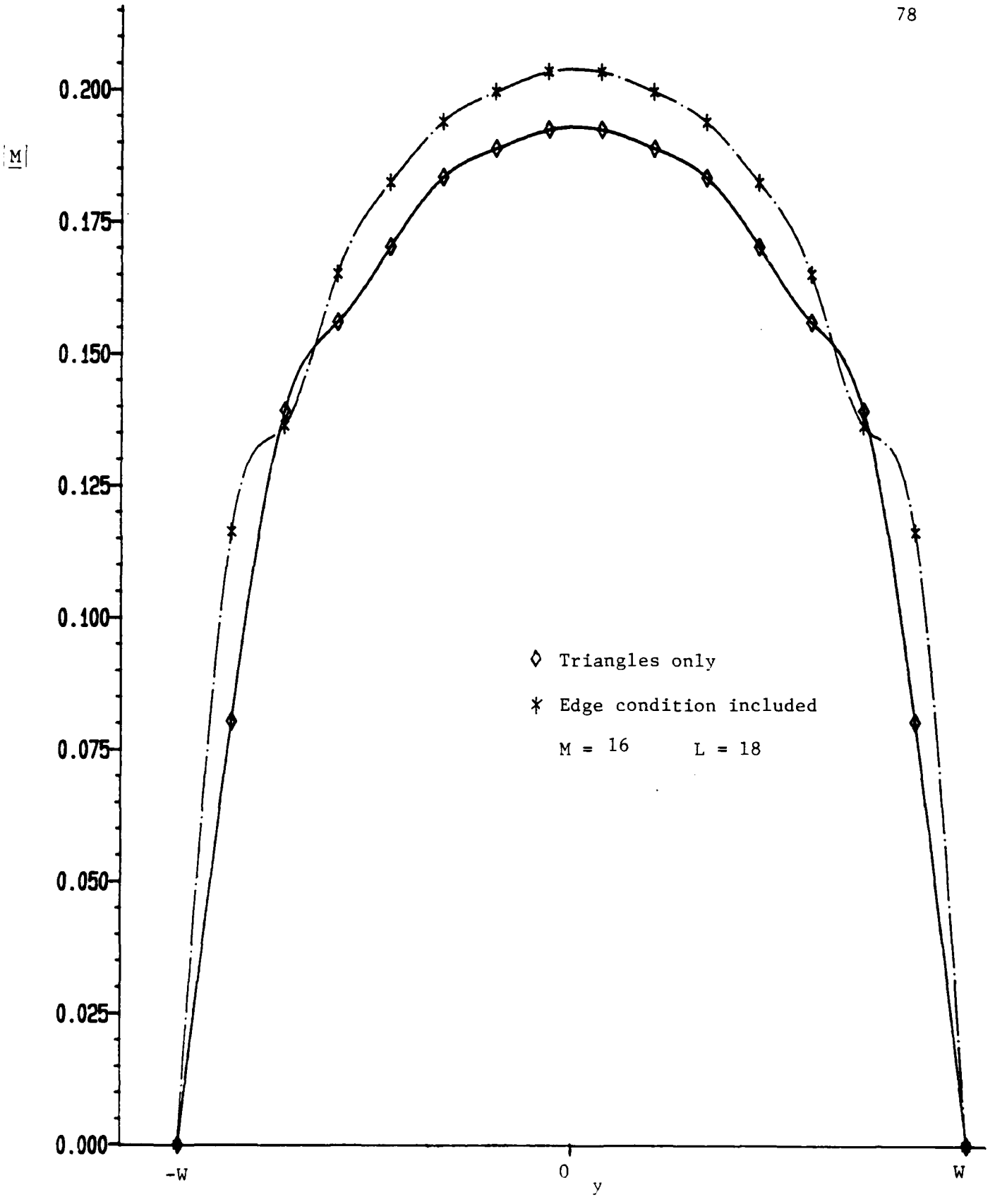

Fig. 21. The magnitude of the magnetic current in the aperture obtained by the pseudo-image method with and without the edge condition included for $\phi^i = 180°$, $\phi_o = 10°$ ka = 1.

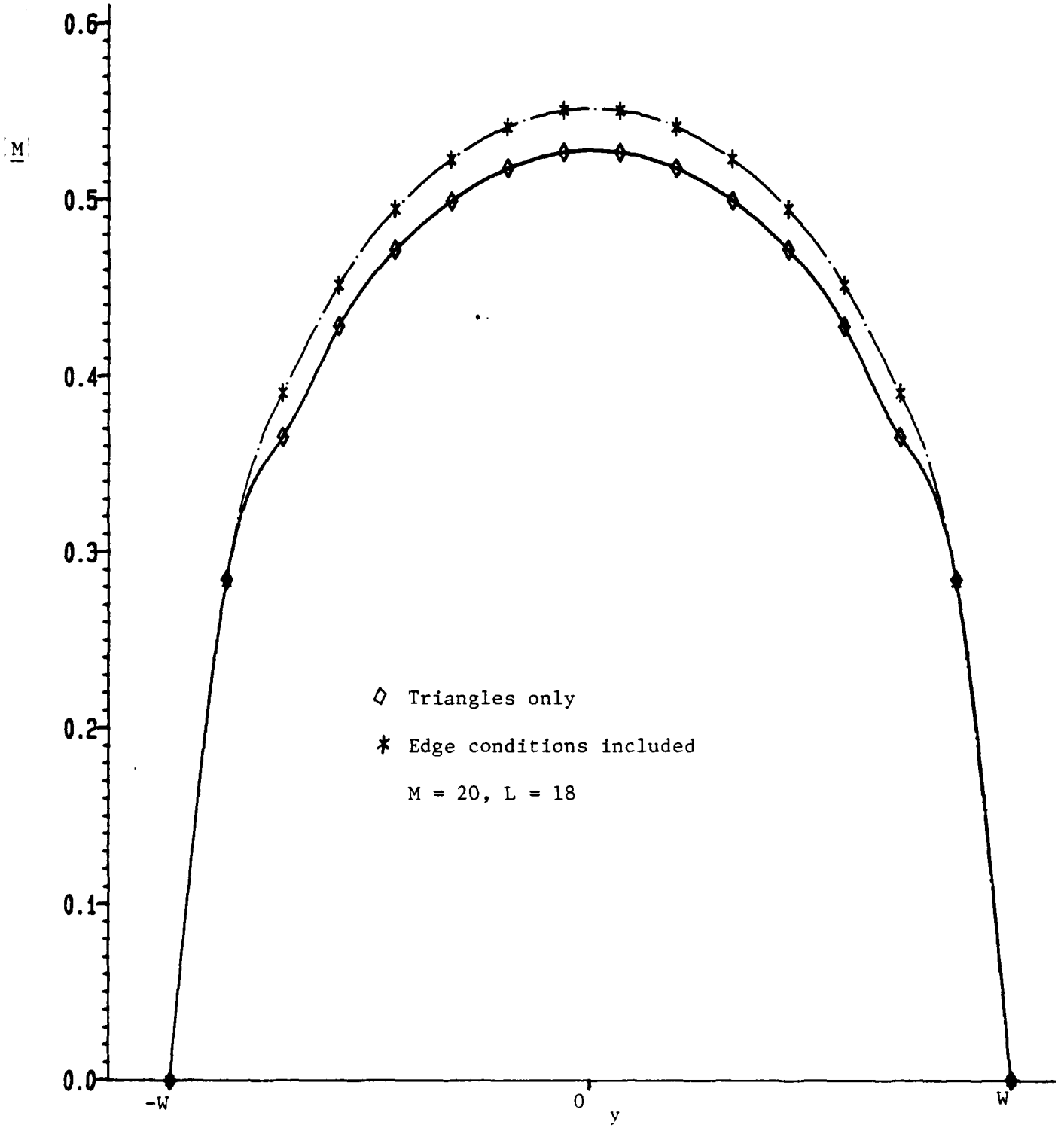

Fig. 22. The magnitude of the magnetic current in the aperture obtained by the pseudo-image method with and without the edge condition included for $\phi^i = 180°$, $\phi_o = 30°$, ka = 1.

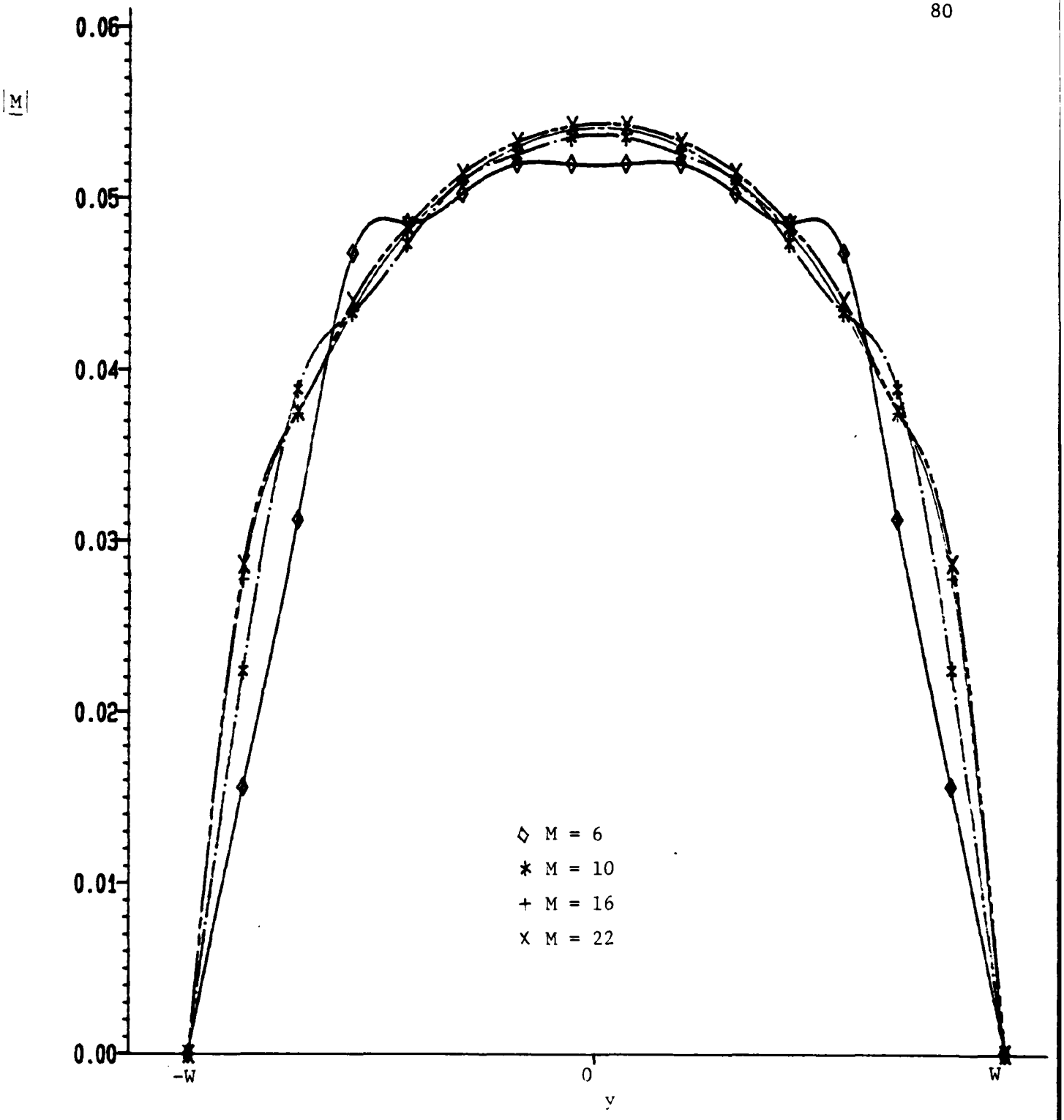

Fig. 23. The speed of convergence of the magnitude of the magnetic current in the aperture for the pseudo-image method with L = 18, ϕ^i = 180°, ϕ_o=1.25°, ka = 2.

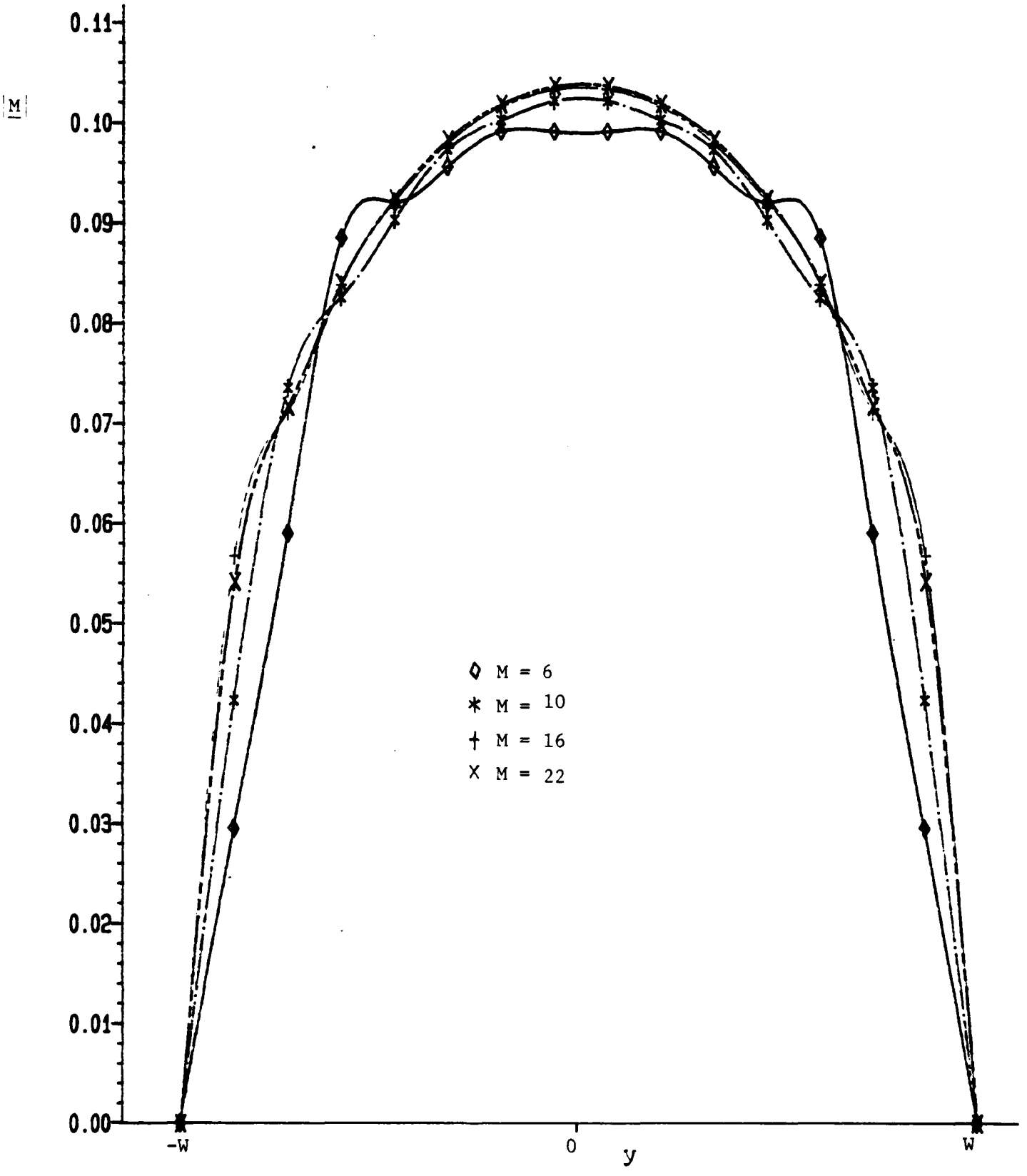

Fig.24 . The speed of convergence of the magnitude of the magnetic current in the aperture for the pseudo-image method with L = 18, ϕ^i = 180°, ϕ_o = 5°, ka = 1.

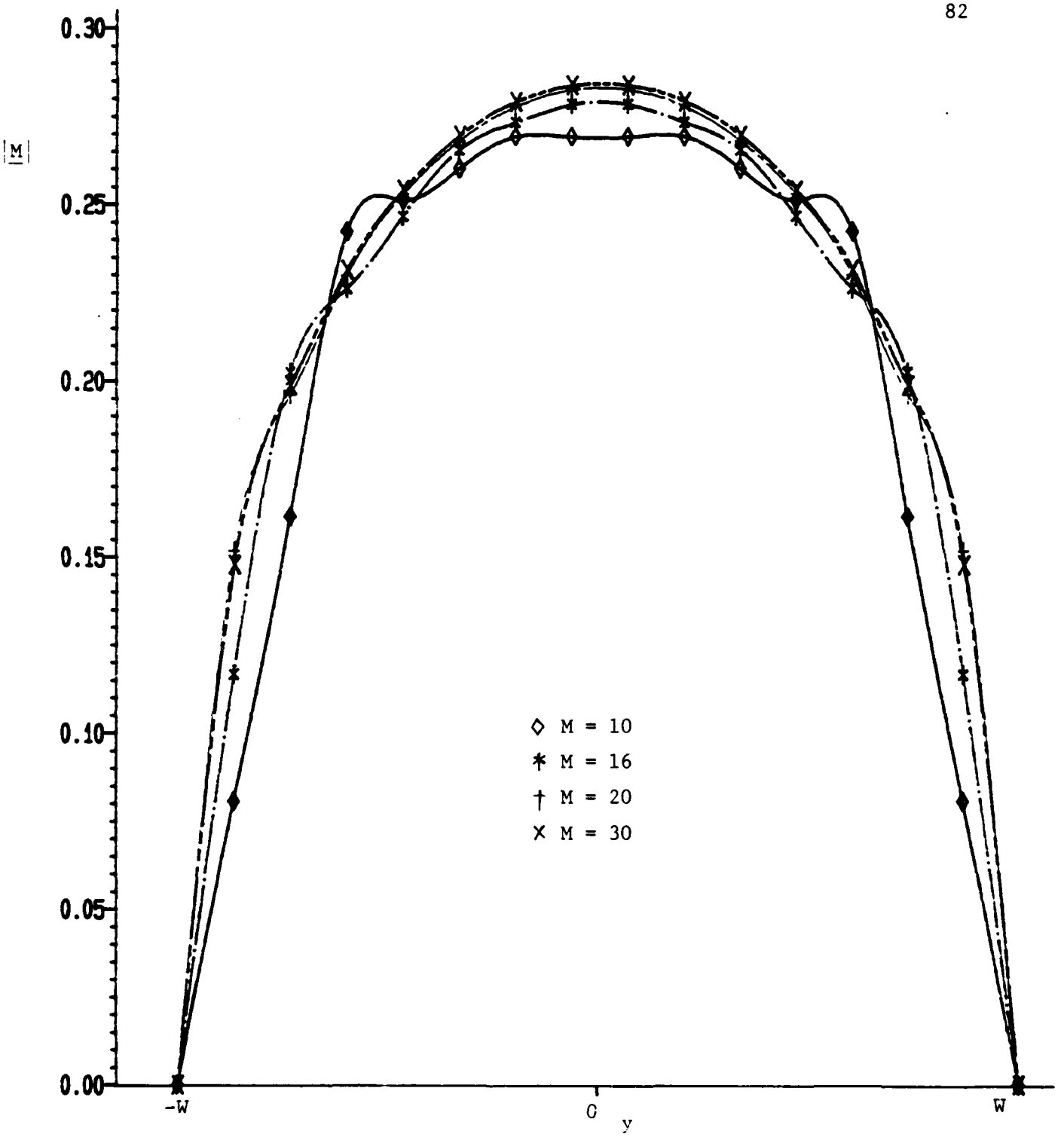

Fig. 25. The Speed of convergence of the magnitude of the magnetic current in the aperture for the pseudo-image method with L = 18, $\phi^i = 180°$, $\phi_o = 15°$, ka = 1.

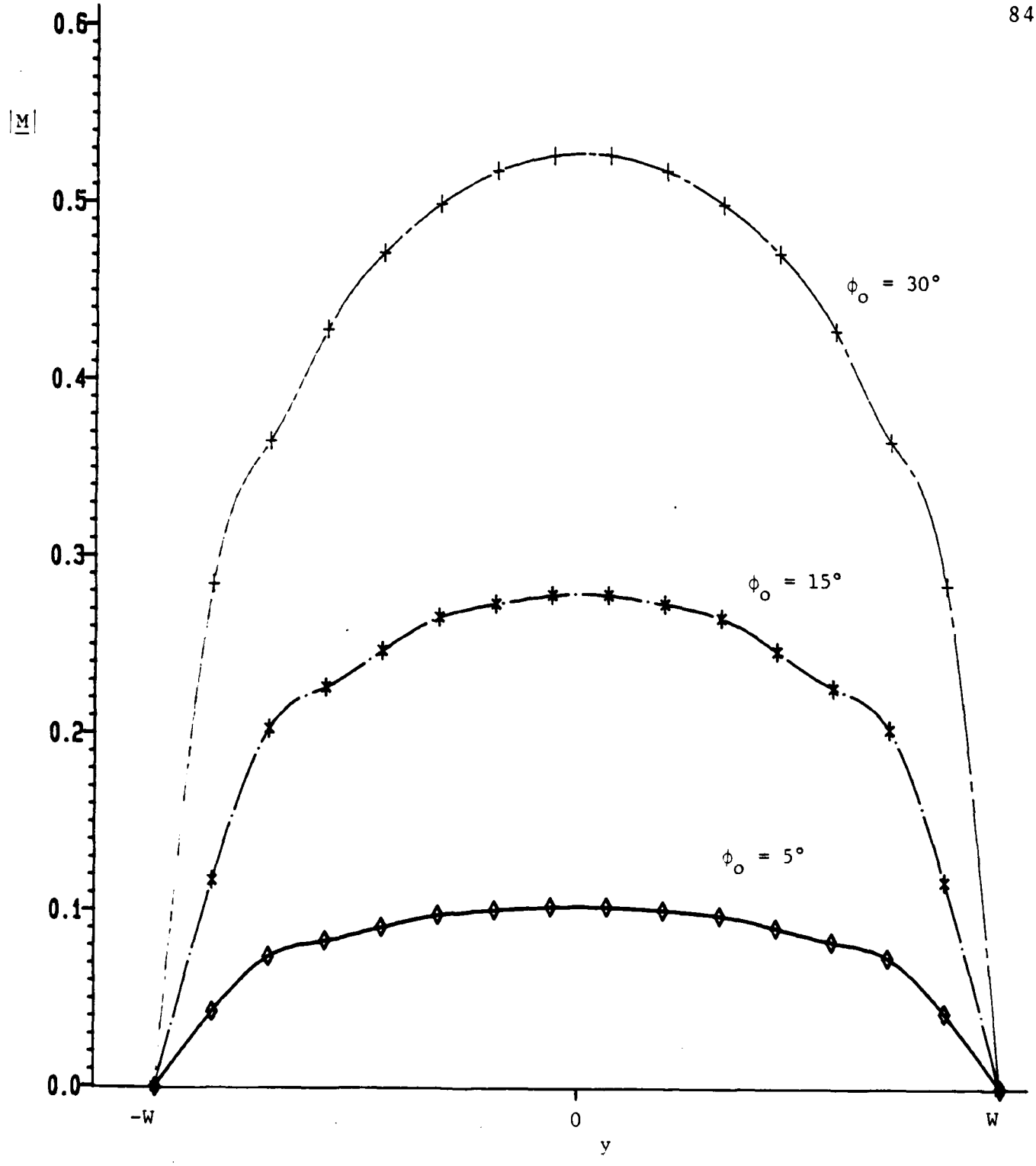

Fig. 27. The magnitude of the magnetic current in the aperture obtained by the pseudo-image method for different sizes of the aperture, where ϕ^i = 180°, ka = 1.

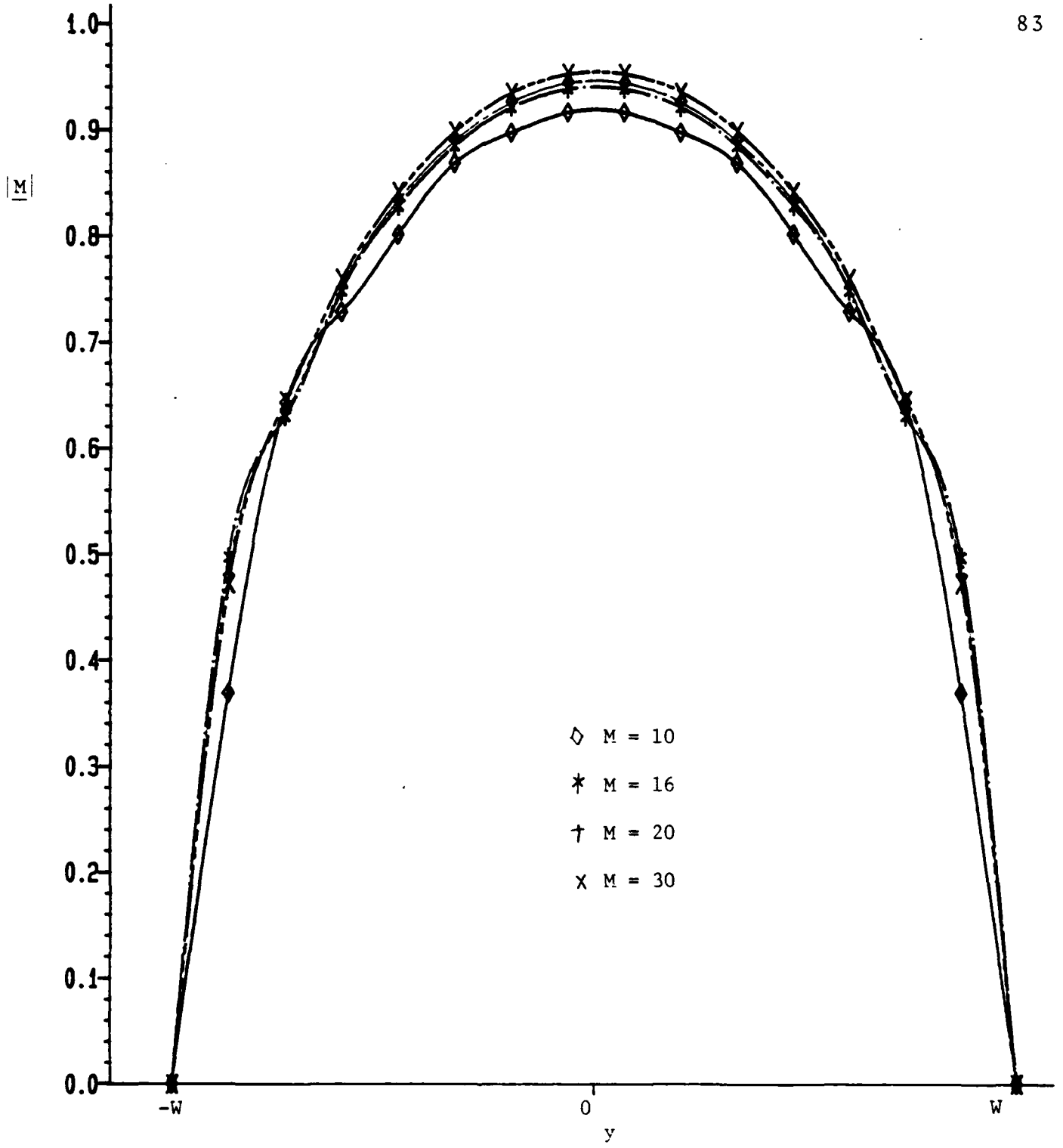

Fig. 26. The Speed of convergence of the magnitude of the magnetic current in the aperture for the pseudo-image method iwth L = 18, ϕ^i = 180°, ϕ_o = 15°, ka = 3.

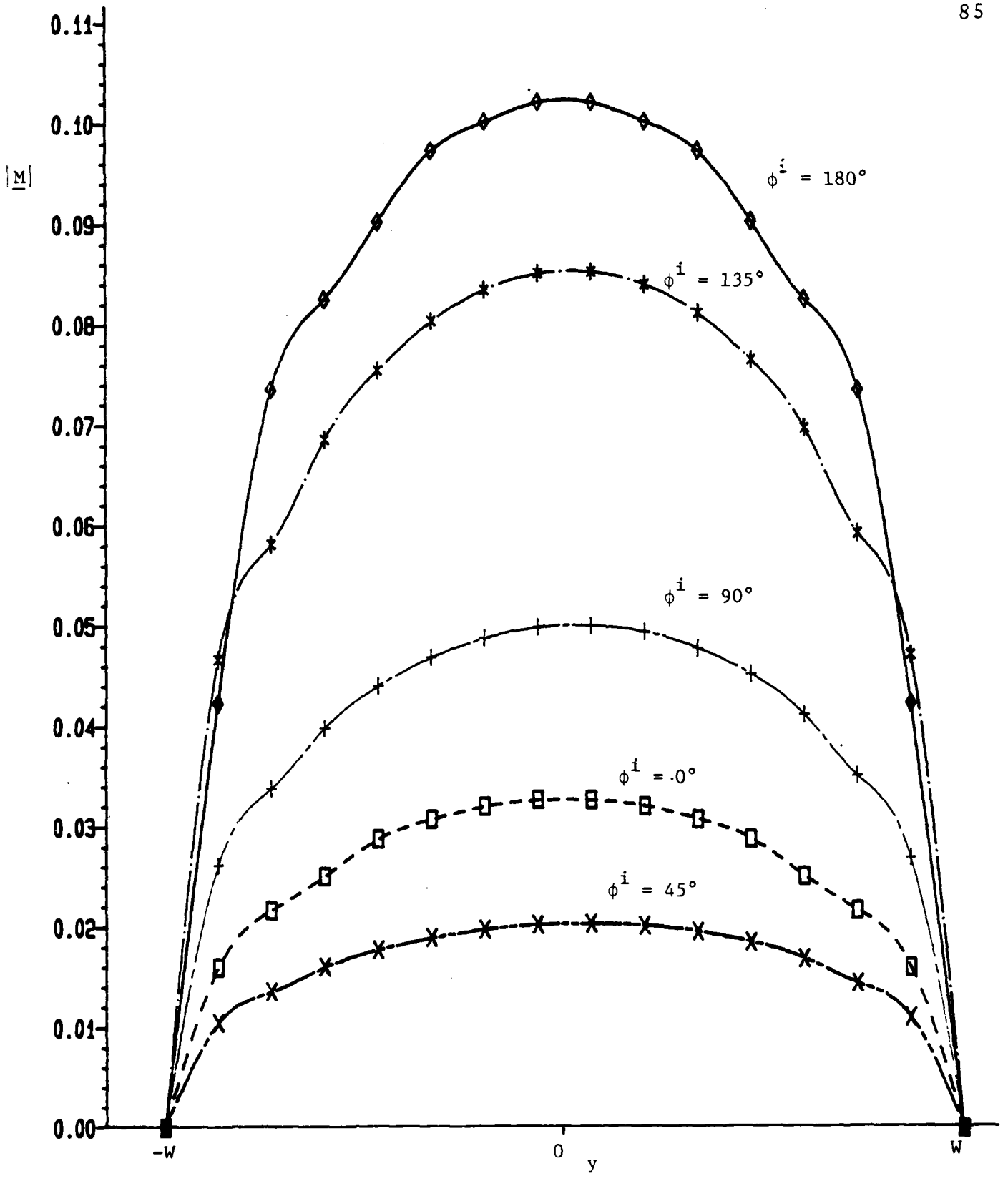

Fig. 28. The magnitude of the magnetic current in the aperture obtained by the pseudo-image method for different incident angles, where $\phi_o = 5°$, ka = 1.

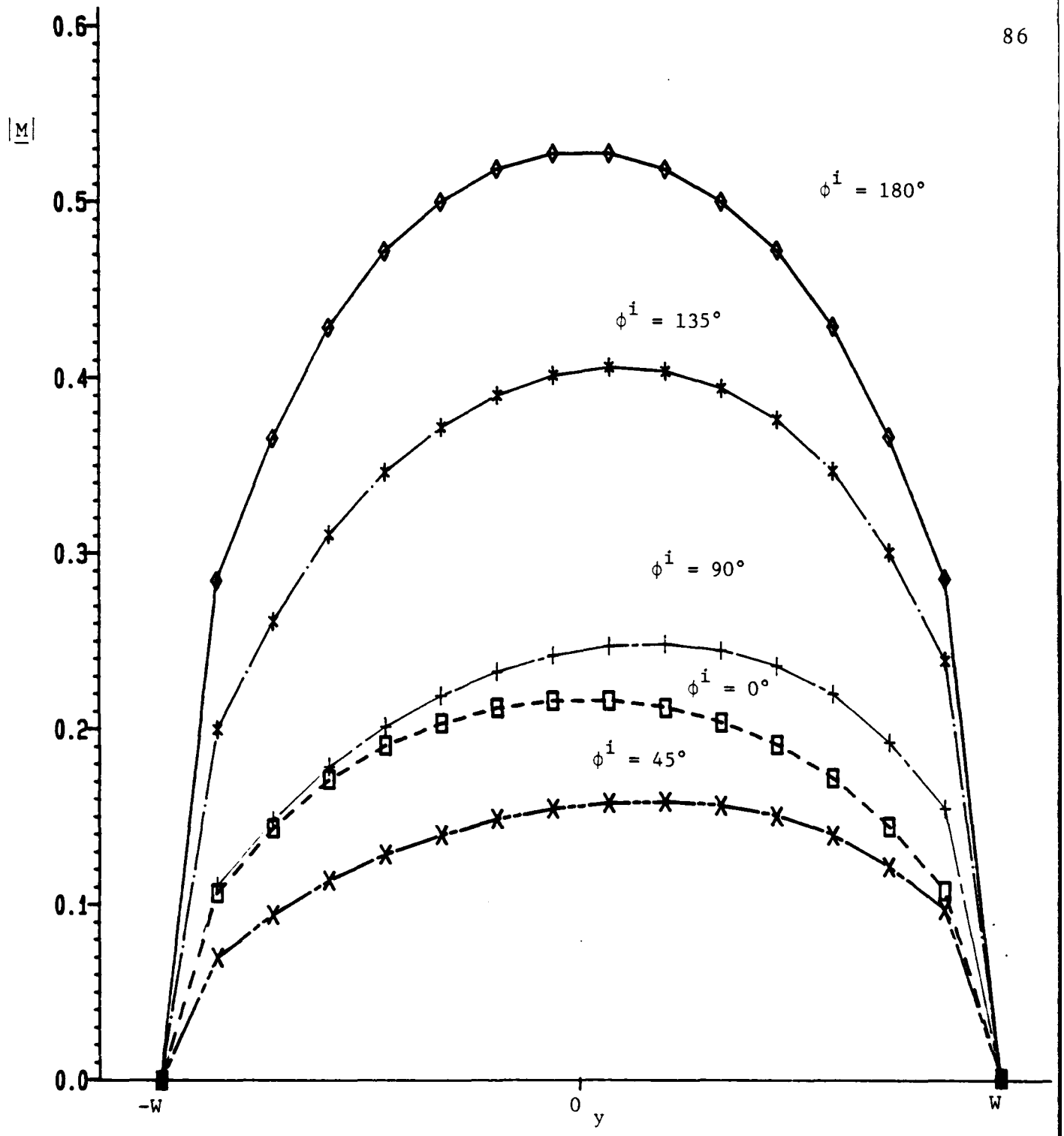

Fig. 29. The magnitude of the magnetic current in the aperture obtained by the pseudo-image method for the different incident angles, where ϕ_o = 30°, ka = 1.

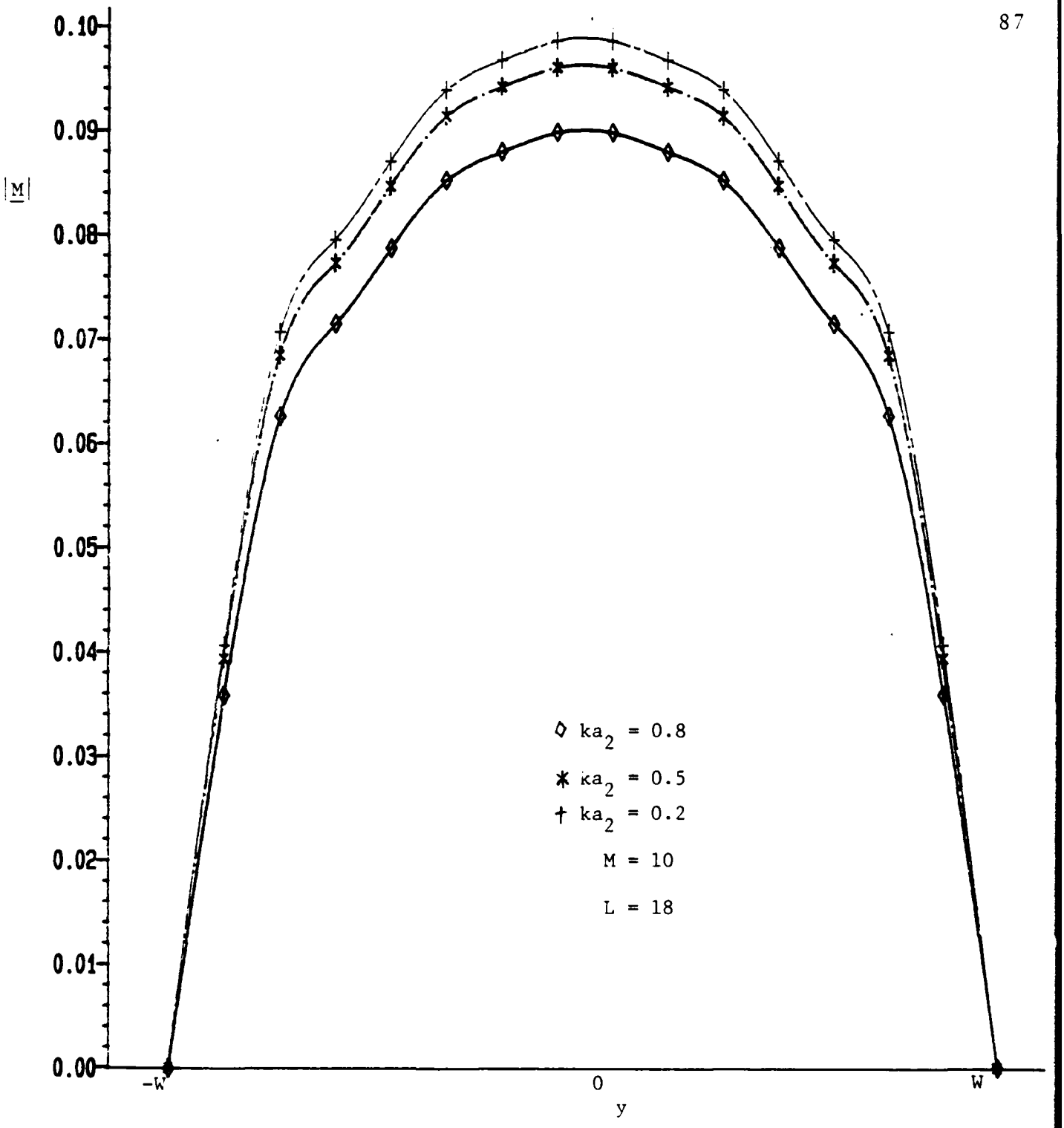

Fig. 30. The magnitude of the magnetic current in the aperture obtained by the pseudo-image method for a cylinder with finite thickness, $\phi^{+} = 180°$, $\phi_o = 5°$, $ka_1 = 1$.

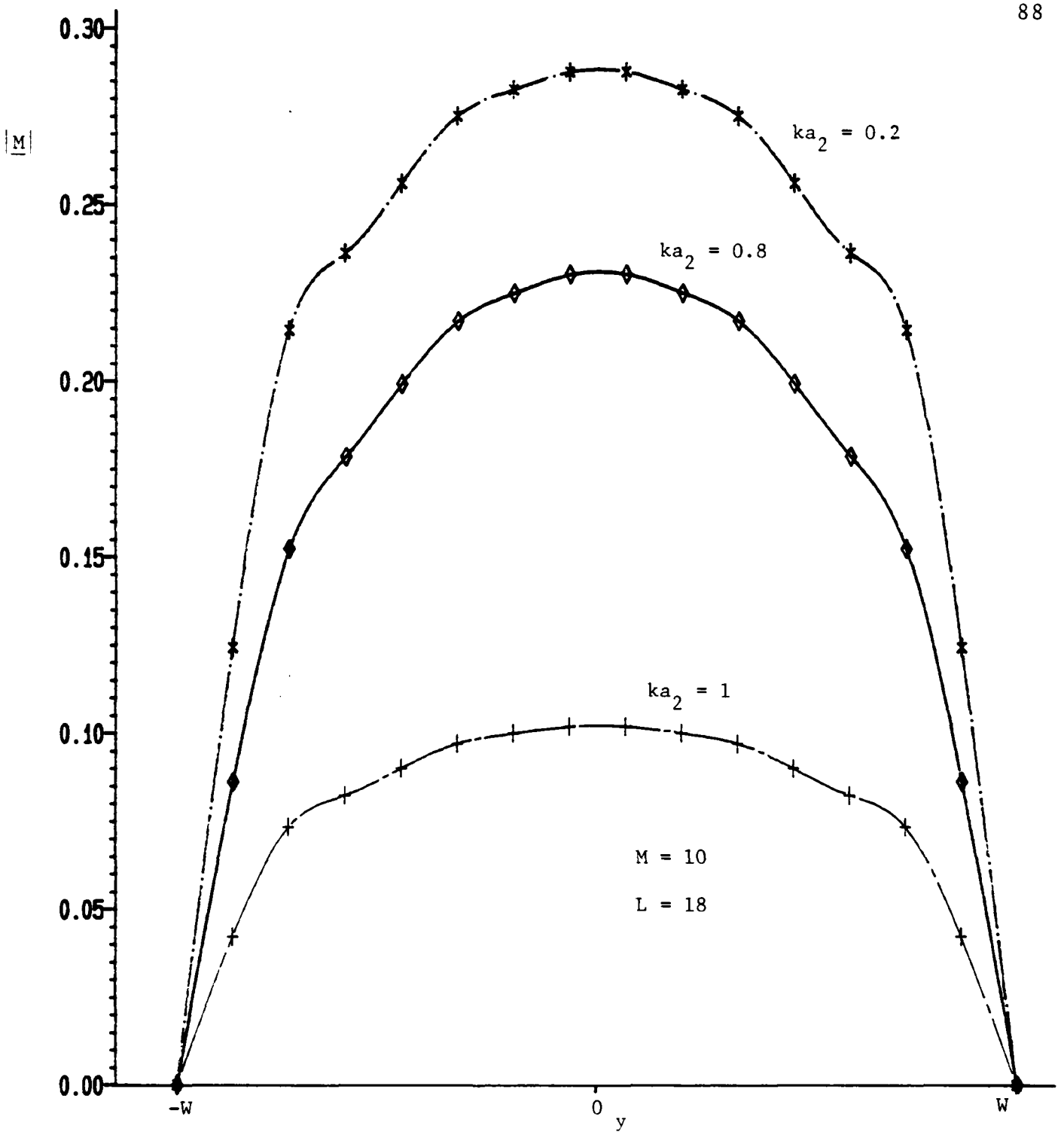

Fig. 31. The magnitude of the magnetic current in the aperture obtained by the pseudo-image method for a cylinder with finite thickness, $\phi^i = 180°$, $\phi_o = 15°$, $ka_1 = 1$.

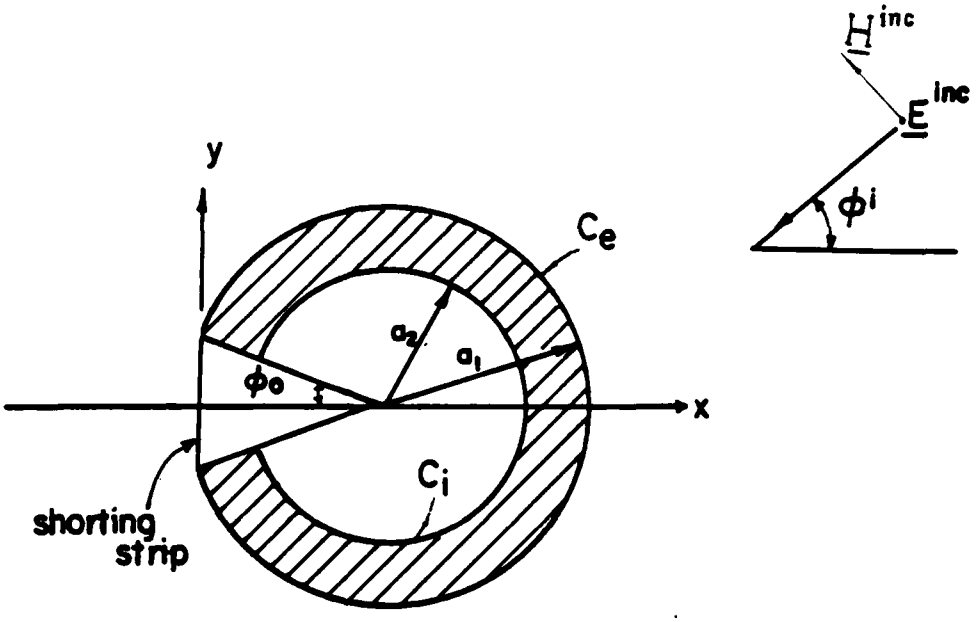

Fig. 32. An infinitely long cylinder with a slot and finite thickness. C_e denotes the outer contour and C_i denotes the rest of the contour. The shaded area is perfectly conducting.

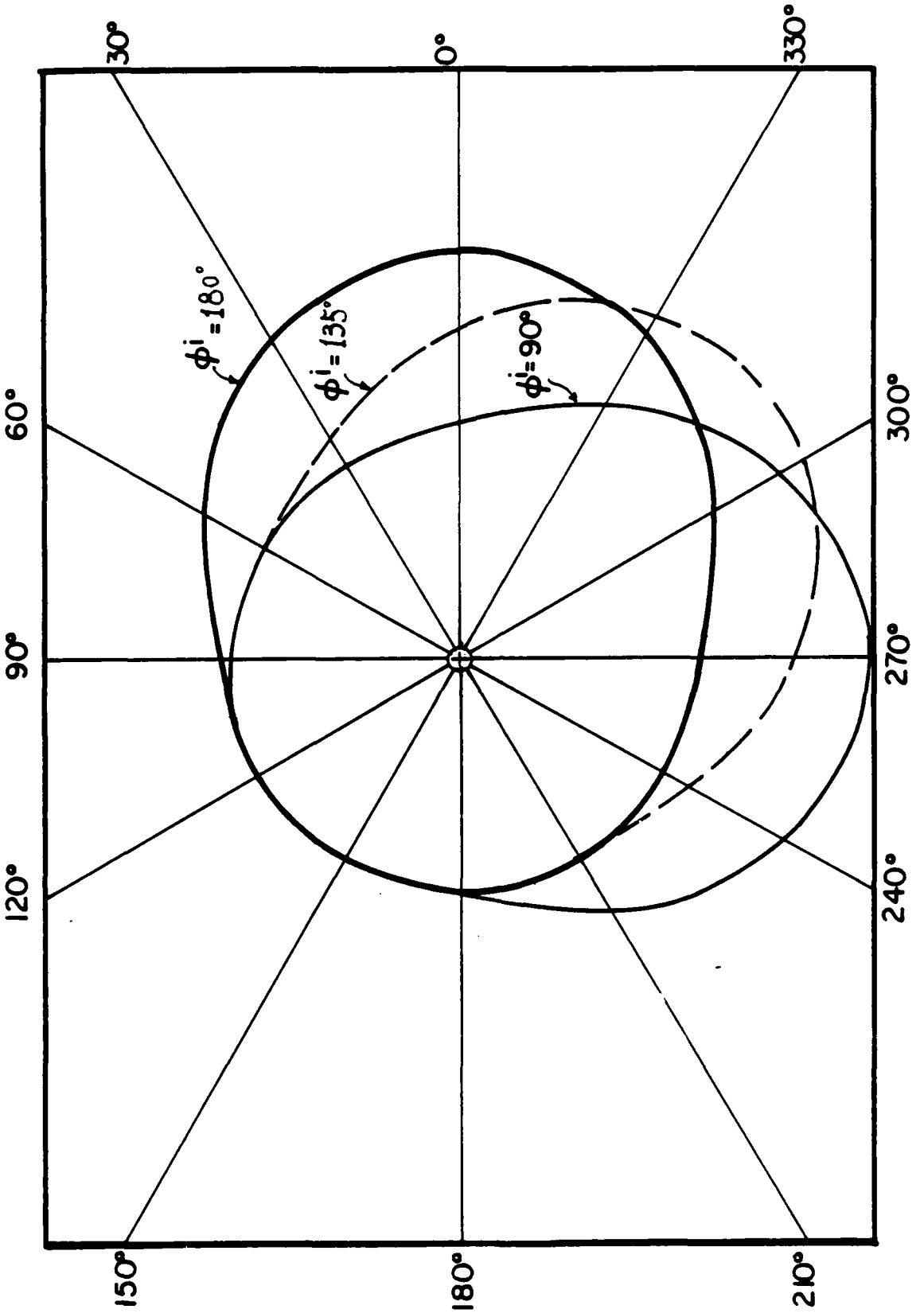

Fig. 33. Far field scattering pattern for $\phi_o = 5°$, ka = 1.

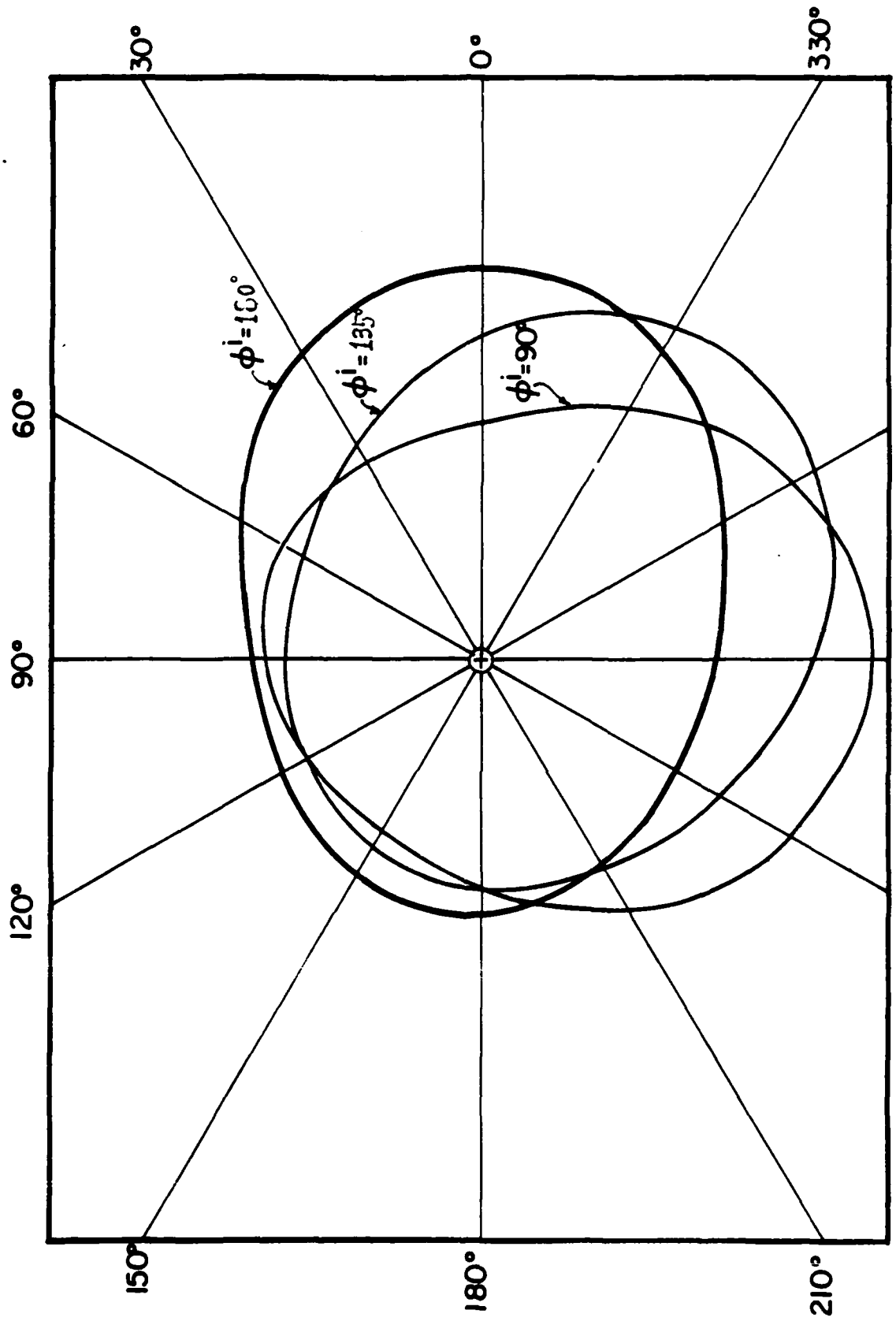

Fig. 34. Far-field pattern for ϕ_o = 30°, ka = 1.

AD-A171 364 THE PSEUDO-IMAGE METHOD FOR COMPUTING ELECTROMAGNETIC FIELD PENETRATION I. (U) SYRACUSE UNIV NY DEPT OF ELECTRICAL AND COMPUTER ENGINEERING X YUAN ET AL. 2/2

UNCLASSIFIED MAY 86 SYRU/DECE/TR-86/1 ARO-21378.6-EL F/G 20/3 NL

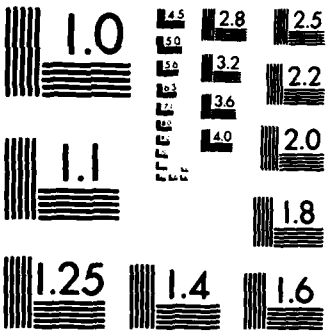

MICROCOPY RESOLUTION TEST CHART
NATIONAL BUREAU OF STANDARDS-1963-A

APPENDIX A

In this Appendix, we express $2k\eta\, Y_{mn}^{ne}$ of (3-88)-(3-91) in terms of integrals whose integrands have no singularity interior to the region of integration. Whenever the argument of $H_o^{(2)}$ is zero at a point interior to the region of integration we subtract out the small argument approximation of $H_o^{(2)}$ and integrate this approximation analytically.

Of all the arguments of the Hankel functions in (3-88), only $k\Delta C|v-v'|$ can be zero at a point interior to the region of integration. Accordingly, we recast (3-88) as

$$2k\eta Y_{11}^{ne} = (k\Delta C)^2 \Bigg[\int_0^1 dv \int_0^1 dv' \left(\sqrt{1-v^2}\sqrt{1-v'^2} + vv'\right) \left(H_o^{(2)}(k\Delta C|v-v'|) - g(k\Delta C|v-v'|)\right) + 2\int_0^1 dv\, v \int_0^1 dv' \sqrt{1-v'^2}\, H_o^{(2)}(k\Delta C|v-v'-1|) + I_1 \Bigg] \tag{A-1}$$

$$- \int_0^1 dv \int_0^1 dv' \left(\frac{v\,v'}{\sqrt{1-v^2}\sqrt{1-v'^2}} + 1\right)\left(H_o^{(2)}(k\Delta C|v-v'|) - g(k\Delta C|v-v'|)\right)$$

$$+ 2\int_0^1 dv \int_0^1 dv' \frac{v'}{\sqrt{1-v'^2}} Ho^{(2)}(k\Delta C|v-v'-1|) - I_2$$

where g is given by (3-20) and

$$I_1 = \int_0^1 dv \int_0^1 dv' \left(\sqrt{1-v^2}\sqrt{1-v'^2} + vv'\right) g(k\Delta C|v-v'|) \tag{A-2}$$

$$I_{\infty} = \int_{\emptyset}^{1} dv \int_{\emptyset}^{1} dv' \left(\frac{v\, v'}{\sqrt{1-v^2}\,\sqrt{1-v'^2}} + 1 \right) g(k_{\Delta c} |v-v'|) \qquad \text{(A-3)}$$

The indentity

$$\int_{\emptyset}^{1} dv \sqrt{1-v^2} \int_{\emptyset}^{1} dv' \sqrt{1-v'^2} \log|v-v'| = \qquad \text{(A-4)}$$

$$\frac{1}{2}\int_{-1}^{1} dv \sqrt{1-v^2} \int_{-1}^{1} dv' \sqrt{1-v'^2} \log|v-v'| - \int_{\emptyset}^{1} dv \sqrt{1-v^2} \int_{\emptyset}^{1} dv' \sqrt{1-v'^2} \log|v+v'|$$

can be verified by expressing each integral over (-1,1) on the right-hand side of (A-4) as the sum of the integral over (-1,Ø) and the integral over (Ø,1) and changing the variable of integration so as to replace the integral over (-1,Ø) by an integral over (Ø,1). Using (3-47), (3-48), and (3-5Ø), we obtain

$$\int_{-1}^{1} dv \sqrt{1-v^2} \int_{-1}^{1} dv' \sqrt{1-v'^2} \log|v-v'| = -\frac{\pi^2}{16} (1 + 4\log 2) \qquad \text{(A-5)}$$

Substitution of (A-5) into (A-4) gives

$$\int_{\emptyset}^{1} dv \sqrt{1-v^2} \int_{\emptyset}^{1} dv' \sqrt{1-v'^2} \log|v-v'| =$$

$$-\frac{\pi^2}{32}(1 + 4\log 2) - \int_{\emptyset}^{1} dv \sqrt{1-v^2} \int_{\emptyset}^{1} dv' \sqrt{1-v'^2} \log|v+v'| \qquad \text{(A-6)}$$

Using [15,formulas 61Ø., 61Ø.1., 61Ø.2., and 61Ø.3.] and working diligently, we obtain

$$\int_{\emptyset}^{1} dv\, v \int_{\emptyset}^{1} dv'\, v' \log|v-v'| = -\frac{7}{16} \qquad \text{(A-7)}$$

It is easy to show that

$$\int_0^1 dv \int_0^1 dv' \left(\sqrt{1-v^2}\sqrt{1-v'^2} + vv'\right) = \frac{\pi^2}{16} + \frac{1}{4} \qquad \text{(A-8)}$$

Substituting (3-20) into (A-2) and using (A-6)-(A-8), we obtain

$$I_1 = \frac{\pi^2}{16} + \frac{1}{4} - j\left(\left(\frac{\pi}{8} + \frac{1}{2\pi}\right)\log b - \frac{\pi}{4}\log 2 - \frac{\pi}{16} - \frac{7}{8\pi}\right)$$

$$+ \frac{j2}{\pi}\int_0^1 dv\sqrt{1-v^2}\int_0^1 dv'\sqrt{1-v'^2}\,\log|v+v'| \qquad \text{(A-9)}$$

where

$$b = \frac{\tau}{2} k_\Delta C \qquad \text{(A-10)}$$

Seeking to evaluate I_2 of (A-3), we consider

$$U_1 = \int_0^1 dv \frac{v}{\sqrt{1-v^2}} \int_0^1 dv' \frac{v'}{\sqrt{1-v'^2}} \log|v-v'| \qquad \text{(A-11)}$$

The substitutions

$$v = \cos\theta \qquad \text{(A-12)}$$

$$v' = \cos\theta' \qquad \text{(A-13)}$$

transform (A-11) to

$$U_1 = \int_0^{\pi/2} d\theta \cos\theta \int_0^{\pi/2} d\theta' \cos\theta' \log|\cos\theta - \cos\theta'| \qquad \text{(A-14)}$$

Substituting [14, eq.(A-2)]

$$\log|\cos\theta - \cos\theta'| = -\log 2 - \sum_{m=1}^{\infty} \frac{2}{m} \cos(m\theta)\cos(m\theta') \qquad \text{(A-15)}$$

into (A-14) and interchanging the order of summation and integration, we obatin

$$U_1 = -\log 2 \left(\int_0^{\pi/2} \cos\theta \, d\theta \right)^2 - \sum_{m=1}^{\infty} \frac{2}{m} \left(\int_0^{\pi/2} \cos\theta \cos(m\theta) \, d\theta \right)^2 \tag{A-16}$$

which first reduces to

$$U_1 = -\log 2 - \frac{\pi^2}{8} - \sum_{m=2}^{\infty} \frac{1}{2m} \left[\frac{\sin((m+1)\pi/2)}{m+1} + \frac{\sin((m-1)\pi/2)}{m-1} \right]^2 \tag{A-17}$$

and finally to

$$U_1 = -\log 2 - \frac{\pi^2}{8} - \sum_{n=1}^{\infty} \frac{1}{n(2n+1)^2(2n-1)^2} \tag{A-18}$$

Using [15, Formulas 610. and 610.1.], we obtain

$$\int_0^1 dv \int_0^1 dv' \, \log|v-v'| = -3/2 \tag{A-19}$$

It is easy to show that

$$\int_0^1 dv \int_0^1 dv' \left(\frac{v\,v'}{\sqrt{1-v^2}\sqrt{1-v'^2}} + 1 \right) = 2 \tag{A-20}$$

Substitution of (A-18)-(A-20) into (A-3) gives

$$I_2 = 2 - j\frac{2}{\pi} \left[\log\left(\frac{b^2}{2}\right) - \frac{3}{2} - \frac{\pi^2}{8} - \sum_{n=1}^{\infty} \frac{1}{n(2n-1)^2(2n-1)^2} \right] \tag{A-21}$$

Now, $2k\eta Y_{11}^{hs}$ of (3-88) is given by (A-1) where I_1 and I_2 are given by (A-9) and (A-21), respectively.

Of all the arguments of the Hankel functions in (3-89), only $k\Delta C|v+v'+n-3|$ can be zero at a point interior to the region of integration. Accordingly, we recast (3-89) as

$$2k\eta Y_{in}^{nn} = (k\Delta C)^{n}\Bigg| \int_0^1 dv\sqrt{1-v^2}\int_0^1 dv'\, v'\,\Big(H_0^{(2)}(k\Delta C|v+v'+n-2|) + H_0^{(2)}(k\Delta C|v-v'+n|)\Big)$$

$$+ \int_0^1 dv\, v\int_0^1 dv'\, v'\, Ho^{(2)}(k\Delta C|v-v'+n-1|) + I_3\Bigg| \qquad \text{(A-22)}$$

$$- \int_0^1 dv\frac{v}{\sqrt{1-v^2}}\int_0^1 dv'\Big(H_0^{(2)}(k\Delta C|v+v'+n-2|)-H_0^{(2)}(k\Delta C|v-v'+n|)\Big)$$

$$- \int_0^1 dv \int_0^1 dv'\, Ho^{(2)}(k\Delta C|v-v'+n-1|) + I_4$$

where

$$I_3 = \int_0^1 dv\, v\int_0^1 dv'\, v'\, H_0^{(2)}(k\Delta C|v+v'+n-3|) \qquad \text{(A-23)}$$

$$I_4 = \int_0^1 dv \int_0^1 dv'\, H_0^{(2)}(k\Delta C|v+v'+n-3|) \qquad \text{(A-24)}$$

If $n \geq 3$, (A-23) and (A-24) are all right as they stand because the argument of $H_0^{(2)}$ can not vanish at any point interior to the region of integration. If n=2, then (A-23) and (A-24) are recast as

$$I_3 = U_2 + \int_0^1 dv\, v\int_0^1 dv' v'\Big(H_0^{(2)}(k\Delta C|v+v'-1|)-g(k\Delta C|v+v'-1|)\Big) \qquad \text{(A-25)}$$

$$I_4 = U_3 + \int_0^1 dv \int_0^1 dv'\, \Big(H_0^{(2)}(k\Delta C|v+v'-1|)-g(k\Delta C|v+v'-1|)\Big) \qquad \text{(A-26)}$$

where

$$U_2 = \int_0^1 dv\, v\int_0^1 dv' v'\, g(k\Delta C|v+v'-1|) \qquad \text{(A-27)}$$

$$U_3 = \int_0^1 dv \int_0^1 dv' \; g(k\Delta C|v+v'-1|) \qquad \text{(A-28)}$$

Using [15, Formulas 610., 610.1., 610.2., and 610.3.] and working diligently, we obtain

$$\int_0^1 dv \; v \int_0^1 dv' v' \log|v+v'-1| = -\frac{5}{16} \qquad \text{(A-29)}$$

Substituting (3-20) into (A-27) and using (A-29), we find that

$$U_\infty = \frac{1}{4} + \frac{j}{8\pi}(5 - 4\log b) \qquad \text{(A-30)}$$

Substitution of (A-30) into (A-25) gives

$$I_3 = \int_0^1 dv \; v \int_0^1 dv' v' (H_\infty^{(\infty)}(k\Delta C|v+v'-1|) - g(k\Delta C|v+v'-1|))$$

$$+\frac{1}{4} + \frac{j}{8\pi}(5 - 4\log b) \quad ,n=2 \qquad \text{(A-31)}$$

where b is given by (A-10).

Seeking to evaluate U_3 of (A-28), we write

$$\int_0^1 dv' \int_0^1 dv' \log|v+v'-1| = -\frac{3}{2} \qquad \text{(A-32)}$$

To verify (A-32), note that if v' is replaced by 1-v' in (A-32), then the left-hand side of (A-32) reduces to that of (A-19). Substituting (3-20) into (A-28) and using (A-32), we obtain

$$U_3 = 1 + \frac{j}{\pi}(3 - 2\log b) \qquad \text{(A-33)}$$

Substitution of (A-33) into (A-26) gives

$$I_4 = \int_0^1 dv \int_0^1 dv' \left(H_0^{(2)}(k\Delta C|v+v'-1|) - g(k\Delta C|v+v'-1|) \right)$$

$$+ 1 + \frac{j}{\pi}\left(3 - 2\log b \right) \qquad ,n=2 \tag{A-34}$$

Now, $2k\eta Y_{1n}^{n=}$ of (3-89) is given by (A-22) where I_3 and I_4 are given by (A-31) and (A-34) for n=2 and by (A-23) and (A-24) for n=3,4,...,M-2.

Of all the arguments of the Hankel functions in (3-90), only $k\Delta C|v+v'+M-4|$ can be zero at a point interior to the region of integration. Accordingly, we recast (3-90) as

$$\begin{aligned} 2k\eta Y_{1,M-1}^{n=} = (k\Delta C)^2 \Bigg| & \int_0^1 dv\sqrt{1-v^2} \int_0^1 dv'\sqrt{1-v'^2}\, H_0^{(2)}(k\Delta C|v+v'+M-2|) \\ & + I_3 + 2\int_0^1 dv\, v \int_0^1 dv' \sqrt{1-v'^2}\, H_0^{(2)}(k\Delta C|v+v'+M-3|) \Bigg| \\ & + \int_0^1 dv \frac{v}{\sqrt{1-v^2}} \int_0^1 dv' \frac{v'}{\sqrt{1-v'^2}} H_0^{(2)}(k\Delta C|v+v'+M-2|) \\ & + I_4 - 2\int_0^1 dv \int_0^1 dv' \frac{v'}{\sqrt{1-v'^2}} H_0^{(2)}(k\Delta C|v+v'+M-3|) \end{aligned} \tag{A-35}$$

where

$$I_3 = \int_0^1 dv\, v \int_0^1 dv'\, v'\, H_0^{(2)}(k\Delta C|v+v'+M-4|) \tag{A-36}$$

$$I_4 = \int_0^1 dv \int_0^1 dv'\, H_0^{(2)}(k\Delta C|v+v'+M-4|) \tag{A-37}$$

If $M \geq 4$, (A-36) and (A-37) are all right as they stand because the argument of $H_0^{(2)}$ can not vanish at any point

interior to the region of integration. If M=3, then the right-hand sides of (A-36) and (A-37) are the same as those of (A-23) and (A-24) with n=2. Hence, from (A-31) and (A-34), we have

$$I_5 = \int_0^1 dv\ v \int_0^1 dv'\ v' \left(H_0^{(e)}(k\Delta C|v+v'-1|) - g(k\Delta C|v+v'-1|) \right)$$

$$+ \frac{1}{4} + \frac{j}{8\pi}\left(5 - 4\log b \right) \qquad ,M=3 \tag{A-38}$$

$$I_6 = \int_0^1 dv \int_0^1 dv' \left(H_0^{(e)}(k\Delta C|v+v'-1|) - g(k\Delta C|v+v'-1|) \right)$$

$$+ 1 + \frac{j}{\pi}\left(3 - 2\log b \right) \qquad ,M=3 \tag{A-39}$$

Now, $2k\eta Y^{hc}_{1,M-1}$ of (3-90) is given by (A-35) where I_5 and I_6 are given by (A-38) and (A-39) for M=3 and by (A-36) and (A-37) for M=4,5,....

We rewrite $2k\eta Y^{hc}_{mn}$ of (3-91) as

$$2k\eta Y^{hc}_{mn} = I_7 + I_8 + I_9 \qquad , \begin{cases} m=2,3,\ldots,M-2 \\ n=2,3,\ldots,M-2 \end{cases} \tag{A-40}$$

where

$$I_7 = \int_0^1 dv \int_0^1 dv' \left((k\Delta C)^2 vv' - 1 \right) \left(H_0^{(e)}(k\Delta C|v-v'+m-n|) \right.$$

$$\left. + H_0^{(e)}(k\Delta C|v-v'+n-m|) \right) \tag{A-41}$$

$$I_8 = \int_0^1 dv \int_0^1 dv' \left((k\Delta C)^2 vv' + 1 \right) H_0^{(e)}(k\Delta C|v+v'+m-n-2|)$$

(A-42)

$$I_{\varphi} = \int_{\varnothing}^{1} dv \int_{\varnothing}^{1} dv' \left((k\Delta C)^{e} vv' + 1 \right) H_{o}^{(e)} (k\Delta C|v+v'+n-m-2|) \tag{A-43}$$

If $m \neq n$, (A-41) is all right as it stands because neither of the arguments of its Hankel functions can vanish at any point interior to the region of integration. If m=n, then (A-41) is recast as

$$I_{7} = 2U_{4} + 2\int_{\varnothing}^{1} dv \int_{\varnothing}^{1} dv' \left((k\Delta C)^{e} vv' - 1 \right) \left(H_{o}^{(e)} (k\Delta C|v-v'|) - g(k\Delta C|v-v'|) \right) \tag{A-44}$$

where

$$U_{4} = \int_{\varnothing}^{1} dv \int_{\varnothing}^{1} dv' \left((k\Delta C)^{e} vv' - 1 \right) g(k\Delta C|v-v'|) \tag{A-45}$$

Using (A-7) and (A-19) to evaluate (A-45), we obtain

$$U_{4} = \frac{(k\Delta C)^{e}}{4} - 1 - \frac{j2}{\pi} \left(\left(\frac{(k\Delta C)^{e}}{4} - 1 \right) \log b - \frac{7}{16} (k\Delta C)^{2} + \frac{3}{2} \right) \tag{A-46}$$

Substitution of (A-46) into (A-44) gives

$$I_{7} = 2\int_{\varnothing}^{1} dv \int_{\varnothing}^{1} dv' \left((k\Delta C)^{e} vv' - 1 \right) \left(H_{o}^{(e)} (k\Delta C|v-v'|) - g(k\Delta C|v-v'|) \right) \tag{A-47}$$

$$+ \frac{(k\Delta C)^{e}}{2} - 2 - \frac{j}{\pi} \left(6 - 4\log b - (k\Delta C)^{e} \left(\frac{7}{4} - \log b \right) \right) \quad , m=n$$

If $m-n \neq 1$, (A-42) is all right as it stands because the argument of $H_{o}^{(e)}$ can not vanish at any point interior to the region of integration. If m-n=1, then (A-42) is recast as

$$I_{\alpha}=U_{\beta}+\int_{0}^{1}dv\int_{0}^{1}dv'((k\Delta C)^{\alpha}vv'+1)(H_{0}^{(\alpha)}(k\Delta C|v+v'-1|)-g(k\Delta C|v+v'-1|)) \tag{A-48}$$

where

$$U_{\beta} = (k\Delta C)^{\alpha}U_{\alpha} + U_{\beta} \tag{A-49}$$

in which U_{α} and U_{β} are given by (A-27) and (A-28). In view of (A-30) and (A-33), substitution of (A-49) into (A-48) gives

$$I_{\alpha} = \int_{0}^{1}dv\int_{0}^{1}dv'((k\Delta C)^{\alpha}vv'+1)(H_{0}^{(\alpha)}(k\Delta C|v+v'-1|)-g(k\Delta C|v+v'-1|))$$

$$+(k\Delta C)^{\alpha}\left(\frac{1}{4}+\frac{j}{8\pi}(5-4\log b)\right)+1+\frac{j}{\pi}(3-2\log b) \qquad ,m-n=1 \tag{A-50}$$

If $n-m \neq 1$, (A-43) is all right as it stands because the argument of $H_{0}^{(\alpha)}$ can not vanish at any point interior to the region of integration. If $n-m=1$, then I_{γ} of (A-43) is what I_{α} of (A-42) would be if $m-n=1$. Hence,

$$I_{\gamma} = I_{\alpha} \qquad , n-m=1 \tag{A-51}$$

where I_{α} is given by (A-50).

Now, $2k\eta Y_{mn}^{h\alpha}$ of (3-91) is given by (A-40) where I_{γ} is given by (A-41) for $m \neq n$ and by (A-47) for $m=n$, I_{α} is given by (A-42) for $m-n \neq 1$ and by (A-50) for $m-n=1$, and I_{γ} is given by (A-43) for $n-m \neq 1$ and by (A-51) for $n-m=1$.

APPENDIX B

In this appendix, we summarize the scattering method, a method in which the aperture remains open and only electric current is involved in the solution. In the original problem in Fig.1, the impressed sources radiate in the presence of the coducting bodies. The resulting field, denoted by $\underline{E}^{imp}(\underline{J}^{imp},\underline{M}^{imp})$, can be viewed as the sum of the field, denoted by $\underline{E}^{inc}$, which would exist if the impressed sources radiated in free space and the field, denoted by $\underline{E}(\underline{J}^{s},\underline{0})$, produced by the eletric current $\underline{J}^{s}$ induced on the perfect conductors radiating in free space.

The boundary condition is that

$$\underline{E}_t^{inc} + \underline{E}_t(\underline{J}^{s},\underline{0}) = \underline{0} \qquad \text{on } S_w,\ S_1,\ \text{and } S_n \qquad \text{(B-1)}$$

where t denotes the tangential componet on the conducting surface and S_w, S_1, and S_n are the surfaces of the perfect conductors. (See Fig.1) (B-1) states that the tangential componet of the electric field vanishes on the surface of the perfect conductors. Rearranging (B-1), we obtain

$$-\underline{E}_t(\underline{J}^{s},\underline{0}) = \underline{E}_t^{inc} \qquad \text{(B-2)}$$

To emphasize, we repeat that $\underline{E}^{inc}$ is the electric field that would exist if the impressed sources radiated in free space, and $\underline{E}(\underline{J}^{s},\underline{0})$ is the electric field due to $\underline{J}^{s}$ radiating in free space as well. $\underline{E}(\underline{J}^{s},\underline{0})$ is usually called the scattered

field. Thus, we refer to the method developed here as the scattering method.

In the following, we obtain $\underline{J}^m$ by the moment method [5]. Let $\underline{J}^m$ be approximated by

$$\underline{J}^m = \sum_{j=1}^{N} I_j^m \, \underline{J}_j^m \tag{B-3}$$

where $\{\underline{J}_j^m\}$ are expansion functions which must be chosen tangent to the conducting surfaces, $\{I_j^m\}$ are coefficients, and N is the number of expansion functions used to approximate $\underline{J}^m$.

Substituting (B-3) into (B-2), we obtain

$$-\sum_{j=1}^{N} I_j^m \, \underline{E}_t(\underline{J}_j^m, \underline{0}) = \underline{E}_t^{inc} \tag{B-4}$$

where $\underline{E}(\underline{J}_j^m, \underline{0})$ is the electric field due to the j^{th} expansion funciton $\underline{J}_j^m$ radiating in free space. Taking the summetric product of (B-4) with $\underline{J}_i^m$, i=1,2,...,N, we obtain

$$[Z^m] \, \vec{I}^m = \vec{V}^m \tag{B-5}$$

where the ij^{th} element of $[Z^m]$ is given by (2-24) with the superscript a replaced by s, the j^{th} element of $\vec{I}^m$ is I_j^m, and the i^{th} element V_i^m of $\vec{V}^m$ is given by

$$V_i^m = \langle \underline{J}_i^m, \underline{E}_t^{inc} \rangle \tag{B-6}$$

After $\vec{I}^m$ is obtained by solving the set of linear equations in (B-5), the fields can be written as

$$\underline{E}^m(\underline{J}^{imp}, \underline{M}^{imp}) = \underline{E}^{inc} + \sum_{j=1}^{N} I_j^m \, \underline{E}(\underline{J}_j^m, \underline{0}) \tag{B-7}$$

$$\underline{H}(\underline{J}^{imp}, \underline{M}^{imp}) = \underline{H}^{inc} + \sum_{j=1}^{N} I_j \, \underline{H}(\underline{J}_j, \underline{0}) \qquad \text{(B-8)}$$

where each field quantity on the right-hand sides of (B-7) and (B-8) is due to its source radiating in free space.

The formulation here is indeed simple. Unfortunately, it will fail to accurately determine the field inside the cavity formed by the walls of a conducting body if this cavity has a very small aperture. This is due to the fact that the field inside the cavity, being the sum of the incident field and the field due to $\underline{J}^m$, will be very small. The field due to $\underline{J}^m$ nearly cancels the incident field. Hence, a small percentage error in $\underline{J}^m$ will give rise to a large percentage error in the field inside the cavity.

REFERENCES

[1] C. M. Butler, Y. Rahmat-Samii, and R. Mittra, "Electromagnetic Penetration through Apertures in Conducting Surfaces," IEEE Trans. Antennas Propagat., Vol. AP-26, pp. 82-93, Jan. 1978.

[2] R. F. Harrington and J. R. Mautz, "A Generalized Network Formulation for Aperture Problems," IEEE Trans. Antennas Propagat., Vol. AP-24, pp. 870-873, Nov. 1976.

[3] R. F. Harrington and J. R. Mautz, "Electromagnetic Transmission through an Aperture in a Conducting Plane," AEÜ, Vol. 31, pp. 81-87, Feb. 1977.

[4] C. M. Butler and K. R. Umashankar, "Electromagnetic Penetration through an Aperture in an Infinite, Planar Screen Separating Two Half Spaces of Different Electromagnetic Properties," Radio Science, Vol. 11, pp. 611-619, July 1976.

[5] R. F. Harrington, Field Computation by Moment Methods, Macmillan, New York, 1968.

[6] R. F. Harrington, Time-Harmonic Electromagnetic Fields, McGraw-Hill Book Company, New York, 1961.

[7] E. Arvas, R. F. Harrington, and J. R. Mautz, "Radiation and scattering from Electrically Small Conducting Bodies of Arbitrary Shape," Report SYRU/DECE/TR-83/2, Department of Electrical and Computer Engineering, Syracuse University, Syracuse, NY 13210, Jan. 1983.

[8] H. A. Bethe, "Theory of Diffraction by Small Holes," Phys. Rev., Vol. 66, pp. 163-182, Oct. 1944.

[9] C. J. Bouwkamp, "On Bethe's Theory of Diffraction by Small Holes," Philips Res. Rep., Vol. 5, pp. 321-332, Oct. 1950.

[10] W. K. Saunders, "On Solutions of Maxwell's Equations in an Exterior Region," Proc. Natl. Acad. Sci., Vol. 38, pp. 342-348, 1952.

[11] D. T. Auckland and R. F. Harrington, "A Nonmodal Formulation for Electromagnetic Transmission through a Filled Slot of Arbitrary Cross Section in a Thick Conducting Screen," IEEE Trans. Microwave Theory Tech., Vol. MTT-28, pp. 548-555, June 1980.

[12] V. I. Krylov, Approximate Calculation of Integrals, Translated by A. H. Stroud, Macmillan, New York, 1962, pp. 107-122.

[13] J. R. Mautz, X. Yuan, and R. F. Harrington, "Electromagnetic Scattering from a Slotted TM Cylindrical Conductor by the Pseudo-Image Method," Report SYRU/DECE/TR-85/3, Department of Electrical and Computer Engineering, Syracuse University, Syracuse, NY 13210, Sept. 1985.

[14] C. M. Butler and D. R. Wilton, "General Analysis of Narrow Strips And Slots", IEEE Trans. Antennas Propagat., Vol. AP-28, pp. 42-48, Jan. 1980.

[15] H. B. Dwright, Tables of Integrals and Other Mathematical Data, Fourth Edition, Macmillan,

New York, 1961.

[16] T. B. A. Senior, "Electromagnetic Field Penetration into a Cylindrical Cavity," IEEE Trans. Electromagn. Compat., Vol. EMC-18, pp. 71-73, May 1976.

[17] T. B. A. Senior, " Field Penetration into a Cylindrical Cavity," Report 012643-2-T, The University of Michigan Radiation Lab., Ann Arbor, MI, Jan. 1975.

[18] A. D. Yaghjian, "Augmented Electric- and Magnetic-Field Integral Equations," Radio Science, Vol. 16, pp. 987-1001, Nov.-Dec. 1981.

END

10-86

DTIC